

GLOBAL JOURNAL

OF RESEARCHES IN ENGINEERING: I

Numerical Methods

The Correction Current Method

Theory for Plane Wave Scattering

} Highlights {

Three-Dimensional Deformation

Unconstrained Quadratic Programming

Discovering Thoughts, Inventing Future

VOLUME 21

ISSUE 1

VERSION 1.0



GLOBAL JOURNAL OF RESEARCHES IN ENGINEERING: I

NUMERICAL METHODS

GLOBAL JOURNAL OF RESEARCHES IN ENGINEERING: I
NUMERICAL METHODS

VOLUME 21 ISSUE 1 (VER. 1.0)

OPEN ASSOCIATION OF RESEARCH SOCIETY

© Global Journal of
Researches in Engineering.
2021.

All rights reserved.

This is a special issue published in version 1.0
of "Global Journal of Researches in
Engineering." By Global Journals Inc.

All articles are open access articles distributed
under "Global Journal of Researches in
Engineering"

Reading License, which permits restricted use.
Entire contents are copyright by of "Global
Journal of Researches in Engineering" unless
otherwise noted on specific articles.

No part of this publication may be reproduced
or transmitted in any form or by any means,
electronic or mechanical, including
photocopy, recording, or any information
storage and retrieval system, without written
permission.

The opinions and statements made in this
book are those of the authors concerned.
Ultraculture has not verified and neither
confirms nor denies any of the foregoing and
no warranty or fitness is implied.

Engage with the contents herein at your own
risk.

The use of this journal, and the terms and
conditions for our providing information, is
governed by our Disclaimer, Terms and
Conditions and Privacy Policy given on our
website [http://globaljournals.us/terms-and-condition/
menu-1463/](http://globaljournals.us/terms-and-condition/menu-1463/).

By referring / using / reading / any type of
association / referencing this journal, this
signifies and you acknowledge that you have
read them and that you accept and will be
bound by the terms thereof.

All information, journals, this journal,
activities undertaken, materials, services and
our website, terms and conditions, privacy
policy, and this journal is subject to change
anytime without any prior notice.

Incorporation No.: 0423089
License No.: 42125/022010/1186
Registration No.: 430374
Import-Export Code: 1109007027
Employer Identification Number (EIN):
USA Tax ID: 98-0673427

Global Journals Inc.

(A Delaware USA Incorporation with "Good Standing"; **Reg. Number: 0423089**)

Sponsors: Open Association of Research Society

Open Scientific Standards

Publisher's Headquarters office

Global Journals® Headquarters
945th Concord Streets,
Framingham Massachusetts Pin: 01701,
United States of America

USA Toll Free: +001-888-839-7392

USA Toll Free Fax: +001-888-839-7392

Offset Typesetting

Global Journals Incorporated
2nd, Lansdowne, Lansdowne Rd., Croydon-Surrey,
Pin: CR9 2ER, United Kingdom

Packaging & Continental Dispatching

Global Journals Pvt Ltd
E-3130 Sudama Nagar, Near Gopur Square,
Indore, M.P., Pin:452009, India

Find a correspondence nodal officer near you

To find nodal officer of your country, please
email us at local@globaljournals.org

eContacts

Press Inquiries: press@globaljournals.org
Investor Inquiries: investors@globaljournals.org
Technical Support: technology@globaljournals.org
Media & Releases: media@globaljournals.org

Pricing (Excluding Air Parcel Charges):

Yearly Subscription (Personal & Institutional)
250 USD (B/W) & 350 USD (Color)

EDITORIAL BOARD

GLOBAL JOURNAL OF RESEARCH IN ENGINEERING

Dr. Ren-Jye Dzung

Professor Civil Engineering, National Chiao-Tung University, Taiwan Dean of General Affairs, Ph.D., Civil & Environmental Engineering, University of Michigan United States

Dr. Iman Hajirasouliha

Ph.D. in Structural Engineering, Associate Professor, Department of Civil and Structural Engineering, University of Sheffield, United Kingdom

Dr. Ye Tian

Ph.D. Electrical Engineering The Pennsylvania State University 121 Electrical, Engineering East University Park, PA 16802, United States

Dr. Eric M. Lui

Ph.D., Structural Engineering, Department of Civil & Environmental Engineering, Syracuse University United States

Dr. Zi Chen

Ph.D. Department of Mechanical & Aerospace Engineering, Princeton University, US Assistant Professor, Thayer School of Engineering, Dartmouth College, Hanover, United States

Dr. T.S. Jang

Ph.D. Naval Architecture and Ocean Engineering, Seoul National University, Korea Director, Arctic Engineering Research Center, The Korea Ship and Offshore Research Institute, Pusan National University, South Korea

Dr. Ephraim Suhir

Ph.D., Dept. of Mechanics and Mathematics, Moscow University Moscow, Russia Bell Laboratories Physical Sciences and Engineering Research Division United States

Dr. Pangil Choi

Ph.D. Department of Civil, Environmental, and Construction Engineering, Texas Tech University, United States

Dr. Xianbo Zhao

Ph.D. Department of Building, National University of Singapore, Singapore, Senior Lecturer, Central Queensland University, Australia

Dr. Zhou Yufeng

Ph.D. Mechanical Engineering & Materials Science, Duke University, US Assistant Professor College of Engineering, Nanyang Technological University, Singapore

Dr. Pallav Purohit

Ph.D. Energy Policy and Planning, Indian Institute of Technology (IIT), Delhi Research Scientist, International Institute for Applied Systems Analysis (IIASA), Austria

Dr. Balasubramani R

Ph.D., (IT) in Faculty of Engg. & Tech. Professor & Head, Dept. of ISE at NMAM Institute of Technology

Dr. Sofoklis S. Makridis

B.Sc(Hons), M.Eng, Ph.D. Professor Department of Mechanical Engineering University of Western Macedonia, Greece

Dr. Steffen Lehmann

Faculty of Creative and Cultural Industries Ph.D., AA Dip University of Portsmouth United Kingdom

Dr. Wenfang Xie

Ph.D., Department of Electrical Engineering, Hong Kong Polytechnic University, Department of Automatic Control, Beijing University of Aeronautics and Astronautics China

Dr. Hai-Wen Li

Ph.D., Materials Engineering, Kyushu University, Fukuoka, Guest Professor at Aarhus University, Japan

Dr. Saeed Chehreh Chelgani

Ph.D. in Mineral Processing University of Western Ontario, Adjunct professor, Mining engineering and Mineral processing, University of Michigan United States

Belen Riveiro

Ph.D., School of Industrial Engineering, University of Vigo Spain

Dr. Adel Al Jumaily

Ph.D. Electrical Engineering (AI), Faculty of Engineering and IT, University of Technology, Sydney

Dr. Maciej Gucma

Assistant Professor, Maritime Univeristy of Szczecin Szczecin, Ph.D.. Eng. Master Mariner, Poland

Dr. M. Meguellati

Department of Electronics, University of Batna, Batna 05000, Algeria

Dr. Haijian Shi

Ph.D. Civil Engineering Structural Engineering Oakland, CA, United States

Dr. Chao Wang

Ph.D. in Computational Mechanics Rosharon, TX, United States

Dr. Joaquim Carneiro

Ph.D. in Mechanical Engineering, Faculty of Engineering, University of Porto (FEUP), University of Minho, Department of Physics Portugal

Dr. Wei-Hsin Chen

Ph.D., National Cheng Kung University, Department of Aeronautics, and Astronautics, Taiwan

Dr. Bin Chen

B.Sc., M.Sc., Ph.D., Xian Jiaotong University, China. State Key Laboratory of Multiphase Flow in Power Engineering Xi'an Jiaotong University, China

Dr. Charles-Darwin Annan

Ph.D., Professor Civil and Water Engineering University Laval, Canada

Dr. Jalal Kafashan

Mechanical Engineering Division of Mechatronics KU Leuven, Belgium

Dr. Alex W. Dawotola

Hydraulic Engineering Section, Delft University of Technology, Stevinweg, Delft, Netherlands

Dr. Shun-Chung Lee

Department of Resources Engineering, National Cheng Kung University, Taiwan

Dr. Gordana Colovic

B.Sc Textile Technology, M.Sc. Technical Science Ph.D. in Industrial Management. The College of Textile? Design, Technology and Management, Belgrade, Serbia

Dr. Giacomo Risitano

Ph.D., Industrial Engineering at University of Perugia (Italy) "Automotive Design" at Engineering Department of Messina University (Messina) Italy

Dr. Maurizio Palesi

Ph.D. in Computer Engineering, University of Catania, Faculty of Engineering and Architecture Italy

Dr. Salvatore Brischetto

Ph.D. in Aerospace Engineering, Polytechnic University of Turin and in Mechanics, Paris West University Nanterre La D?fense Department of Mechanical and Aerospace Engineering, Polytechnic University of Turin, Italy

Dr. Wesam S. Alaloul

B.Sc., M.Sc., Ph.D. in Civil and Environmental Engineering, University Technology Petronas, Malaysia

Dr. Ananda Kumar Palaniappan

B.Sc., MBA, MED, Ph.D. in Civil and Environmental Engineering, Ph.D. University of Malaya, Malaysia, University of Malaya, Malaysia

Dr. Hugo Silva

Associate Professor, University of Minho, Department of Civil Engineering, Ph.D., Civil Engineering, University of Minho Portugal

Dr. Fausto Gallucci

Associate Professor, Chemical Process Intensification (SPI), Faculty of Chemical Engineering and Chemistry Assistant Editor, International J. Hydrogen Energy, Netherlands

Dr. Philip T Moore

Ph.D., Graduate Master Supervisor School of Information Science and engineering Lanzhou University China

Dr. Cesar M. A. Vasques

Ph.D., Mechanical Engineering, Department of Mechanical Engineering, School of Engineering, Polytechnic of Porto Porto, Portugal

Dr. Jun Wang

Ph.D. in Architecture, University of Hong Kong, China Urban Studies City University of Hong Kong, China

Dr. Stefano Invernizzi

Ph.D. in Structural Engineering Technical University of Turin, Department of Structural, Geotechnical and Building Engineering, Italy

Dr. Togay Ozbakkaloglu

B.Sc. in Civil Engineering, Ph.D. in Structural Engineering, University of Ottawa, Canada Senior Lecturer University of Adelaide, Australia

Dr. Zhen Yuan

B.E., Ph.D. in Mechanical Engineering University of Sciences and Technology of China, China Professor, Faculty of Health Sciences, University of Macau, China

Dr. Jui-Sheng Chou

Ph.D. University of Texas at Austin, U.S.A. Department of Civil and Construction Engineering National Taiwan University of Science and Technology (Taiwan Tech)

Dr. Houfa Shen

Ph.D. Manufacturing Engineering, Mechanical Engineering, Structural Engineering, Department of Mechanical Engineering, Tsinghua University, China

Prof. (LU), (UoS) Dr. Miklas Scholz

Cand Ing, BEng (equiv), PgC, MSc, Ph.D., CWEM, CEnv, CSci, CEng, FHEA, FIEMA, FCIWEM, FICE, Fellow of IWA, VINNOVA Fellow, Marie Curie Senior, Fellow, Chair in Civil Engineering (UoS) Wetland Systems, Sustainable Drainage, and Water Quality

Dr. Yudong Zhang

B.S., M.S., Ph.D. Signal and Information Processing, Southeast University Professor School of Information Science and Technology at Nanjing Normal University, China

Dr. Minghua He

Department of Civil Engineering Tsinghua University Beijing, 100084, China

Dr. Philip G. Moscoso

Technology and Operations Management IESE Business School, University of Navarra Ph.D. in Industrial Engineering and Management, ETH Zurich M.Sc. in Chemical Engineering, ETH Zurich, Spain

Dr. Stefano Mariani

Associate Professor, Structural Mechanics, Department of Civil and Environmental Engineering, Ph.D., in Structural Engineering Polytechnic University of Milan Italy

Dr. Ciprian Lapusan

Ph. D in Mechanical Engineering Technical University of Cluj-Napoca Cluj-Napoca (Romania)

Dr. Francesco Tornabene

Ph.D. in Structural Mechanics, University of Bologna Professor Department of Civil, Chemical, Environmental and Materials Engineering University of Bologna, Italy

Dr. Kitipong Jaojaruek

B. Eng, M. Eng, D. Eng (Energy Technology, Asian Institute of Technology). Kasetsart University Kamphaeng Saen (KPS) Campus Energy Research Laboratory of Mechanical Engineering

Dr. Burcin Becerik-Gerber

University of Southern California Ph.D. in Civil Engineering Ddes, from Harvard University M.S. from University of California, Berkeley M.S. from Istanbul, Technical University

Hiroshi Sekimoto

Professor Emeritus Tokyo Institute of Technology Japan Ph.D., University of California Berkeley

Dr. Shaoping Xiao

BS, MS Ph.D. Mechanical Engineering, Northwestern University The University of Iowa, Department of Mechanical and Industrial Engineering Center for Computer-Aided Design

Dr. A. Stegou-Sagia

Ph.D., Mechanical Engineering, Environmental Engineering School of Mechanical Engineering, National Technical University of Athens, Greece

Diego Gonzalez-Aguilera

Ph.D. Dep. Cartographic and Land Engineering, University of Salamanca, Avilla, Spain

Dr. Maria Daniela

Ph.D in Aerospace Science and Technologies Second University of Naples, Research Fellow University of Naples Federico II, Italy

Dr. Omid Gohardani

Ph.D. Senior Aerospace/Mechanical/ Aeronautical,
Engineering professional M.Sc. Mechanical Engineering,
M.Sc. Aeronautical Engineering B.Sc. Vehicle
Engineering Orange County, California, US

Dr. Paolo Veronesi

Ph.D., Materials Engineering, Institute of Electronics,
Italy President of the master Degree in Materials
Engineering Dept. of Engineering, Italy

CONTENTS OF THE ISSUE

- i. Copyright Notice
- ii. Editorial Board Members
- iii. Chief Author and Dean
- iv. Contents of the Issue

- 1. Unconstrained Quadratic Programming Problem with Uncertain Parameters. *1-7*
- 2. New Full Wave Theory for Plane Wave Scattering by a Rough Dielectric Surface – The Correction Current Method. *9-14*
- 3. An Accurate Three-Dimensional Deformation Measurement Method in Wind Turbine Blade Static Loading Test. *15-22*
- 4. Optimized Mesh-free Analysis for the Singularity Subtraction Technique of Linear Elastic Fracture Mechanics. *23-50*

- v. Fellows
- vi. Auxiliary Memberships
- vii. Preferred Author Guidelines
- viii. Index



Unconstrained Quadratic Programming Problem with Uncertain Parameters

By Sie Long Kek, Fong Peng Lim & Harley Ooi

Universiti Tun Hussein Onn Malaysia

Abstract- In this paper, an unconstrained quadratic programming problem with uncertain parameters is discussed. For this purpose, the basic idea of optimizing the unconstrained quadratic programming problem is introduced. The solution method of solving linear equations could be applied to obtain the optimal solution for this kind of problem. Later, the theoretical work on the optimization of the unconstrained quadratic programming problem is presented. By this, the model parameters, which are unknown values, are considered. In this uncertain situation, it is assumed that these parameters are normally distributed; then, the simulation on these uncertain parameters are performed, so the quadratic programming problem without constraints could be solved iteratively by using the gradient-based optimization approach. For illustration, an example of this problem is studied. The computation procedure is expressed, and the result obtained shows the optimal solution in the uncertain environment. In conclusion, the unconstrained quadratic programming problem, which has uncertain parameters, could be solved successfully.

Keywords: *quadratic programming, gradient approach, uncertain parameters, risk simulator, the system of linear equations.*

GJRE-I Classification: FOR Code: 010399



Strictly as per the compliance and regulations of:



Unconstrained Quadratic Programming Problem with Uncertain Parameters

Sie Long Kek^α, Fong Peng Lim^σ & Harley Ooi^ρ

Abstract- In this paper, an unconstrained quadratic programming problem with uncertain parameters is discussed. For this purpose, the basic idea of optimizing the unconstrained quadratic programming problem is introduced. The solution method of solving linear equations could be applied to obtain the optimal solution for this kind of problem. Later, the theoretical work on the optimization of the unconstrained quadratic programming problem is presented. By this, the model parameters, which are unknown values, are considered. In this uncertain situation, it is assumed that these parameters are normally distributed; then, the simulation on these uncertain parameters are performed, so the quadratic programming problem without constraints could be solved iteratively by using the gradient-based optimization approach. For illustration, an example of this problem is studied. The computation procedure is expressed, and the result obtained shows the optimal solution in the uncertain environment. In conclusion, the unconstrained quadratic programming problem, which has uncertain parameters, could be solved successfully.

Keywords: quadratic programming, gradient approach, uncertain parameters, risk simulator, the system of linear equations.

I. INTRODUCTION

In nonlinear optimization, quadratic programming is the most simple optimization problem, and its applications have been widely studied [1], which are ranged from engineering [2, 3, 4] to business [5, 6, 7]. For allocating resources, the quadratic programming problem, which has an objective function in the quadratic form and subject to a set of constraints, is employed. Consequently, a quantitative decision could be made by referring to the optimal solution obtained from solving the quadratic programming problem, especially with the fuzzy parameters [8, 9, 10]. Also, the computational techniques for solving the quadratic programming problem under the probabilistic environment [11] and the related robust solution [12] are actively studied.

By the use of quadratic programming, this paper aims to discuss the uncertain parameters, which are presented in quadratic programming problem

without constraints. In doing so, a general unconstrained quadratic programming problem [13, 14, 15, 16] is considered, and the analytical solution is discussed. In the uncertain parameters, the analytical solution does not exist unless an assumption of knowing these uncertain parameters is made. Hence, the quadratic programming problem could be handled practically, where the uncertain parameters are assumed to be normally distributed. On this basis, the simulation [17] is performed on the uncertain parameters to give a possible optimal solution to the quadratic programming problem.

The paper is organized as follows. In Section 2, the unconstrained quadratic programming problem is described in general, and the analytical solution is provided. In Section 3, the presence of the uncertain parameters in the quadratic programming problem is taken into consideration. These parameters are assumed from the normal distribution, and the simulation is made to identify these parameters. The solution procedure is then summarized. In Section 4, an illustrative example is further discussed. Finally, a concluding remark is made.

II. PROBLEM STATEMENT

Consider a general unconstrained quadratic programming problem [13, 14], given by

$$\text{Minimize } f(\mathbf{x}) = \mathbf{x}^T \mathbf{A} \mathbf{x} + \mathbf{b}^T \mathbf{x} + c \quad (1)$$

where $\mathbf{x} \in \mathcal{R}^n$ is an n -vector of decision variables, $\mathbf{A} \in \mathcal{R}^{n \times n}$ is a symmetry positive definite matrix, $\mathbf{b} \in \mathcal{R}^n$ is an n -vector of coefficients, and $c \in \mathcal{R}$ is a constant. Under the certainty situation, the values for parameters \mathbf{A} , \mathbf{b} , and c are known and complete. Thus, to determine the optimal solution of the problem in (1), the first-order necessary condition [15, 16],

$$\nabla f(\mathbf{x}) = \mathbf{0} \quad (2)$$

is derived from giving

$$\mathbf{A} \mathbf{x} + \mathbf{b} = \mathbf{0} \quad (3)$$

Note that (3) is a system of linear equations, and its solution can be obtained from

Author ^α: Universiti Tun Hussein Onn Malaysia, Pagoh Campus, Muar, Johor, Malaysia. e-mail: slkek@uthm.edu.my

Author ^σ: Universiti Putra Malaysia, Serdang, Seri Kembangan, Selangor, Malaysia. e-mail: fongpeng@upm.edu.my

Author ^ρ: Edustats Solutions, Kuala Lumpur, Malaysia. e-mail: harley@edustats.com.my

$$\mathbf{x} = -\mathbf{A}^{-1}\mathbf{b}. \quad (4)$$

However, the analytical solution given by (4) would not exist if the parameters \mathbf{A} , \mathbf{b} , and c are unknown and incomplete information. From this point of view, a computational procedure is required to handle these uncertain parameters, so the unconstrained quadratic programming could be solved in practice.

III. OPTIMIZATION MODELLING APPROACH

Now, assume that the uncertain parameters are normally distributed, where mean and covariance are known necessarily [17, 18, 19]. Therefore, a simulation procedure is properly performed in handling these uncertain parameters. It is followed by using any optimization gradient techniques to solve the unconstrained quadratic programming problem for the possible optimal solution.

a) Uncertain Parameters Simulation

Suppose the values of the elements in the matrix $\mathbf{A} = (a_{ij})$ and the vector $\mathbf{b} = (b_i)$, for $i = 1, 2, \dots, n$, and $j = 1, 2, \dots, n$, are unknown, and these values are defined in the uncertainty set U , that is,

$$U = \{a_{ij}, b_i\} \quad (5)$$

where

$$a_{ij} \sim N(m_a, \sigma_a^2) \quad \text{and} \quad b_i \sim N(m_b, \sigma_b^2) \quad (6)$$

are assumed to be normally distributed with m_a is the mean vector and σ_a^2 is the covariance matrix for the elements of the matrix $\mathbf{A} = (a_{ij})$, and m_b is the mean vector and σ_b^2 is the covariance matrix for the elements of the vector $\mathbf{b} = (b_i)$.

By considering the simulation of the normal distribution, the uncertain parameters are determined from

$$a_{ij} = m_a + z_{a,\alpha} \sigma_a \quad (7)$$

$$b_i = m_b + z_{b,\alpha} \sigma_b \quad (8)$$

where α is the confidence level, $z_{a,\alpha}$ is the z-score at the confidence level α for the parameters a_{ij} , and $z_{b,\alpha}$ is the z-score at the confidence level α for the parameters b_i .

b) Calculation Solution Procedure

After the simulation is carried out to the uncertain parameters, the unconstrained quadratic programming problem is solved by using the optimization gradient approach [13, 15], which is given by

$$\mathbf{x}^{(k+1)} = \mathbf{x}^{(k)} + \beta_k \cdot \nabla f^{(k)} \quad (9)$$

where β_k represents the step size at the iteration number k , calculated from

$$\beta_k = \arg \min f(\mathbf{x}^{(k)} + \beta \cdot \nabla f(\mathbf{x}^{(k)})) \quad (10)$$

and

$$\nabla f^{(k)} = \nabla f(\mathbf{x}^{(k)}) \quad (11)$$

is the gradient function at $\mathbf{x}^{(k)}$, that is,

$$\nabla f(\mathbf{x}^{(k)}) = \mathbf{A}\mathbf{x}^{(k)} + \mathbf{b}. \quad (12)$$

From the discussion above, the calculation procedure for solving the unconstrained quadratic programming problem, where uncertain parameters exist, is summarized as follows.

Algorithm 1

Data \mathbf{A} , \mathbf{b} , c , m_a , σ_a , m_b , and σ_b . Set the iteration number $k = 0$, the initial value $\mathbf{x}^{(0)}$, the tolerance ε , and the number of simulation trials n .

Step 1 Simulate the uncertain parameters a_{ij} and b_i , respectively, from (7) and (8).

Step 2 Calculate the gradient from (12).

Step 3 Compute the parameter β_k from (10).

Step 4 Obtain the optimal solution $\mathbf{x}^{(k+1)}$ from (9).

Step 4 Evaluate the value of the objective function $f(\mathbf{x}^{(k+1)})$ from (1).

Step 5 Update the simulation trial number. If $\|\nabla f^{(k)}\| < \varepsilon$, stop the calculation, else, set $k = k + 1$, and repeat from Step 1.

Remark

The optimal solution to the unconstrained quadratic programming problem would be different for each simulation cycle. Hence, the simulation values for the decision variable are determined by solving the unconstrained quadratic problem. For this reason, the possible optimal solution shall be preferred in this situation.

IV. ILLUSTRATIVE EXAMPLE

Consider a quadratic programming problem with no constraint [14, 16] given by

$$\begin{aligned} \text{Minimize } f(x_1, x_2, x_3) \\ = \frac{5}{2}x_1^2 + \frac{7}{2}x_2^2 + 3x_3^2 + x_1x_2 + 3x_1x_3 \\ + 2x_2x_3 + 4x_1 + 9x_2 + 8x_3 + 10 \end{aligned} \quad (13)$$

This problem is solved by using the risk simulator software [18, 19, 20]. With the complete information of the matrix **A** and the vector **b**, the optimal solution is $(0.0, -1.0, -1.0)^T$, and the objective function has a minimum value of 1.50.

For the uncertain situation, two cases are further investigated. In Case 1, only the matrix **A** is assumed to have an uncertain value of entries, while in Case 2, both matrix **A** and vector **b** are assumed to have uncertain entries. The number of simulation trials is set to 500, and the number of optimization runs is set to 20.

Case 1:

Assume that the parameters in matrix **A** have mean and standard deviation given by

$$m_a = \begin{pmatrix} 5 & 1 & 3 \\ 1 & 7 & 2 \\ 3 & 2 & 6 \end{pmatrix} \quad \text{and} \quad \sigma_a = \begin{pmatrix} 0.5 & 0.1 & 0.3 \\ 0.1 & 0.7 & 0.2 \\ 0.3 & 0.2 & 0.6 \end{pmatrix}. \quad (14)$$

Suppose $\mathbf{b} = (4, 9, 8)^T$ and $c = 10$ are known. The simulation results for the decision variables and the objective function are shown in Table 1 and Table 2.

Table 1: Simulation Result for Decision Variables, Case 1

Decision Variable	Initial Value	Final Value	Mean Value
x_1	-0.00105	0.00068	0.000277
x_2	-1.00107	-1.01098	-1.00118
x_3	-0.99732	-0.99795	-0.99865

Table 2: Simulation Result for Objective Function, Case 1

Objective Function	Initial value	Final Value	Iteration Numbers
f	1.46040	1.46006	6

The graphical result for the objective function f is shown in Fig. 1, while the simulation values for decision variables X_1 , X_2 , and X_3 are shown in Figs. 2, 3, and 4, respectively. Notice that the figures' bars

represent the respective simulation values, and the lines show the relative cumulative distribution values.

Case 2:

To observe the possible results that might be obtained under the uncertainty, consider the entries of the matrix **A** has mean and covariance as given in (14), and assume the entries of the vector **b** is normally distributed with mean and variance given by

$$m_b = \begin{pmatrix} 4 \\ 9 \\ 8 \end{pmatrix} \quad \text{and} \quad \sigma_b = \begin{pmatrix} 0.4 \\ 0.9 \\ 0.8 \end{pmatrix}. \quad (15)$$

Table 3 and Table 4 show the simulation results for the decision variables and the objective function, respectively.

Table 3: Simulation Results for Decision Variables, Case 2

Decision Variable	Initial Value	Final Value	Mean Value
x_1	-0.01137	-0.00226	-0.0019
x_2	-1.00806	-0.99402	-1.00016
x_3	-0.97891	-0.98902	-0.99607

Table 4: Simulation Result for Objective Function, Case 2

Objective Function	Initial value	Final Value	Iteration Numbers
f	1.63204	1.63127	9

The graphical result of the objective function and the simulation values for the decision variables X_1 , X_2 , and X_3 are shown in Figs. 5, 6, 7, and 8, respectively.

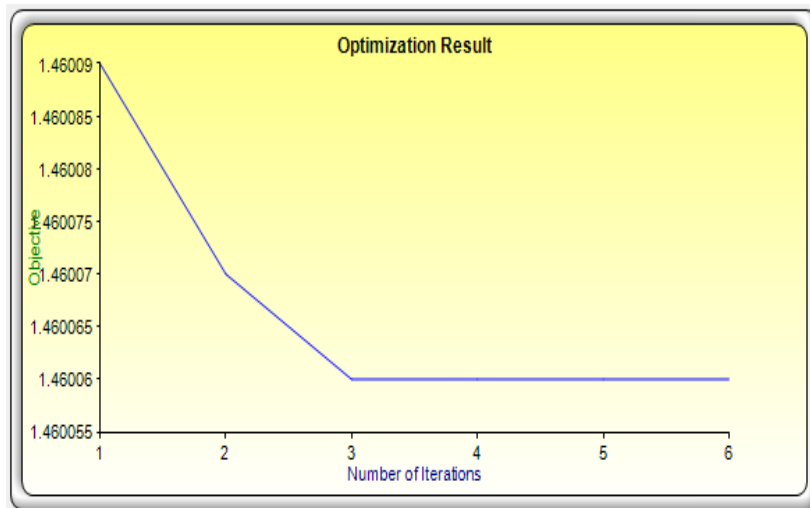


Fig. 1: Objective function, Case 1

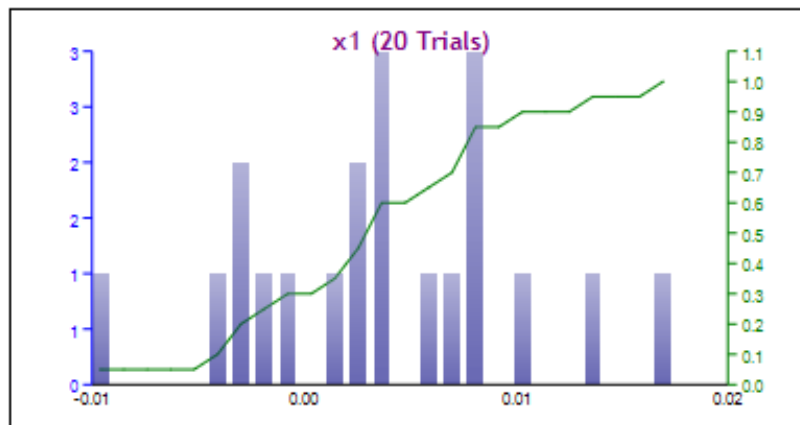


Fig. 2: Simulation values for decision variable X_1 , Case 1.

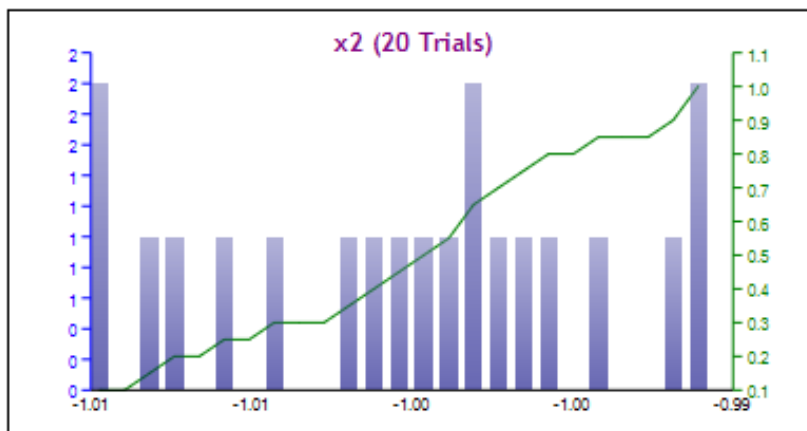


Fig. 3: Simulation values for decision variable X_2 , Case 1.

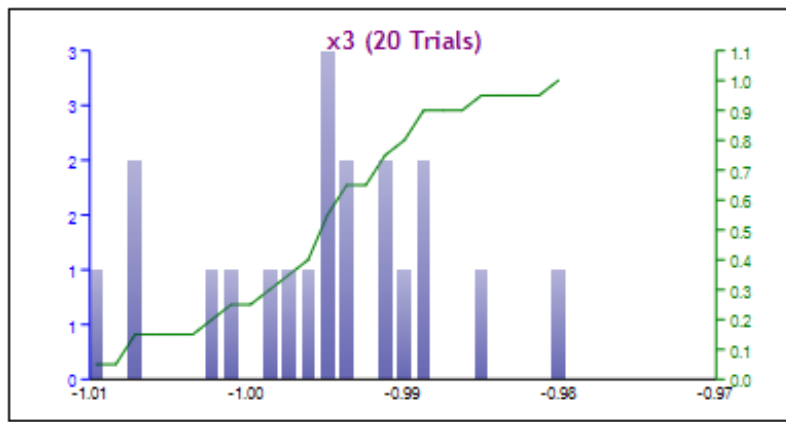


Fig. 4: Simulation values for decision variable X_3 , Case 1.

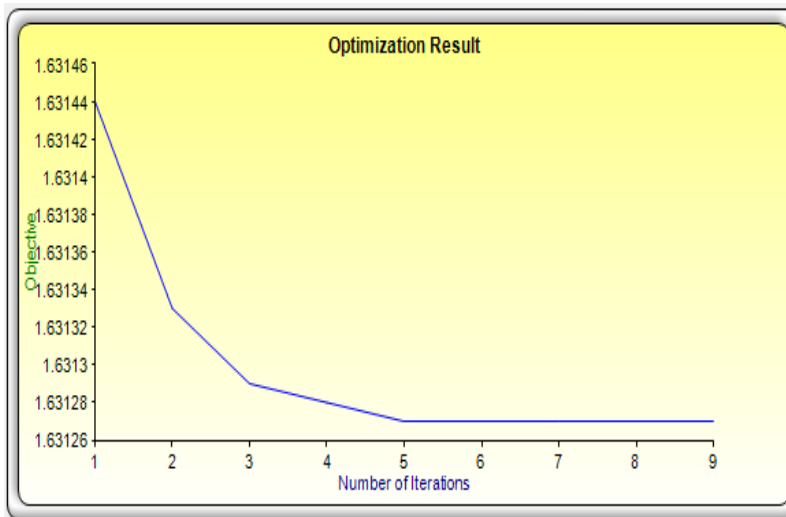


Fig. 5: Objective function, Case 2.

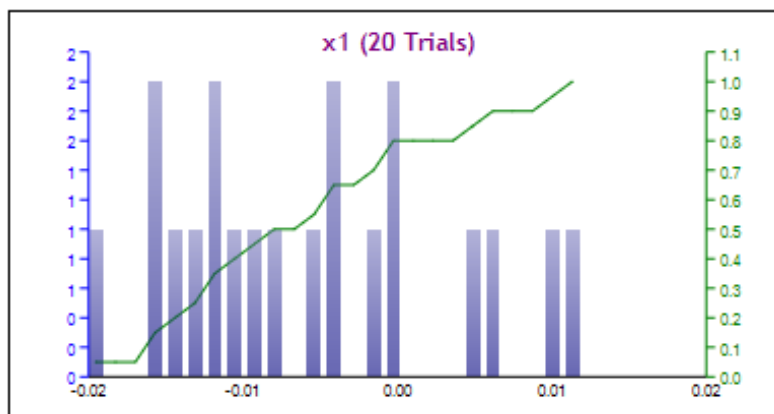


Fig. 6: Simulation values for decision variable X_1 , Case 2.

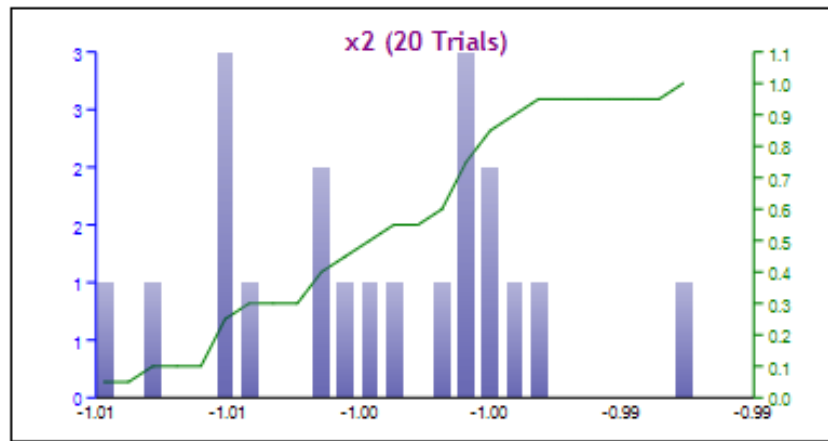


Fig. 7: Simulation values for decision variable X_2 , Case 2.

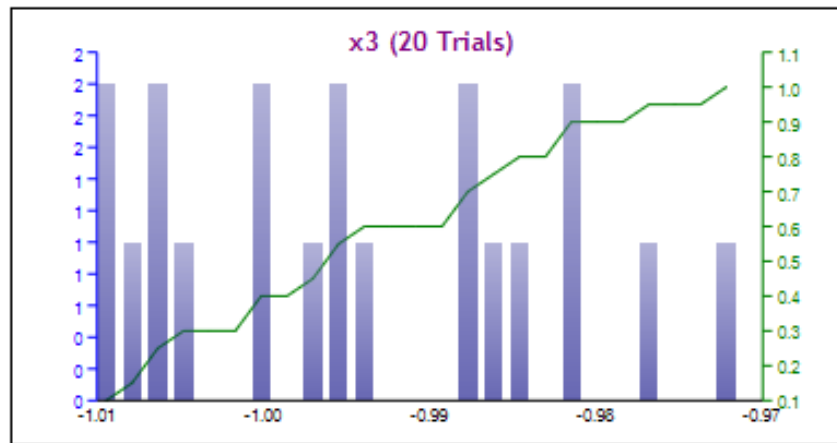


Fig. 8: Simulation values for decision variable X_3 , Case 2.

Therefore, assuming the uncertain parameters are normally distributed and applying the simulation procedure, the unconstrained quadratic programming problem could be solved in advance. The possible optimal solution obtained mainly depends on the simulation performed to the uncertain parameters and the gradient approach used.

V. CONCLUDING REMARKS

This paper has discussed the unconstrained quadratic programming problem with the presence of uncertain parameters. It is assumed that these parameters are normally distributed, and their values are determined from the simulation process. Accordingly, the unconstrained quadratic programming problem is solved by using the optimization gradient approach. The resulted simulation values of decision values are identified to obtain the possible optimal solution to the problem. In conclusion, the computation procedure used could handle the uncertain quadratic programming problem practically. For future research direction, it is recommended to cover the constraints, both for equality and inequality constraints, in solving the quadratic programming problems.

ACKNOWLEDGMENT

The authors would like to thank the Ministry of Education Malaysia (MOE) for supporting this research under the Fundamental Research Grant Scheme Vot No. FRGS/1/2018/STG06/UTHM/02/5 and partially sponsored by Universiti Tun Hussein Onn Malaysia.

REFERENCES RÉFÉRENCES REFERENCIAS

1. Carl, B.A., Moskowitz, H. and Furtan, H., Quadratic Programming Applications, *Omega*, 1977, Vol. 5, Iss. 1, pp. 43-55.
2. Guo, P. Huang, G.H. and Li, Y.P., Interval Stochastic quadratic Programming approach for Municipal Solid Waste Management, *Journal of Environment Engineering and Science*, 2008, Vol. 7, Iss. 6 pp. 569-579.
3. Sunarsih, S., Multi-Period Quadratic Programming Model for Sewon-Bantul Facultative Ponds Optimization, *Advances in Science, Technology and Engineering System Journal*, 2019, Vol. 4, Iss. 6, pp. 397-401.
4. Zhou, J., A New Spatial Branch and Bound Algorithm for Quadratic Program with One Quadratic Constraint and Linear Constraints,

- Mathematical Problems in Engineering*, Vol. 2020, Article ID 5717301, 2020, 8 pages.
5. Shi, Y., Peng Y., Kou G. and Chen, Z., Classssifying Credit Card Accounts for Business Intelligence and Decision Making: A Multiple-Criteria Quadratic Programming Approach, *International Journal of Information Technology and Decision Making*, 2005, Vol. 4, pp. 581-599.
 6. Cui,X. Zhu, S., Li, D. and Sun, J., Mean-Variance Portfolio Optimization with Parameter Sensitivity Control, *Optimization Methods and Software*, 2016, Vol. 31, Iss.4, pp. 755-774.
 7. Zhao, W., Wang, L., Yin, Y. Wang, B. and Tang, Y., Sequential Quadratic Programming Enhanced Backtracking Search Algorithm, *Frontiers of Computer Science*, 2018, Vol. 12, pp. 316-330.
 8. Gabr, W.I., Quadratic and Nonlinear Programming Problems Solving and Analysis in Fully Fuzzy Environment, *Alexandria Engineering Journal*, 2015, Vol. 54, Iss. 3, pp. 457-472.
 9. Mirmohseni, S.M. and Nasser, H., A Quadratic Programming with Triangular Fuzzy Numbers, *Journal of Applied Mathematics and Physics*, 2017, Vol. 5, 2218-2227.
 10. Taghi-Nezhad, N.A. and Taleshian, F., A Solution Approach for Solving Fully Fuzzy Quadratic Programming Problems, *Journal of Applied Research on Industrial Engineering*, 2018, Vol. 5, No. 1, pp. 50-61.
 11. Barik, S.K. and Biswal, M.P., Probabilistic Quaratic Programming Problems with Some Fuzzy Parameters, *Advances in Operations Research*, Vol. 2012, Article ID 635282, 2012, 13 pages.
 12. Mittal, A., Gokalp, C. and Hanasusanto, G.A., Robust Quadratic Programming with Mixed-Integer Uncertainty, *INFORMS Journal of Computing*, 2019, Vol. 32, No. 2, pp. 201-218.
 13. Chong, E.K.P. and Zak, H.S., *An Introduction to Optimization*, 4th Ed., John-Wiley & Sons, Inc., 2013.
 14. Luenberger, D.G. and Ye, Y., *Linear and Nonlinear Programming*, 4th Ed., New York: Springer, 2016.
 15. Sinha, S.M., *Mathematical Programming: Theory and Methods*, Elsevier Science, 2006.
 16. Nocedal, J. and Wright, S.J., *Numerial Optimization*, New York: Springer, 1999.
 17. Anderson, D.R., Sweeney, D.J., Williams, T.A. Camm, J.D. and Cochran, J.J., *An Introduction to Management Science: Quantitative Approaches to Decision Making*, 14th Ed., Cengage Learning, 2015.
 18. Johnathan, M., *Risk Simulator User Manual*, Real Option Valuation Press, 2015.
 19. Johnathan, M., *Modeling Risk: Applying Monte Carlo Risk Simulation, Strategic Real Optiions, Stochastic Forecasting, Portfolio Optimization, Data Analytics, Business Intelligence, and Decision Modeling*, Real Option Valuation Press, 2015.
 20. Johnathan, M., *Advanced Analytical Models: Applications in ROV Modeling Toolkit*, 2nd Ed., Create Space Independent Publishing Platform, 2016.



This page is intentionally left blank



GLOBAL JOURNAL OF RESEARCHES IN ENGINEERING: I
NUMERICAL METHODS

Volume 21 Issue 1 Version 1.0 Year 2021

Type: Double Blind Peer Reviewed International Research Journal

Publisher: Global Journals

Online ISSN: 2249-4596 & Print ISSN: 0975-5861

New Full Wave Theory for Plane Wave Scattering by a Rough Dielectric Surface – The Correction Current Method

By Felix Schwering, Gerald Whitman & Henry Tsai

Abstract- A new full wave theory for scattering by one dimensional perfectly conducting rough surface has been formulated recently. It provides enhanced physical insights into rough surface scattering processes, includes multiple scattering effects, quantifies field errors and furnishes a quantitative measure of the method's accuracy, permits a systematic procedure for obtaining higher-order terms in the iterative solution of the scatter problem, and satisfies reciprocity using only the first-order solution. The first- order solution of this new full wave method has been shown to reduce to the small perturbation and the Kirchhoff approximation in their regions of validity. It has also been numerically applied to surfaces with Gaussian height and slope variations and shown to be more accurate than the small-perturbation and the Kirchhoff methods in regions where neither are considered valid. This paper extend the theory to the more general and important case of scattering by a dielectric interface, where one of the two halfspaces is lossy.

GJRE-I Classification: FOR Code: 240501p



Strictly as per the compliance and regulations of:



New Full Wave Theory for Plane Wave Scattering by a Rough Dielectric Surface – The Correction Current Method

Felix Schwering^α, Gerald Whitman^σ & Henry Tsai^ρ

Abstract- A new full wave theory for scattering by one dimensional perfectly conducting rough surface has been formulated recently. It provides enhanced physical insights into rough surface scattering processes, includes multiple scattering effects, quantifies field errors and furnishes a quantitative measure of the method's accuracy, permits a systematic procedure for obtaining higher-order terms in the iterative solution of the scatter problem, and satisfies reciprocity using only the first-order solution. The first-order solution of this new full wave method has been shown to reduce to the small perturbation and the Kirchhoff approximation in their regions of validity. It has also been numerically applied to surfaces with Gaussian height and slope variations and shown to be more accurate than the small-perturbation and the Kirchhoff methods in regions where neither are considered valid. This paper extend the theory to the more general and important case of scattering by a dielectric interface, where one of the two halfspaces is lossy.

I. FORMULATION OF PROBLEM BY USE OF CC-METHOD

Subject of this paper is a new theory of scattering from rough dielectric surfaces of the type shown in Fig 1. The interface between an air halfspace and a dielectric halfspace is rough over a length $2L$ and planar beyond this region. The roughness profile is one-dimensional, i.e. the local height D varies with z but is constant with y .

A plane wave is incident under the angle ϕ_0 upon the interface; it may be incident from above or below. This incident wave and the resulting scattering field are TE- polarized, i.e. these fields consist of components E_y , H_x and H_z .

The technique used in this paper to formulate the problem is the Correction Current (CC) method, a new full wave method which has recently been established for plane wave scattering from metal surfaces [1] and subsequently extended to dielectric surfaces, with the lower halfspace at first assumed to be lossless but in the work presented here allowed to be lossy¹.

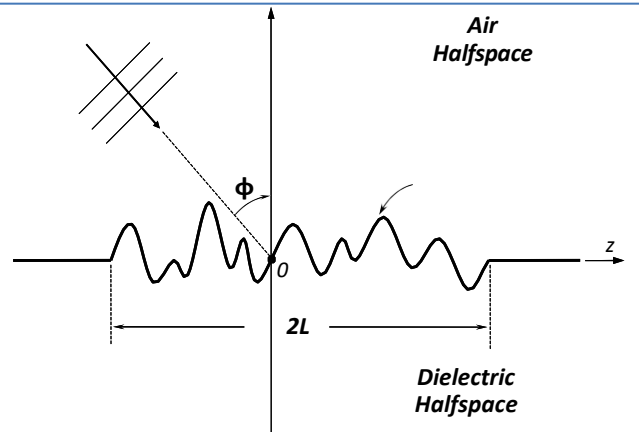


Fig. 1: Scatter Problem Geometry

The CC-method defines a primary field and a complete system of scatter fields, called radiation modes. Each of these fields consists of an incident, reflected and transmitted plane wave. These component waves, however, are modified such that each of the radiation modes as well as the primary field satisfies the boundary conditions at the interface, individually and rigorously. Since these fields are simple in structure (i.e. consisting of suitably modified plane waves) and comply with the boundary conditions at the rough interface, they will no longer satisfy Maxwell's equations¹. This is remedied by introducing fictitious current distributions, called passive currents that are assumed to be associated with each of these fields and chosen such that they exactly cancel the field errors of these fields; the passive current distribution of course varies from mode to mode. Thus, while not being solutions of Maxwell's source free equations, the primary field and radiation modes are solutions of Maxwell's equations with sources². The passive currents exist only in the corrugation region $|z| \leq L$; outside this region, where the interface is planar, the primary field and radiation modes are exact solutions of Maxwell's source free equations and no correction is needed.

¹ For a review of established theoretical methods for the analysis of rough surface scattering see [2]-[4].

² Alternatively, the passive currents may be interpreted as quantifying the field errors.

Author ^α p: US Army CERDEC Fort Monmouth, NJ.

Author ^σ: NJIT Newark, NJ. e-mail: gerald.whitman@njit.edu

In addition, it is assumed that each radiation mode is generated by an “active” sheet current distribution residing in a plane $z =$ termed the reference plane of this mode. These reference planes exist in the corrugation region $|Z| \leq L$ only, and all active currents of the mode system are limited to the same region as the passive currents. An important feature of these active currents is that taken together they form a complete orthogonal system so that any (passive) current distribution in the region $|Z| \leq L$ can be expanded into, or nullified by the active currents.

The total field is then written as a superposition of the primary field and the radiation modes. This combined field, of course, is not allowed to contain any active or passive current distribution, and this “zero-current” condition is then used to determine the unknown amplitudes of the radiation modes by an iterative procedure which in, a step-by-step fashion, eliminates the passive currents of the primary field and the radiation modes by the active currents of the radiation modes. The completeness, mentioned above, of the active currents allows us to do this consistently. The resulting combined field will satisfy the boundary conditions at the interface and the radiation condition at infinity while all active and passive currents are eliminated by mutual compensation. Thus the combined field is the solution of the scatter problem. For numerical efficiency, the iterative process is typically cut-off after the first iteration.

Using this approach the dielectric surface scatter problem has recently been solved for the case that the dielectric halfspace is loss free. Scattering patterns have been obtained in the form of single integrals over elementary functions which are easily evaluated numerically. The patterns have been computed for both deterministic and random rough surfaces. Comparison with the corresponding patterns obtained by a Method of Moments (MoM) procedure has shown that the first order iteration theory is of good accuracy over a wide parameter region. A paper reporting on this study, which was conducted at CERDEC and NJIT, is close to completion and will be submitted for publication in the near future.

The extension of the theory to lossy dielectrics is currently pursued under the 2007 In-house Laboratory Independent Research (ILIR) program. This extension is not straight forward, however. The problem geometry consists of two halfspaces; and two groups of radiation modes are required for full characterization of the problem. This holds for the lossy as well as for the lossless case. But when these two mode groups for the lossy case are defined in direct analogy to the two mode groups for the lossless case one of the groups diverges, i.e. increases exponentially with $|x|$, which is unacceptable. Hence the radiation modes need to be redefined, which has a significant effect on the theory. In

the development of this theory it is consistently assumed that $[\epsilon_r]$ is finite; it may be small, but is not allowed to be arbitrarily small. Comparison to the results of the lossless theory will be made only after all formulas for fields and radiation patterns have been fully established.

II. ANALYTICAL RESULTS AND DISCUSSION

In the following it is assumed that the incident plane wave is situated in the upper (air) halfspace. If it is located in the lower halfspace, the expressions obtained for fields and patterns will be different, of course. But the overall trends observed are similar.

It is interesting to note that the scatter fields associated with the two locations of the incident wave are related by a simple symmetry relation. Assume that a plane wave of amplitude E_0 and phase constant (in the z -direction) incident in the air halfspace – generates a scatter field $\beta_0 - E^s(x, z; k_0, k_\epsilon, D(z))$. Assume, furthermore, that a plane wave of amplitude E_ϵ and phase constant β_ϵ – incident in the dielectric halfspace – creates a scatter field $\bar{E}_y^s(x, z; k_0, k_\epsilon, D(z))$. Then these two scatter fields are related by the condition.

$$\frac{\bar{E}_y^s(x, z; k_0, k_\epsilon, D(z))}{E_\epsilon} = \frac{E_y^s(-x, z; k_\epsilon, k_0, -D(z))}{E_0} \quad (1)$$

for

$$\beta_\epsilon = \beta_0$$

with

$$k_\epsilon = k_0 \sqrt{\epsilon_r}$$

This relation holds for all x and z , i.e. in both halfspaces. Thus, if E_y^s has been determined \bar{E}_y^s , follows by a simple substitution of coordinates and parameters³; and vice versa.

Symmetry relation (1) must be satisfied for the exact scatter fields. But it is satisfied already for the first order iteration approximation used in this paper which may be taken as an indication that the first order method is of good accuracy.

In this first order approximation the CC-theory leads to the following expression for the scatter field in the upper (air) halfspace $x > D$:

³ Note that since $\epsilon_r = (\kappa_\epsilon / \kappa_0)^2$ the parameter substitution replaces ϵ_r by $1 / \epsilon_r$.

$$\begin{aligned}
 E_y^{(1)}(x, z) = & -\frac{E_0 u_0}{\pi(u_0 + v_0)} \left[\int_{u=0}^{\infty} \int_{\tilde{z}=-L}^{+L} \left\{ \frac{1 - e^{+j(u_0+u)\tilde{D}}}{u_0 + u} \right. \right. \\
 & \cdot \left[1 + 2j\delta(z - \tilde{z}) \frac{\beta_1}{u_0^2 - u^2} \right] - \left(\frac{1}{u_0 + u} - \frac{1}{v_0 + v_1} \right) \cdot \\
 & \cdot \tilde{D}'^2 e^{+j(u_0+u)\tilde{D}} \left\{ (u + v_1)e^{+ju(x-2D)} + (u - v_1)e^{-ju(x-2D)} \right\} \\
 & \cdot e^{-j\beta_0 \tilde{z} - j\beta_1 |z - \tilde{z}|} \cdot \frac{u}{\beta_1} du d\tilde{z} - \\
 & - 2 \int_{u=0}^{\infty} \int_{\tilde{z}=-L}^{+L} \left\{ \frac{1 - e^{+j(u_0-u)\tilde{D}}}{u_0 - u} \left[1 + 2j\delta(z - \tilde{z}) \frac{\beta_2}{u_0^2 - v_2^2} \right] - \right. \\
 & - \left(\frac{1}{u_0 - v_2} - \frac{1}{v_0 + u} \right) \tilde{D}'^2 e^{+j(u_0-u)\tilde{D}} \left\{ e^{+jv_2 x + j(u-v_2)D} \right. \\
 & \cdot e^{-j\beta_0 \tilde{z} - j\beta_2 |z - \tilde{z}|} \frac{u^2}{\beta_2} du d\tilde{z} \left. \right] \quad (2a)
 \end{aligned}$$

for $x > D$

Where E_0 is the amplitude of the incident plane wave \tilde{D} stands for $D(\tilde{z})$ and k_0 is the free-space wave number; furthermore

$$u_0 = k_0 \cos \varphi_0$$

$$\begin{aligned}
 v_0 &= k_0(\varepsilon_r - \sin^2 \varphi_0)^{1/2}, \quad \beta_0 = k_0 \sin \varphi_0 \\
 v_1 &= [u^2 + k_0^2(\varepsilon_r - 1)]^{1/2}, \quad \beta_1 = (k_0^2 - u^2)^{1/2} \\
 v_2 &= [u^2 - k_0^2(\varepsilon_r - 1)]^{1/2}, \quad \beta_2 = (k_0^2 \varepsilon_r - u^2)^{1/2}
 \end{aligned} \quad (2b)$$

The path of the u -integration runs along the positive real axis⁴. The propagation constants v_0 , v_1 , β_1 and β_2 are positive real and/or negative imaginary while is positive real and positive imaginary.

The first double integral in (2a) represents the contribution of the first mode group to the scatter field and the second double integral shows the contribution of the second mode group. A formally similar representation is obtained for the scatter field in the lower (lossy dielectric) halfspace but for brevity is not spelled out here.

In the far field region, where

$$k_0 \rho = k_0 (x^2 + z^2)^{1/2} \gg k_0 L \text{ and } \gg 2\pi,$$

eq. (2) can be simplified by substituting

$$x = \rho \cos \varphi, \quad z = \rho \sin \varphi$$

where the scatter angle φ is in the region

$$-\frac{\pi}{2} \leq \varphi \leq +\frac{\pi}{2} \quad (\text{upper halfspace})$$

The formula may then be evaluated asymptotically for $k_0 \rho \rightarrow \infty$ using the method of stationary phase which eliminates the u -integration. Only the first double integral in (2a) contributes to the far field and one obtains

$$E_y^{(1)} = \left(\frac{2}{\pi} \right)^{1/2} E_0 \frac{e^{-j(k_0 \rho - \pi/4)}}{(k_0 \rho)^{1/2}} S_0(\varphi, \varphi_0) \quad (3a)$$

$$\text{for } -\frac{\pi}{2} \leq \varphi, \varphi_0 \leq +\frac{\pi}{2}, \quad k_0 \rho \rightarrow \infty$$

where the scatter pattern $S_0(\varphi, \varphi_0)$ takes the form

$$\begin{aligned}
 S_0(\varphi, \varphi_0) = & -k_0(\varepsilon_r - 1) \frac{\cos \varphi \cos \varphi_0}{\cos \varphi + \cos \varphi_0} \cdot \\
 & \cdot \frac{1}{[\cos \varphi + (\varepsilon_r - \sin^2 \varphi)^{1/2}][\cos \varphi_0 + (\varepsilon_r - \sin^2 \varphi_0)^{1/2}]}
 \end{aligned}$$

⁴ Except when a $(u-u)^{-1}$ singularity occurs on the real u -axis. In this case the u -integration bypasses the singularity by a local deformation of the integration path into the positive imaginary u -halfspace.

$$\cdot \int_{\tilde{z}=-L}^{+L} \left\{ 1 - \left[1 + \left(1 - \frac{\cos \varphi + \cos \varphi_0}{(\varepsilon_r - \sin^2 \varphi)^{1/2} + (\varepsilon_r - \sin^2 \varphi_0)^{1/2}} \right) \tilde{D}'^2 \right] \right\} \cdot e^{+jk_0 \tilde{D}(\cos \varphi + \cos \varphi_0)} \cdot e^{+jk_0 \tilde{z}(\sin \varphi - \sin \varphi_0)} d\tilde{z} \quad (3b)$$

This expression for the scatter pattern in the air halfspace $x > D$ is identical to the one obtained by the previously developed theory for $\varepsilon_r = \text{real}$, but it is now confirmed to be valid for complex ε_r as well. Eq. (3b) also shows that S_0 vanishes, as required, in the no-contrast case that $\varepsilon_r \rightarrow 1$, and that it satisfies the reciprocity relation $S_0(\varphi, \varphi_0) = S_0(-\varphi_0, -\varphi)$.

Similar to expression (2) for the scatter field in the upper halfspace, the formula obtained for the lower halfspace (not shown here) consists of two double integrals representing the contributions of the two mode groups. However, due to the lossy nature of the dielectric halfspace, the scatter field will decrease here

exponentially away from the corrugated interface, and the two double integrals in general cannot be simplified. Simplification is possible only if $\text{Im}[\varepsilon_r]$ is either very small, so that a far field of reasonable magnitude exists, or if $\text{Im}[\varepsilon_r]$ is rather large, so that the scatter field in the lower halfspace is in effect confined to a neighborhood of the scatter surface.

In the case that $|\text{Im}[\varepsilon_r]|$ is very small, the scatter field in the region far away from the corrugated section of the interface can be obtained by the method of steepest descent, which eliminates the integration over \tilde{z} . One finds that $E_y^{(1)}$ in the lower halfspace $x < D$ is of the form

$$E_y^{(1)} = \sqrt{\frac{2}{\pi}} \cdot E_0 \left[\frac{e^{-j(k_\varepsilon \rho - \pi/4)}}{(k_\varepsilon \rho)^{1/2}} S_\varepsilon(\varphi, \varphi_0) + F_\varepsilon(\rho, \varphi) T_\varepsilon(\varphi_0) \right] \quad (4a)$$

where $k_\varepsilon = k_0 \sqrt{\varepsilon_r}$ and

$$F_\varepsilon(\rho, \varphi) = \begin{cases} \frac{e^{-jk_0 \rho [\sin \varphi - (\varepsilon_r - 1)^{1/2} \cos \varphi]}}{\left[k_0 \rho \left(\sin \varphi + \frac{\cos \varphi}{(\varepsilon_r - 1)^{1/2}} \right) \right]^{3/2}} & \text{for } \text{Im}[\varepsilon_r] < 0 \\ 0 & \text{for } \text{Im}[\varepsilon_r] = 0 \end{cases} \quad (4b)$$

for $\frac{\pi}{2} \leq |\varphi| \leq \pi$, $k_0 \rho \rightarrow \infty$

The scatter field in this case consists of two parts which may be interpreted in the following way. In contrast to the scatter field in the upper halfspace, the scatter pattern in the lower halfspace is generated by two different mechanisms which are illustrated by Fig. 2. The first mechanism, as in the case of the lossless upper halfspace, is simply the scattering of the incident plane wave at the corrugated part of the interface. The second mechanism comes about because the scatter field in the lower, lossy halfspace decreases with ρ exponentially, i.e. much faster than the scatter field in the upper halfspace. But the scatter field must be continuous at the interface. As a consequence there is a continuous leakage of energy from the upper halfspace into the lower halfspace, which constitutes the second mechanism generating the scatter field in the lower halfspace⁵. The first mechanism causes a conventional scatter field where in the far zone the ρ - and φ -

dependence are separated, but with the ρ -dependence in this case decreasing exponentially; see eq.(4a). This field will dominate at scatter angle φ close to $\pm 180^\circ$. In the asymptotic field caused by the second mechanism, on the other hand, the ρ - and φ -dependence remain coupled also in the asymptotic region. This part of the field will be dominant near the interface, i.e. for φ near $\pm 90^\circ$.

⁵ No such energy transfer occurs when ε_r is real, since the energy density in both half spaces decreases with ρ^{-1} .

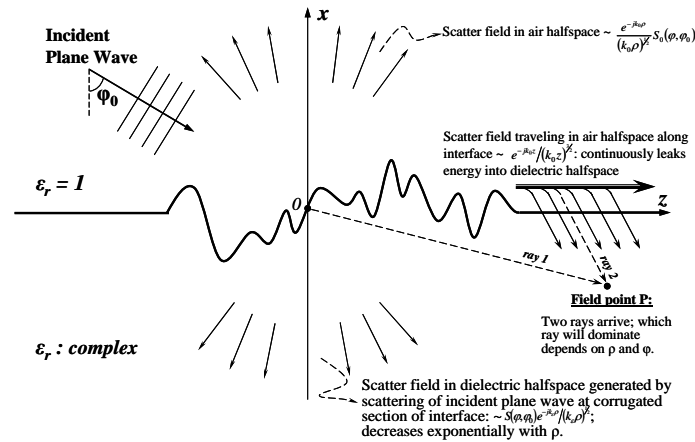


Fig. 2: Scatter field in lower (lossy) halfspace is generated by two mechanisms

- (1) Scattering of primary field at corrugated section of interface
 - (2) Energy transfer from scatter field in upper halfspace to asymptotic scatter field in lower half space
- ($x = \rho \cos \varphi$, $z = \rho \sin \varphi$, $k_z = k_0 \sqrt{\epsilon_r}$)

A possible problem is the following. If $|\text{Im}[\epsilon_r]|$ is very small then the denominator of F_ϵ in (4b) will have a near-zero at $\sin \varphi = |\epsilon_r|^{-1/2}$ resulting in a sharp peak of F_ϵ . The authors are not sure that this is correct and eq. (4b) will require further study.

As mentioned above, if $\text{Im}[\epsilon_r]$ is sizeable then eq. (4), even if mathematically correct, will lose its physical meaning. The equation holds in the far zone, i.e. at large distances from the corrugated part of the interface, and if $\text{Im}[\epsilon_r]$ is significant then the scatter field at such distances will be exceedingly small and undetectable for all practical purpose.

Conceptually it is obvious that, in the case of large $\text{Im}[\epsilon_r]$, the scatter field in the lower halfspace will be of significant magnitude only in a narrow region adjacent to the interface, while this field, whether generated by the first or the second mechanism mentioned above, will decrease rapidly with increasing distance from the interface. The general representation of the scatter fields in terms of two double integrals (i.e. a representation akin to eq. (2a)) allows to quantify this, but the analytical procedure is rather lengthy and tedious, and not included in this paper.

One last remark: The scatter pattern (3b) in the upper halfspace includes a factor $\cos \varphi$ and will be zero for $\pm 90^\circ$, i.e. at the interface, indicating that E_y along the

interface declines faster than $\frac{e^{-jk_0 z}}{|k_0 z|^{1/2}}$. The scatter field

in the direct vicinity of the interface can be determined by an asymptotic evaluation of (2) for

$$|k_0 z| \gg k_0 L \text{ and } \gg 2\pi, \quad |k_0 x| < |k_0 z|^{1/2}$$

i.e. in a region where z is large but x remains small compared to z (Fresnel Region). One obtains

$$E_y^{(1)} = -j\left(\frac{2}{\pi}\right)^{1/2} E_0 k_0^2 \frac{u_0}{u_0 + v_0} \int_{z=-L}^{+L} \frac{1 - e^{+ju_0 \tilde{z}}}{u_0} -$$

$$\left[\frac{1}{u_0} - \frac{1}{v_0 + k_0(\epsilon_r - 1)^{1/2}} \right] \tilde{D}'^2 e^{+ju_0 \tilde{D}} \left] e^{-j(\beta_0 \mp k_0) \tilde{z}} d\tilde{z} \cdot \frac{e^{-j(k_0 |z| - \frac{\pi}{4})}}{(k_0 |z|)^{3/2}} \begin{cases} [1 + jk_0(\epsilon_r - 1)^{1/2}(x - D)], & x > D(z) \\ e^{+jk_0(\epsilon_r - 1)^{1/2}(x - D)}, & x < D(z) \end{cases}$$

The formula shows that E_y near the interface decrease with $\frac{e^{-jk_0 |z|}}{|k_0 z|^{3/2}}$, i.e. the energy density will decrease here with ρ^{-3} rather than with ρ^{-1} , the rate of decrease for $|\varphi| < 90^\circ$. With x , the field below the surface decreases exponentially, indicating a transmitted wave while above the surface it varies linearly with x indicating the interaction between an incident and a reflected wave. All this is consistent with a continuous leakage of energy from the air halfspace into the lossy dielectric halfspace, i.e. with the second mechanism mentioned above for generating the scatter field in the lower halfspace.

As mentioned earlier, the discussion and formulas presented in this paper apply to the case that the primary wave is incident in the upper (air) halfspace. If the antenna generating the incident wave is situated in the lower (dielectric) halfspace, the symmetry relation (1) applies; the formulas are analogous; and similar overall trends are observed.

The theory for the lossy dielectric case summarized in this paper has been developed under the 2007 CERDEC ILIR program in cooperation with NJIT and is near completion, though some points need further investigation. Final results will be tested by comparison to data obtained by a MoM technique. This work is schedule for 2008.

Numerical Techniques such as the MoM and FDTD methods can be relied on to provide very

accurate results. Analytical methods as the one presented in this paper, even though approximate, have the advantage of showing parameter dependencies explicitly, thus providing physical insight. In addition, the field and pattern formulas – often obtained in the form of single integrals over elementary functions – are amenable to efficient computer evaluation and may be useful for real-time modeling.

REFERENCES RÉFÉRENCES REFERENCIAS

1. F. K. Schwing, G. M. Whitman and A. A. Triolo, "New full-wave theory for scattering from rough metal surfaces- the correction current method: the TE-polarization case," *Waves and Random Media*, vol. 14, pp.23-60, 2004.
2. P. Beckmann and A. Spizzichino, *The Scattering of Electromagnetic Wave from Rough Surfaces*, New York: Macmillan, 1963.
3. J. Ogilvy, *Theory of Wave Scattering from Random Rough Surfaces*, Philadelphia Institute of Physics, 1991.
4. A.G. Voronovich, *Wave Scattering from Rough Surfaces*, 2nd ed., Berlin: Springer Verlag, 1998.



An Accurate Three-Dimensional Deformation Measurement Method in Wind Turbine Blade Static Loading Test

By Yongfeng Yu

Abstract- The accurate deflection measurement of wind turbine blade is one of the key step in its full-scale static loading test. In order to measure the blade deflection accurately in the three-dimensional space, an effective spatial displacement measurement mathematical model has been established on the basis of geometric transformation method. At the same time, the finite element method is used to calculate the change of the blade deflection under the static loading force. Based on the above three-dimensional deflection measurement model, corresponding data measurement system was development. In the end, the three-dimensional measurement method was applied to wind turbine blade static test for blade tip measurement. The test results show that the maximum error rate of the three directions is only 4.1%, 3.8% and 4.3%, compared with the results of theoretical calculation, which has a very broad engineering application prospect.

Keywords: *measurement methods; mathematical model; three-dimensional deformation; wind turbine blade; static loading test.*

GJRE-I Classification: FOR Code: 010301



Strictly as per the compliance and regulations of:



An Accurate Three-Dimensional Deformation Measurement Method in Wind Turbine Blade Static Loading Test

Yongfeng Yu

Abstract- The accurate deflection measurement of wind turbine blade is one of the key step in its full-scale static loading test. In order to measure the blade deflection accurately in the three-dimensional space, an effective spatial displacement measurement mathematical model has been established on the basis of geometric transformation method. At the same time, the finite element method is used to calculate the change of the blade deflection under the static loading force. Based on the above three-dimensional deflection measurement model, corresponding data measurement system was development. In the end, the three-dimensional measurement method was applied to wind turbine blade static test for blade tip measurement. The test results show that the maximum error rate of the three directions is only 4.1%, 3.8% and 4.3%, compared with the results of theoretical calculation, which has a very broad engineering application prospect.

Keywords: measurement methods; mathematical model; three-dimensional deformation; wind turbine blade; static loading test.

I. INTRODUCTION

The wind power industry is becoming a focus of the national new energy industry. The blade as one of the core components of the wind turbine, its quality determines the healthy development of wind power industry. Due to the blade not only to withstand strong wind load, but also to bear the impact of sand and gravel, ultraviolet radiation and other external erosion in the process of work (Chen et al., 2014; Kong et al., 2005; Lee et al., 2015; Shi et al., 2011; Liu et al., 2013), coupled with wind power accidents occurred in recent years, so the wind vane full-size structure detection has become very important in the areas of research. The static test is the most important part of the blade certification in order to verify whether the blade is under ultimate load (such as 50 a worst hurricane). According to the third party authority Certification body Germany GL (Germanischer Lloyd) classification of the Guideline for the Certification of Wind Turbine (Germanischer Lloyd, 2003) and IEC61400-23 Full - scale Structural Testing of Wind Turbine Blades Testing standard, static load evaluation is the essential link of blade structure performance Testing. For the new development or process to make major changes in the leaves, is

required to do a full-size static loading test, which the purpose is to verify the static strength of the blade. However, field tests show that the coupling force is stored between the loading force during the static test, loading force of any node changes, resulting in irregular fluctuations in the loading force of other nodes, resulting in the uncoordinated and uniform change between the loading forces. Resulting in serious distortion of the test data, so the coordinated control between the loading force becomes very important. Deflection measurement is a key parameter that must be collected during the static loading test. It is an important theoretical basis for checking whether the blade structure design is qualified. Most domestic and foreign scholars focus on testing control methods and equipment development, that is, how to improve the loading precision and made no mention of the blade deflection measurement. The adaptive sliding mode control algorithm is proposed in the literature (Benitro and Hedrick, 2009), which is applied to the three axis swing table control system, and a better control effect is obtained. The distributed control method is proposed in (Hua et al., 2010), and the feasibility of the method is proved by the theoretical analysis and experimental results. Currently in the process of static testing, only one rope sensor / laser rangefinder is usually used to realize single direction deflection measurement. For example, the full scale static test of large-scale wind turbine blade is only in a single direction of the deflection measurement in the literature (Wang et al., 2014; Li et al., 2013), which can't make accurate measurement of the three-dimensional space displacement of the wind turbine blade.

Aiming at the above problems, based on the analysis of the coupling law of load force and dynamic command method, this paper proposes a simple and accurate three - dimensional space displacement measurement model is constructed by using the geometric transformation method, and the corresponding data acquisition system is developed.

II. WIND TURBINE BLADE FULL-SIZE STATIC LOADING SCHEME

Wind turbine blade full-scale static loading scheme is shown in Fig. 1. The wind turbine blade is fixed on base by many high strength bolts. Clamps on

Author: Lianyungang Zhongfu Lianzhong Composite Group Co., Ltd., Jiangsu 222006, China. e-mail: yuyongfeng@lzfrp.com

the blade is connected to the load node through the wire rope, and a tension sensor is connected in series between the wire rope to collect the current loading force. Each loading node is mainly composed of loading bracket, hydraulic winch, hydraulic drive system and electronic control system. Static loading test was usually

divided into four stages, namely, according to the maximum load of 40%-60%-80%-100% for loading/unloading, and the 100% stage requires a duration of not less than ten seconds. When the loading stage is completed, the load in reverse is order to unloading.

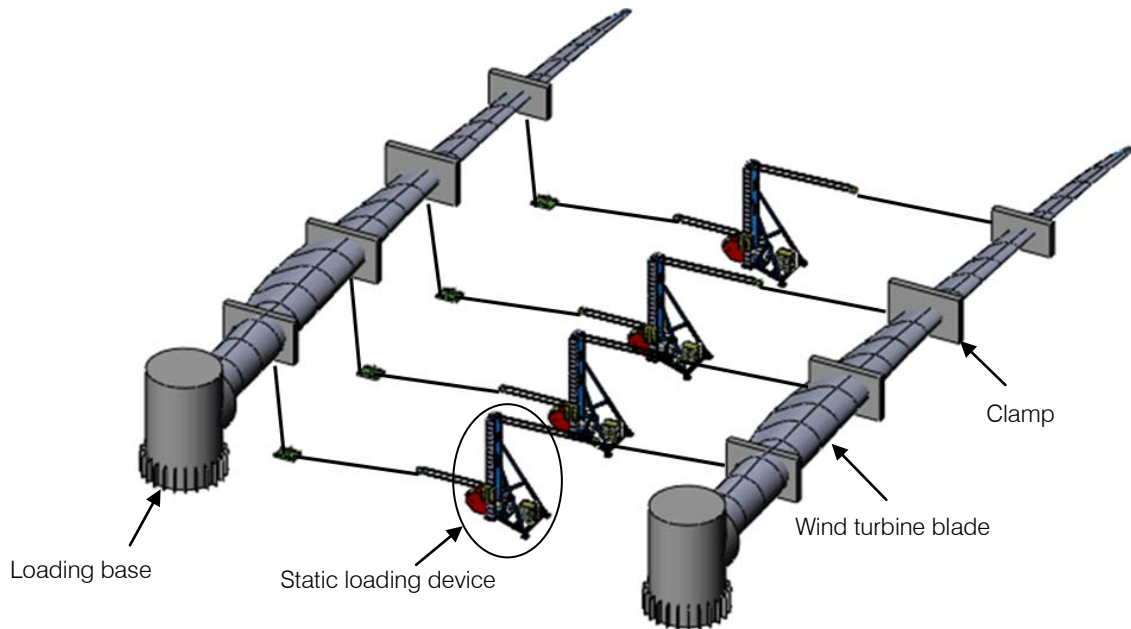


Fig. 1: Wind turbine blade full-scale static loading scheme

Taking the flapwise direction of aeroblade2.5-57wind turbine blades as the controlled object, the static loading test is carried out with four nodes. The four loading position are 14, 26, 32 and 40m, respectively

along the spanwise direction of the blade. The loading force value of each node in the every stage is shown in Table 1.

Table 1: Load value at flapwise direction

Load Step	13.0m	24.0m	33.0m	46.0m
40% up/KN	37.85	39.07	27.34	53.09
60% up/KN	56.78	58.24	40.42	79.98
80% up/KN	75.71	78.13	52.78	106.87
100%/KN	94.63	97.60	67.76	134.47

The finite element model of the blade under the above load is constructed in order to compare with the test results. The deformation of the blade under the above load is shown in Fig. 2. Take the 100% stage for

example, the three-dimensional deflection simulation of the blade along the Span of 28m, 42m, 57 m are shown in Table 2.

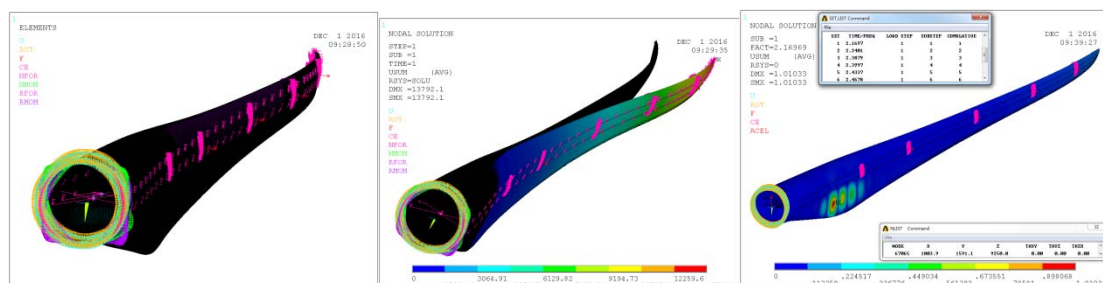


Fig. 2: Wind turbine blade deformation of finite element model

Table 2: Three-dimensional deflection simulation results

Location	28m	42m	57m
x direction/m	0.258	1.015	5.045
y direction/m	0.143	0.305	1.256
z direction/m	2.431	6.045	17.032

III. THREE-DIMENSIONAL MEASUREMENT MATHEMATICAL MODEL

Three-dimensional deformation system is established. The four-node static loading test is carried out by using the horizontal loading method, which is shown in Fig. 3. PLC controller is applied to the static

load scheme. In the measurement scheme, the blade tip is the measured point, under which three rope-type displacement sensors are fixed, and the sensor is fixed at the measured point, and finally the signal is transmitted to the monitoring system for data calculation and collection.

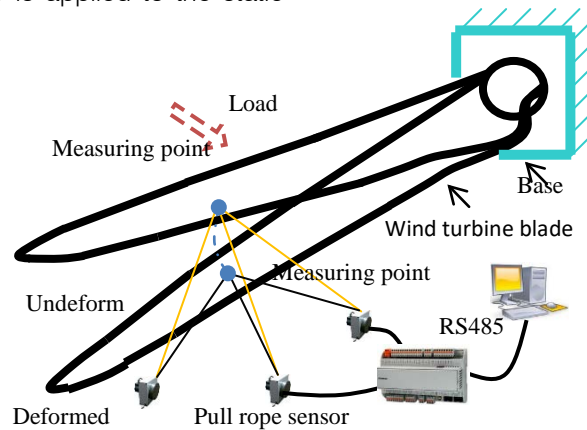


Fig. 3: The measurement scheme

After selecting the coordination control algorithm, in order to make accurate measurement of the displacement in the three-dimensional space, it is necessary to establish a suitable three-dimensional space measurement model. Firstly, set up the three-dimensional coordinate system xyz , the measured point is recorded as o , the deformation of the location is recorded as o' . Then determine the location of the three sensors in the space coordinate system, so that points a, b, c for the three sensor position, before the test to measure the fixed distance between the three sensors, recorded as: ab, bc, ac . Determine the measured points, then measured the elongation of three pull rope

sensors', recorded as: oa, ob, oc . After applying a static load to the blade, the current measured value of the sensor is collected and recorded as: $o'a, o'b, o'c$. From the point o to the line ab for the vertical line oc' , to a point c' , from the point o to the bottom of the vertical line $o'd$, to a point d . From the point d to the line ab for the vertical line dn , to a point n . Nc' is the precise deformation of the measured point o in the x direction, $o'd-oc'$ is the precise deformation amount in the y direction, dn is the precise deformation amount in the z direction, and the deformation of spatial structure is shown in Fig.4. Respectively, connect $ad, bd, cd, c'd$, the specific calculation steps are as follows:

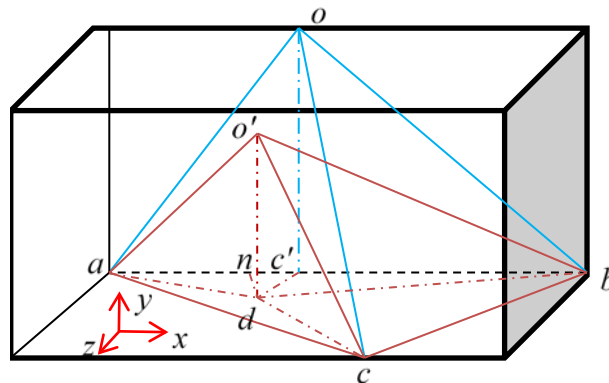


Fig. 4: Space deformation of measured point

Step 1: According to the Euler tetrahedron theory, the volume of tetrahedron $oabc$ and $o'abc$ (Respectively before and after deformation is recorded as V_1 and V_2) is expressed as:

$$V_1 = \frac{1}{12} (4oa^2ob^2oc^2 + (oa^2 + ob^2 - ab^2) \times (oa^2 + oc^2 - ac^2) \times (oc^2 + ob^2 - cb^2) - oc^2(oa^2 + ob^2 - ab^2)^2 - oa^2(oc^2 + ob^2 - cb^2)^2 - ob^2(oa^2 + oc^2 - ac^2)^2)^{1/2} \quad (1)$$

$$V_2 = \frac{1}{12} (4o'a^2o'b^2o'c^2 + (o'a^2 + o'b^2 - a'b^2) \times (o'a^2 + o'c^2 - a'c^2) \times (o'c^2 + o'b^2 - c'b^2) - o'c^2(o'a^2 + o'b^2 - a'b^2)^2 - o'a^2(o'c^2 + o'b^2 - c'b^2)^2 - o'b^2(o'a^2 + o'c^2 - a'c^2)^2)^{1/2} \quad (2)$$

Step 2: The circumference of $\triangle abc$ is recorded as d_1 , according to Helen formula the area of $\triangle abc$ is recorded as S_1 :

$$d_1 = ac + bc + ab \quad (3)$$

$$S_1 = \sqrt{\frac{d_1}{2} \left(\frac{d_1}{2} - ac \right) \left(\frac{d_1}{2} - ab \right) \left(\frac{d_1}{2} - bc \right)} \quad (4)$$

Step 3: Find the height of oc' and $o'd$ from the tetrahedral quadrature formula:

$$oc' = \frac{3V_1}{S_1} \quad (5)$$

$$o'd = \frac{3V_2}{S_1} \quad (6)$$

Step 4: From the formula (8) to calculate the measured point o in the y direction of the precise change:

$$\Delta y = oc' - o'd \quad (7)$$

Step 5: Calculating the length of the $c'b$ in the $Rt\triangle o'bc$:

$$c'b = \sqrt{ob^2 - oc'^2} \quad (8)$$

Calculating the length of the db in the $Rt\triangle o'db$:

$$db = \sqrt{o'b^2 - o'd^2} \quad (9)$$

Calculating the length of the dc in the $Rt\triangle o'c$:

$$dc = \sqrt{o'c^2 - o'd^2} \quad (10)$$

Calculating the length of the ad in the $Rt\triangle o'a$:

$$ad = \sqrt{oa'^2 - o'd^2} \quad (11)$$

Step 6: Calculating the perimeter d_2 and d_3 of $\triangle adc$ and $\triangle dbc$:

$$d_2 = ad + dc + ac \quad (12)$$

$$d_3 = dc + db + bc \quad (13)$$

Step 7: According to the Helen formula, the areas S_2 and S_3 of $\triangle adc$ and $\triangle dbc$ are expressed as:

$$S_2 = \sqrt{\frac{d_2}{2}(\frac{d_2}{2} - ac)(\frac{d_2}{2} - dc)(\frac{d_2}{2} - ad)} \quad (14)$$

$$S_3 = \sqrt{\frac{d_3}{3}(\frac{d_3}{3} - bc)(\frac{d_3}{3} - bd)(\frac{d_3}{3} - dc)} \quad (15)$$

Step 8: According to the formula (17) and (18), the area S_4 of the $\triangle adb$ is expressed as:

$$S_4 = S_1 - S_2 - S_3 \quad (16)$$

$$S_4 = \frac{1}{2}ab \times dn \quad (17)$$

Step 9: Common formula (17) and (18), find the value of dn , you can calculate the measured point o in the z direction of the precise deformation:

$$\Delta z = dn = \frac{2S_4}{ab} \quad (18)$$

Step 10: Calculating the length of nb in the $Rt\triangle dnb$:

$$nb = \sqrt{db^2 - nd^2} \quad (19)$$

Step 11: Common formula (21), find the value of nc , you can calculate the measured point o in the x direction of the precise deformation:

$$\Delta x = nc' = nb - bc' \quad (20)$$

IV. TEST VERIFICATION

a) Loading test

The LZ2.5-57-V4 blade is the main beam of glass fiber and the structure of double web. The main girder is 830mm wide and high modulus unidirectional cloth, and the shell skin is made of multi axial fiber cloth, sandwiched sandwich structure of Balsa and PVC, which can effectively provide the buckling resistance of the shell. The blade is a marine wind turbine, which is resistant to typhoon.

According to the above measurement scheme, this paper developed a space trajectory measurement system based on the mathematical model which is constructed above. The system consists of three pull rope type displacement sensors (Range: 0-30m, 4-20mA current output) and PLC analog acquisition module, the monitoring interface using software (MCGS) to configure. The pull rope type displacement sensor will transmit the analog signal to the PLC controller. The control system will get the precise deflection value after the mathematical operation, and will be transmitted to the man-machine interface through the RS485 Bus, which is shown in Fig. 5. Take the blade tip as an example, the test site is shown in Fig. 6. Three pull rope type displacement sensors were fixed on the ground, and the active ends of the three ropes were connected to the tip of blade. Test parameters were shown in Table.3.

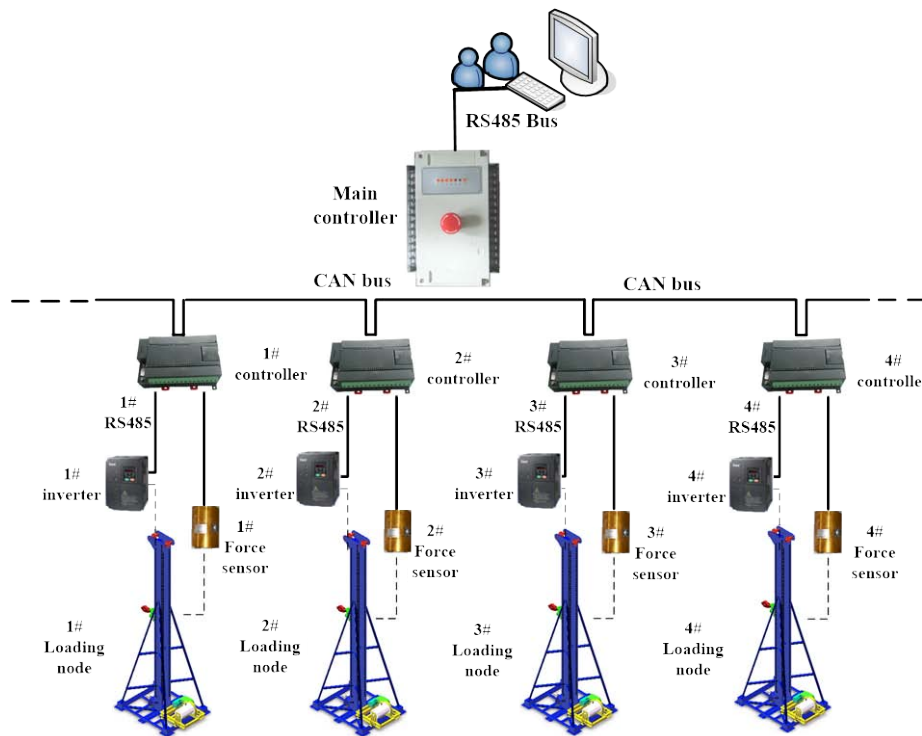


Fig. 5: Control scheme



Fig. 6: Static loading test

Table 3: Test parameter

Parameter	Value
Blade rated power /MW	2.5
Blade length/m	57
Number of loading nodes/ea	4
Tension sensor model	DBSL-25T
Maximum capacity of loading nodes/KN	250
Room temperature/°C	29
Humidity/RH	56

b) Result analysis

In the process of static loading, the blade produces irregular space torsion, and all of them have deformation in three directions. Under the action of the above static load, the deflection measurement of the four stages in the static test of the blade is carried out respectively. The test results are shown in Fig. 7(a). At

the same time, compared with the experimental results of the previous finite element simulation, the error obtained is shown in Fig. 7 (b).

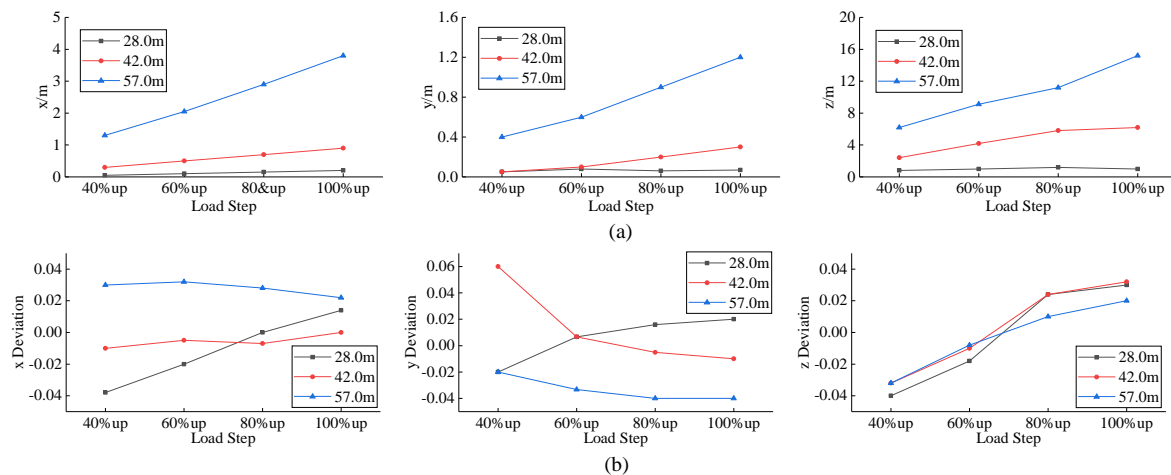


Fig. 7: Relative deviation of deflections for all load levels

From Fig. 7, it can be found that the blade has deflection in three directions. With the increase of loading load, the trend is increasing. By comparing the results of the finite element calculation with the test, the error of three directions is only 4.1%, 3.8% and 4.3%, which verifies the accuracy of the mathematical model.

V. CONCLUSION

There are complex nonlinear and strong coupling characteristics under the wind turbine blade full-scale static test. The deflection is used as a key parameter to check whether the blade is qualified. At present, the measurement of its deflection is usually done with a rope sensor or laser range finder, this traditional method is not only poor precision, but also get the deflection change of a single direction. In this paper, a precise mathematical model of the three-dimensional deflection of the blade is developed, and then the experimental verification is carried out, and the following conclusions are obtained.

1. Using three pull rope type displacement sensors and spatial geometric transformation method, a mathematical model of precision spatial deflection is deduced, which can calculate the accurate deflection change in three directions at the same time.
2. Based on the mathematical model, a set of spatial deflection measurement system was developed. The blade tip change which in a certain type of wind turbine blade static test as a testing object, and the tip system was measured by the measuring system. The results show that the system can track the spatial trajectory of the blade tip, and the data acquisition result is stable and accurate. In addition, since the rope sensor has been stretched during the test, it does not produce severe jitter and improves the stability of the test results.
3. The mathematical model and system can not only measure the irregular torsion caused by the static

test of wind power blade, but also apply to the space deformation measurement of irregular parts such as cantilever beam, which has extremely wide application prospect of engineering application.

It was successfully applied to the full-scale static test of four nodes wind turbine blade. The above research results can provide a solid theoretical basis and detailed experimental data for the next step of blade re-design, which has great engineering application value.

ACKNOWLEDGMENTS

This work was supported by National Key R&D Program of China (grant number 2018YFB1501203), Natural Science Foundation of Shandong Province, China (grant number ZR2019MEE076) and A Project of Shandong Province Higher Educational Science and Technology Program (grant number 2019KJB013).

REFERENCES RÉFÉRENCES REFERENCIAS

1. Chen, X., Zhao, W., Zhao, X. L., & Xu, J. Z. (2014). Failure test and finite element simulation of a large wind turbine composite blade under static loading. *Energies*, 7(4), 2274-2297.
2. Kong, C., Bang, J., & Sugiyama, Y. (2005). Structural investigation of composite wind turbine blade considering various load cases and fatigue life. *Energy*, 30(11-12), 2101-2114.
3. Lee, H. G., Kang, M. G., & Park, J. (2015). Fatigue failure of a composite wind turbine blade at its root end. *Composite Structures*, 133, 878-885.
4. Kezhong, S., Xiaolu, Z., & Jianzhong, X. (2011). Research on fatigue test of large horizontal axis wind turbine blade [J]. *Acta Energiæ Solaris Sinica*, 32(8), 1264-1268.
5. Liu, D., Dai, J., Hu, Y., & Shen, X. (2013). Status and development trends of modern large-scale wind turbines. *Zhongguo Jixie Gongcheng (China Mechanical Engineering)*, 24(1), 125-135.

6. Lloyd, G. (2003). Rules and regulations IV-Non-marine technology, Part 1. Wind Energy.
7. FERNÁNDEZ R, B. E. N. I. T. O., & Hedrick, J. K. (1987). Control of multivariable non-linear systems by the sliding mode method. *International Journal of Control*, 46(3), 1019-1040.
8. Hua, M., Hu, H., Xing, Y., & He, Z. (2011). Distributed control for AC motor drive inverters in parallel operation. *IEEE Transactions on Industrial Electronics*, 58(12), 5361-5370.
9. Zhou, H. F., Dou, H. Y., Qin, L. Z., Chen, Y., Ni, Y. Q., & Ko, J. M. (2014). A review of full-scale structural testing of wind turbine blades. *Renewable and Sustainable Energy Reviews*, 33, 177-187.
10. Li, R., Ge, P., Zhou, J. (2013). Research of structure test based on the large load/deformation turbine blade [J]. *Structure & Environment Engineering*, 40(5), 53-56.





Optimized Mesh-free Analysis for the Singularity Subtraction Technique of Linear Elastic Fracture Mechanics

By Tiago Oliveira & Artur Portela

University of Brasília

Abstract- In linear elastic fracture mechanics, the stress field is singular at the tip of a crack. Since the representation of this singularity in a numerical model raises considerable numerical difficulties, the paper uses a strategy that regularizes the elastic field, subtracting the singularity from the stress field, known as the singularity subtraction technique (SST). In this paper, the SST is implemented in a local mesh-free numerical model, coupled with modern optimization schemes, used for solving twodimensional problems of the linear elastic fracture mechanics.

The mesh-free numerical model (ILMF) considers the approximation of the elastic field with moving least squares (MLS) and implements a reduced numerical integration. Since the ILMF model implements the singularity subtraction technique that performs a regularization of the stress field, the mesh-free analysis does not require a refined discretization to obtain accurate results and therefore, is a very efficient numerical analysis.

Keywords: *local mesh-free, singularity subtraction technique, stress intensity factors and genetic algorithm.*

GJRE-I Classification: *FOR Code: 010301p*



Strictly as per the compliance and regulations of:



Optimized Mesh-free Analysis for the Singularity Subtraction Technique of Linear Elastic Fracture Mechanics

Tiago Oliveira* ^α & Artur Portela ^ο

Abstract- In linear elastic fracture mechanics, the stress field is singular at the tip of a crack. Since the representation of this singularity in a numerical model raises considerable numerical difficulties, the paper uses a strategy that regularizes the elastic field, subtracting the singularity from the stress field, known as the singularity subtraction technique (SST). In this paper, the SST is implemented in a local mesh-free numerical model, coupled with modern optimization schemes, used for solving two-dimensional problems of the linear elastic fracture mechanics.

The mesh-free numerical model (ILMF) considers the approximation of the elastic field with moving least squares (MLS) and implements a reduced numerical integration. Since the ILMF model implements the singularity subtraction technique that performs a regularization of the stress field, the mesh-free analysis does not require a refined discretization to obtain accurate results and therefore, is a very efficient numerical analysis.

Mesh-free numerical methods control the accuracy and efficiency of the model through the size of compact supports, the size of integration domains and the distribution of nodes in the body, which are usually heuristically determined through an expensive and time consuming calibration effort. The leading innovation of this paper is the automatic definition of these parameters and the nodal distribution by means of a multi-objective optimization, based on genetic algorithms (GA), with reliable and efficient objective functions. The optimization scheme effectively automates the whole pre-processing phase of a numerical analysis with mesh-free methods.

Benchmark problems were analyzed to assess the accuracy and efficiency of the modeling strategy. The results presented in the paper are in perfect agreement with those of reference solutions and therefore, make reliable and robust this mesh-free numerical analysis, coupled with a multi-objective optimization, for linear elastic fracture mechanics problems.

Keywords: local mesh-free, singularity subtraction technique, stress intensity factors and genetic algorithm.

1. INTRODUCTION

In a linear elastic analysis, it is well known that, at the tip of a crack the stress field becomes infinite and thus, is singular. The strength of this singularity is measured by the SIF that is thus defined at the crack tip. The presence of the stress singularity in the numerical model raises considerable numerical difficulties, by virtue of the need of simultaneously representing the singular and the finite stresses in the numerical model. Instead of representing the stress singularity in the numerical model, Oliveira and Portela [26] used an elegant strategy that subtracts the singularity from the elastic field which is known as the singularity subtraction technique (SST). Hence, the SST performs a regularization of the stress field, which introduces the SIF as primary unknowns of the numerical method used in the analysis. These two features, which are the analysis of the regularized stress field and the direct computation of SIF, make very efficient the SST solution strategy. The paper considers the SST, a very efficient and accurate technique for solving two-dimensional problems of linear elastic fracture mechanics, as reported by Oliveira et al. [27], implemented in the ILMF mesh-free model of numerical analysis.

Mesh-free numerical methods eliminate the mesh of the discretization, an intrinsic feature of the finite element and finite difference numerical methods of the first-generation in computational mechanics. On the other hand, the development of the boundary element method, as a second-generation numerical method, was motivated by the reduction of the analysis dependency on the mesh discretization,

*Corresponding author ^α: Department of Civil and Environmental Engineering, Faculty of Technology, University of Brasília, Brasília-DF, 70910-900, Brasil. e-mail: tiago.antuney@gmail.com

Author ^ο: Department of Civil and Environmental Engineering, Faculty of Technology, University of Brasília, Brasília-DF, 70910-900, Brasil.

used only on the boundary of the domain. Mesh-free methods are third-generation numerical methods which consider only a nodal discretization and completely overcome the difficulties posed by the mesh of the first and second-generation numerical methods in computational mechanics. This paper considers a domain mesh-free method of analysis, with the MLS approximation of the elastic field, coupled with a multi-objective optimization process that automatically generates optimal nodal arrangements of the mesh-free discretization, to compute the SIF of two-dimensional linear elastic fracture mechanics problems.

Thorough reviews of mesh-free methods and their applications in science and engineering were recently presented by Chen et al. [6] and Huerta et al. [17]. The most popular of local mesh-free methods is the MLPG method, presented by Atluri and Zhu [2] to Atluri and Shen [1], which implements the MLS approximation. Other local mesh-free methods of reference are the LPIM method, see Liu and Gu [21] and the LRPIM method, see Liu et al. [22]. The ILMF linearly integrated local mesh-free method, presented by Oliveira et al. [27], performs a linear reduced integration, which leads to an increase of the solution accuracy with high efficiency.

Until now, the discretization process of local mesh-free methods has been heuristically implemented, which requires an expensive and time consuming calibration of the nodal arrangements or parameters of the discretization that refer to the size of the compact supports and the size of the integration domain of each node. This is a huge drawback since the definition of these discretization parameters is not unique and therefore cannot be easily implemented into an automatic process.

Some researchers tried to overcome the drawback of heuristically defined mesh-free discretization parameters, as is the case of Baradaran and Mahmoodabadi [4], Bagheri et al. [3] and Ebrahimnejad et al. [12]. The successful attempts of these authors required an analytical solution to be performed and therefore their modeling process is not efficient. Recently, Santana et al. [31] and Oliveira and Portela [26], presented a strategy that performs the optimization of the size of compact supports and the size of the local integration domain of given mesh-free nodal distributions.

Thus, there is room for the alternative modeling strategy of this paper, that is the automatic generation of optimal mesh-free parameters and nodal discretization, through an optimization process that completely overcomes the issues of the heuristic process of discretization. As a consequence, the modeling strategy of this paper ensures robustness, accuracy and efficiency of the analysis, features required to be able to make reliable statements in the high fidelity modeling of engineering applications.

The use of optimization has been applied in many different areas, such as elastostatics, see Denk et al. [10], Proos et al. [29] and Zolfagharian et al. [37], heat conduction, see Dede [8], Denk et al. [11], Gersborg-Hansen et al. [14] and Kim et al. [20], fluid mechanics, see Dede et al. [9], electrostatics, see Gupta et al. [15], or structural dynamics, see Kim et al. [20] and Proos et al. [29].

The field of optimization is expansive, and the choice of a suitable algorithm is highly problem dependent, as reported by Zingg et al. [36]. The *No free lunch theorems* for optimization, presented by Wolpert and Macready [35], suggests that different algorithms are better than others for particular classes of problems. The multi-objective optimization of mesh-free numerical models deals with two main difficulties. The first one concerns the number of optimal solutions, generated by competing goals, instead of a single optimal solution. The second difficulty regards the large and complex search space that cannot be dealt with classic optimization

methods. Consequently, to overcome these difficulties, non-gradient methods of optimization must be used, instead of classic methods. Evolutionary algorithms are non-gradient methods, quite robust in locating the global optimum, that do not require continuity or predictability over the design space. This paper considers the use of evolutionary genetic algorithms (GA), for the multi-objective optimization of nodal arrangements of the mesh-free discretization. GA perform a search and optimization procedure motivated by the principles of natural genetics and natural selection, originally proposed by Holland [16]. They are a robust and flexible approach that can be applied to a wide range of optimization problems, as reported for instance by Kelner and Leonard [19], McCall [23] and Ebrahimnejad et al. [12].

The paper organization is as follows. The modeling of the structural body and the local mesh-free method is presented in Section 2 that is followed by the implementation of the SST in the mesh-free formulation, presented in Section 3. Section 4 presents the multi-objective optimization implementation and algorithm formulation. Numerical results, obtained for benchmark problems, in order to illustrate the accuracy, efficiency and robustness of the strategies adopted in this work, are presented in Section 5. Finally, the concluding remarks are presented in Section 6.

II. MESH-FREE MODELING OF THE STRUCTURAL BODY

The local mesh-free numerical analysis of the structural body is carried out by the ILMF model presented by Oliveira et al. [27]. It is defined in a body with domain Ω and boundary $\Gamma = \Gamma_u \cup \Gamma_t$, with constrained displacements $\bar{\mathbf{u}}$ prescribed on the kinematic boundary Γ_u and loaded by an external system of distributed surface and body forces, with densities represented respectively by $\bar{\mathbf{t}}$, applied on the static boundary Γ_t , and \mathbf{b} , applied in Ω , as Figure 1 schematically represents. Assign to

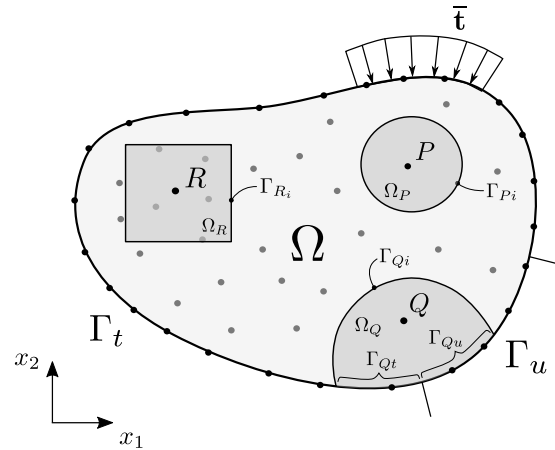


Figure 1: Mesh-free discretization of a body with domain Ω and boundary $\Gamma = \Gamma_u \cup \Gamma_t$; Ω_P , Ω_Q and Ω_R are local domains assigned to reference nodes P , Q and R ; Ω_Q has boundary $\Gamma_Q = \Gamma_{Qi} \cup \Gamma_{Qt} \cup \Gamma_{Qu}$, in which Γ_{Qi} is the interior local boundary and $\Gamma_{Qt} \in \Gamma_t$ and $\Gamma_{Qu} \in \Gamma_u$.

point Q an arbitrary local domain Ω_Q , such that $Q \in \Omega_Q \in \Omega \cup \Gamma$, with boundary $\Gamma_Q = \Gamma_{Qi} \cup \Gamma_{Qt} \cup \Gamma_{Qu}$, in which Γ_{Qi} is the interior local boundary and Γ_{Qt} and Γ_{Qu} are local boundaries that share respectively the global boundaries Γ_t and Γ_u , as Figure 1 schematically represents.

The work theorem is used to formulate the ILMF model. The mechanical equilibrium of the local domain Ω_Q can be defined through the rigid-body kinematic formulation of the work theorem, as presented by Oliveira et al. [27], which is

written, in the case of no body forces, as

$$\int_{\Gamma_Q - \Gamma_{Qt}} \mathbf{t} \, d\Gamma = - \int_{\Gamma_{Qt}} \bar{\mathbf{t}} \, d\Gamma \quad (1)$$

and describes the equilibrium of boundary tractions in Ω_Q . This equation, used to generate the stiffness matrix of each node of a mesh-free discretization, is integrated by Gauss quadrature. Finally, in order to allow for a unique solution of the elastic field, displacement boundary conditions must be enforced, on the kinematic boundary Γ_u , as

$$\mathbf{u} = \bar{\mathbf{u}}. \quad (2)$$

Since ILMF is a local model, each node of the discretization has assigned its local integration domain, as schematically represented in Figure 1, which has rectangular or circular shape, as Figure 2 schematically represents. Whenever a linear

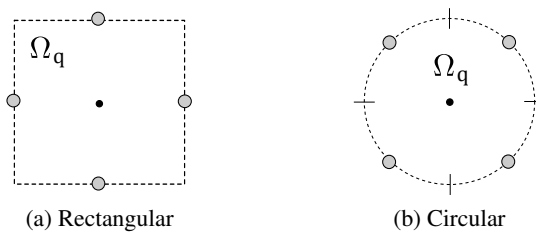


Figure 2: Schematic representation of local integration domains, with 1 integration point per boundary, or quadrant, of the local domain, for the computation of local equilibrium equations.

variation of tractions is defined, along each segment of the boundary of the local domain, equilibrium equations (1) can be exactly evaluated with 1 integration point, centered on each segment of the local boundary, as represented in Figure 2, which leads to a point-wise discrete form of mechanical equilibrium, represented by

$$\frac{L_i}{n_i} \sum_{j=1}^{n_i} \mathbf{t}_{\mathbf{x}_j} = - \frac{L_t}{n_t} \sum_{k=1}^{n_t} \bar{\mathbf{t}}_{\mathbf{x}_k}, \quad (3)$$

where the number of integration points, or segments, defined on, respectively the interior boundary $\Gamma_{Qi} = \Gamma_Q - \Gamma_{Qt} - \Gamma_{Qu}$, of length L_i , and the static boundary Γ_{Qt} , of length L_t , are denoted, respectively by n_i and n_t .

The MLS approximation of variables is used with the ILMF model. Therefore, traction components are evaluated in terms of the unknown nodal parameters $\hat{\mathbf{u}}$ and thus, equations (1) lead to the system of algebraic equations of the order $2 \times 2n$ (n is the number of nodes of the influence domain of the reference node Q), given by

$$\int_{\Gamma_Q - \Gamma_{Qt}} \mathbf{n} \mathbf{D} \mathbf{B} \, d\Gamma \hat{\mathbf{u}} = - \int_{\Gamma_{Qt}} \bar{\mathbf{t}} \, d\Gamma \quad (4)$$

represented by

$$\mathbf{K}_Q \hat{\mathbf{u}} = \mathbf{F}_Q, \quad (5)$$

in which \mathbf{K}_Q is the stiffness matrix

$$\mathbf{K}_Q = \int_{\Gamma_Q - \Gamma_{Qt}} \mathbf{n} \mathbf{D} \mathbf{B} \, d\Gamma \quad (6)$$

and \mathbf{F}_Q is the vector of forces

$$\mathbf{F}_Q = - \int_{\Gamma_{Qt}} \bar{\mathbf{t}} \, d\Gamma. \quad (7)$$

For a nodal arrangement with N nodes, in which M are interior and static-boundary nodes, the assembly of equations (5) leads to the system of equations of the order $2M \times 2N$

$$\mathbf{K} \hat{\mathbf{u}} = \mathbf{F}. \quad (8)$$

The remaining algebraic equations are generated from the $N - M$ kinematic-boundary nodes, through the direct interpolation of the boundary condition (2) prescribed as

$$\mathbf{u}_k = \Phi_k \hat{\mathbf{u}} = \bar{\mathbf{u}}_k, \quad (9)$$

with $k = 1, 2$, where $\bar{\mathbf{u}}_k$ is the constrained displacement component. Equations (9) are directly assembled into the global system (8).

For each node of a local mesh-free discretization there are two key parameters, respectively the size r_{Ω_s} of the compact support Ω_s and the size r_{Ω_q} of the local integration domain Ω_q that strongly affect the performance of the solution. For a generic node i , these parameters are defined through arbitrary constants, α_s and α_q , respectively as

$$r_{\Omega_s} = \alpha_s c_i \quad (10)$$

and

$$r_{\Omega_q} = \alpha_q c_i, \quad (11)$$

in which c_i is the distance of the node i to the nearest neighboring node. Equations (10) and (11) show that the accuracy of a mesh free numerical application can be controlled through a proper specification of the discretization parameters α_s and α_q .

It is important to enhance the different roles that these parameters play, in any numerical application. The size of the influence domain of a point, determined by the size of the compact support of each node, completely defines the number of nodes used to build MLS shape functions of that point. Consequently, the parameter α_s , sometimes referred to as MLS discretization parameter, is primarily linked to the accuracy of the numerical application. On the other hand, since the integration domain of each node is used to compute the respective nodal stiffness matrix, it must be entirely defined within the domain of the body, without intersecting the respective boundary. Consequently, the parameter α_q , sometimes referred to as the local domain parameter, is linked primarily to the efficiency of the application.

Until now, these parameters have been heuristically defined with values that depend on the pattern of the nodal distribution of each mesh-free application. When changes are made to the nodal distribution of a problem, these parameters also change, becoming an interactive process. In general, they have been considered in the range, respectively of $\alpha_s > 1.0$ and $\alpha_q < 1.0$, as reported by Oliveira et al.

[27]. In this paper, the appropriate values of α_s , α_q and the nodal distribution of nodes are obtained automatically, through a multi-objective optimization process.

III. THE SINGULARITY SUBTRACTION TECHNIQUE - SST

To overcome difficulties raised by the presence of unbounded stress in the numerical method, an alternative strategy which considers the subtraction of singularities from the original elastic field is used. The leading feature of this formulation is the regularization the elastic field, through the subtraction of the crack tip singularity from the original elastic field, which introduces the SIF as additional primary unknowns of the regularized numerical model.

a) Regularized Elastic Field

In the linear elastic fracture mechanics, the stress field is singular at a crack tip and therefore, it is convenient to modify the original problem before its solution by the ILMF numerical model. As the linear behavior allows the principle of superposition, the elastic field can be decomposed into a regular (R) and a singular (S) component as

$$\sigma_{ij} = (\sigma_{ij} - \sigma_{ij}^S) + \sigma_{ij}^S = \sigma_{ij}^R + \sigma_{ij}^S \quad (12)$$

and

$$u_i = (u_i - u_i^S) + u_i^S = u_i^R + u_i^S, \quad (13)$$

where $\sigma_{ij}^R = \sigma_{ij} - \sigma_{ij}^S$ and $u_i^R = u_i - u_i^S$ represent the regular parts, respectively of the stress and displacement of the initial problem; σ_{ij}^S and u_i^S denote, respectively the stress and displacement of a particular solution, of the initial problem, which represent the singular field. When suitable functions are used for the particular singular field, equations (12) and (13) regularize the initial problem, since the stress σ_{ij}^R become non-singular.

With this regularization, the analysis of the initial problem can be performed with the regular elastic field only, since the components σ_{ij}^S and u_i^S automatically satisfy the field equations identically, because they represent a particular solution of the initial problem. Therefore, the elasticity equations are written as

$$\mathbf{L}^T \boldsymbol{\sigma}^R = \mathbf{0} \quad (14)$$

$$\boldsymbol{\varepsilon}^R = \mathbf{L} \mathbf{u}^R \quad (15)$$

$$\boldsymbol{\sigma}^R = \mathbf{D} \boldsymbol{\varepsilon}^R \quad (16)$$

in domain Ω , with boundary conditions

$$\mathbf{u}^R = \bar{\mathbf{u}} - \mathbf{u}^S \quad \text{on } \Gamma_u \quad (17)$$

and

$$\mathbf{t}^R = \bar{\mathbf{t}} - \mathbf{t}^S \quad \text{on } \Gamma_t. \quad (18)$$

Note that the boundary conditions (17) and (18) include additional terms, respectively \mathbf{u}^S and \mathbf{t}^S , components of a singular particular solution of the initial problem.

b) William's Singular Solution

Components σ_{ij}^S and u_i^S of the particular solution, used in equations (12) and (13), represent the singular field around the crack tip, which can be defined through the first term of the William's [34] eigen-expansion, derived for a semi-infinite edge crack. The stress components are

$$\sigma_{11}^S = \frac{K_I}{\sqrt{2\pi r}} \cos \frac{\theta}{2} \left(1 - \sin \frac{\theta}{2} \sin \frac{3\theta}{2} \right) + \frac{K_{II}}{\sqrt{2\pi r}} \sin \frac{\theta}{2} \left(2 + \cos \frac{\theta}{2} \cos \frac{3\theta}{2} \right), \quad (19)$$

$$\sigma_{22}^S = \frac{K_I}{\sqrt{2\pi r}} \cos \frac{\theta}{2} \left(1 + \sin \frac{\theta}{2} \sin \frac{3\theta}{2} \right) - \frac{K_{II}}{\sqrt{2\pi r}} \sin \frac{\theta}{2} \cos \frac{\theta}{2} \cos \frac{3\theta}{2} \quad (20)$$

and

$$\sigma_{12}^S = \frac{K_I}{\sqrt{2\pi r}} \cos \frac{\theta}{2} \sin \frac{\theta}{2} \cos \frac{3\theta}{2} + \frac{K_{II}}{\sqrt{2\pi r}} \cos \frac{\theta}{2} \left(1 - \sin \frac{\theta}{2} \sin \frac{3\theta}{2} \right) \quad (21)$$

and the displacements are

$$u_1^S = \frac{K_I}{4\mu} \sqrt{\frac{r}{2\pi}} \left[(2\kappa - 1) \cos \frac{\theta}{2} - \cos \frac{3\theta}{2} \right] + \frac{K_{II}}{4\mu} \sqrt{\frac{r}{2\pi}} \left[(2\kappa + 3) \sin \frac{\theta}{2} + \sin \frac{3\theta}{2} \right] \quad (22)$$

and

$$u_2^S = \frac{K_I}{4\mu} \sqrt{\frac{r}{2\pi}} \left[(2\kappa + 1) \sin \frac{\theta}{2} - \sin \frac{3\theta}{2} \right] + \frac{K_{II}}{4\mu} \sqrt{\frac{r}{2\pi}} \left[(2\kappa - 3) \cos \frac{\theta}{2} + \cos \frac{3\theta}{2} \right], \quad (23)$$

where K_I and K_{II} represent the SIF, respectively of the opening and sliding modes; the constant $\kappa = 3 - 4\nu$ is defined for plain strain and $\kappa = (3 - \nu)/(1 + \nu)$ for plain stress, in which ν is Poisson's ratio; the constant μ is the shear modulus. A polar coordinate reference system (r, θ) , centered at the crack tip, is defined such that $\theta = 0$ is the crack axis, ahead of the crack tip. Note that the order $r^{-1/2}$ of the stress field becomes singular when r tends to zero. Caicedo and Portela [5] demonstrated that the first term of the William's eigen-expansion, derived for an edge crack, can also be used to represent the elastic field around the crack-tip, for the case of internal piecewise-flat multi-cracked finite plates, under mixed-mode deformation.

At a boundary point, the singular stress components, of equations (19) to (21), are used in the definition of traction components as

$$\mathbf{t}^S = \begin{bmatrix} t_1^S \\ t_2^S \end{bmatrix} = \begin{bmatrix} \sigma_{11}^S & \sigma_{21}^S \\ \sigma_{12}^S & \sigma_{22}^S \end{bmatrix} \begin{bmatrix} n_1 \\ n_2 \end{bmatrix} = \begin{bmatrix} g_{11} & g_{12} \\ g_{21} & g_{22} \end{bmatrix} \begin{bmatrix} K_I \\ K_{II} \end{bmatrix} = \mathbf{g} \mathbf{k}, \quad (24)$$

where n_i refers to the i -th component of the unit normal to the boundary, outwardly directed; functions $g_{ij} = g_{ij}(r^{-1/2}, \theta)$ were introduced for a simple notation of equations (19) to (21) and the vector \mathbf{k} contains the SIF components.

The displacement field, of equations (22) and (23), can be similarly defined in a vector form as

$$\mathbf{u}^S = \begin{bmatrix} u_1^S \\ u_2^S \end{bmatrix} = \begin{bmatrix} f_{11} & f_{12} \\ f_{21} & f_{22} \end{bmatrix} \begin{bmatrix} K_I \\ K_{II} \end{bmatrix} = \mathbf{f} \mathbf{k}, \quad (25)$$

where functions $f_{ij} = f_{ij}(r^{1/2}, \theta)$ are a simple notation of equations (22) and (23).

c) *Mesh-Free Model Equations*

An approximate solution of the regularized problem, equations (14) to (16) with boundary conditions (17) and (18), obtained with the ILMF numerical model, is now considered.

The equilibrium equations (1), of the domain Ω_Q associated with the node $Q \in \Omega_Q \cup \Gamma_Q$, are now rewritten as

$$\int_{\Gamma_Q - \Gamma_{Qt}} \mathbf{t}^R d\Gamma = - \int_{\Gamma_{Qt}} (\bar{\mathbf{t}} - \mathbf{t}^S) d\Gamma, \quad (26)$$

in which the static boundary conditions (18), of the regularized problem, are considered. For a linear reduced integration, along each boundary segment of the local domain, equation (26) simply leads to

$$\frac{L_i}{n_i} \sum_{j=1}^{n_i} \mathbf{t}_{\mathbf{x}_j}^R = - \frac{L_t}{n_t} \sum_{k=1}^{n_t} \bar{\mathbf{t}}_{\mathbf{x}_k} + \int_{\Gamma_{Qt}} \mathbf{t}^S d\Gamma, \quad (27)$$

in which n_i and n_t denote the total number of integration points, or boundary segments, defined on, respectively the interior local boundary $\Gamma_{Qi} = \Gamma_Q - \Gamma_{Qt} - \Gamma_{Qu}$, with length L_i , and the local static boundary Γ_{Qt} , with length L_t .

Discretization of the local form (27) is done with the MLS approximation, see Oliveira *et al.* [25], in terms of the unknown nodal parameters $\hat{\mathbf{u}}^R$, which leads to the system of two linear algebraic equations

$$\frac{L_i}{n_i} \sum_{j=1}^{n_i} \mathbf{n}_{\mathbf{x}_j} \mathbf{D} \mathbf{B}_{\mathbf{x}_j} \hat{\mathbf{u}}^R = - \frac{L_t}{n_t} \sum_{k=1}^{n_t} \bar{\mathbf{t}}_{\mathbf{x}_k} + \int_{\Gamma_{Qt}} \mathbf{g} d\Gamma \quad \mathbf{k} \quad (28)$$

that can be written as

$$\mathbf{K}_Q \hat{\mathbf{u}}^R + \mathbf{G}_Q \mathbf{k} = \mathbf{F}_Q, \quad (29)$$

in which the stiffness matrix \mathbf{K}_Q , of the order $2 \times 2n$ (n is the number of nodes included in the influence domain of the node Q) is given by

$$\mathbf{K}_Q = \frac{L_i}{n_i} \sum_{j=1}^{n_i} \mathbf{n}_{\mathbf{x}_j} \mathbf{D} \mathbf{B}_{\mathbf{x}_j}, \quad (30)$$

matrix \mathbf{G}_Q , of the order 2×2 , computed from equations (24), is given by

$$\mathbf{G}_Q = - \int_{\Gamma_{Qt}} \mathbf{g} d\Gamma \quad (31)$$

and \mathbf{F}_Q is the force vector given by

$$\mathbf{F}_Q = - \frac{L_t}{n_t} \sum_{k=1}^{n_t} \bar{\mathbf{t}}_{\mathbf{x}_k}. \quad (32)$$

Note that, in the case of an interior node, matrix \mathbf{G}_Q and vector \mathbf{F}_Q are null. For a problem with N nodes, the assembly of equations equations (29) for all M interior and static-boundary nodes generates the global system of $2M \times (2N + 2)$ equations

$$\mathbf{K} \hat{\mathbf{u}}^R + \mathbf{G} \mathbf{k} = \mathbf{F}. \quad (33)$$



The $N - M$ kinematic-boundary nodes, are used to generate the remaining equations of the discretization, implementing the kinematic boundary conditions of the regularized problem, equations (17). Thus, for a kinematic-boundary node, the boundary conditions of the regularized problem are enforced by a direct interpolation method as

$$\mathbf{u}_k^R = \Phi_k \hat{\mathbf{u}}^R = \bar{\mathbf{u}}_k - \mathbf{u}_k^S = \bar{\mathbf{u}}_k - \mathbf{f}_k \mathbf{k}, \quad (34)$$

with $k = 1, 2$, where $\bar{\mathbf{u}}_k$ denotes the specified displacement component and $\mathbf{u}_k^S = \mathbf{f}_k \mathbf{k}$ is the displacement component of the singular solution, obtained from equations (25). For the sake of simplicity, equations (34) are written in the same form of equations (29), for a point Q , as

$$\mathbf{K}_{Q_k} \hat{\mathbf{u}}^R + \mathbf{G}_{Q_k} \mathbf{k} = \mathbf{F}_{Q_k}, \quad (35)$$

in which $\mathbf{K}_{Q_k} = \Phi_k$, while $\mathbf{G}_{Q_k} = \mathbf{f}_k$ and $\mathbf{F}_{Q_k} = \bar{\mathbf{u}}_k$. Local equations (35) are assembled into the global system of equations (33) which, after this operation, is written as

$$[\mathbf{K} \ \mathbf{G}] \begin{bmatrix} \hat{\mathbf{u}}^R \\ \mathbf{k} \end{bmatrix} = [\mathbf{F}], \quad (36)$$

in which \mathbf{K} is a matrix of the order $2N \times 2N$, \mathbf{G} is a matrix of the order $2N \times 2$ and \mathbf{F} is a vector of the order $2N$; the unknowns are the vector $\hat{\mathbf{u}}^R$, of the order $2N$, and the vector \mathbf{k} of the order 2. Note that this global system of equations introduce the SIF K_I and K_{II} , in the vector \mathbf{k} , as additional unknowns of the numerical method. Therefore, to have a well-posed problem, with a unique solution, it is necessary to specify additional constraint equations, one for each mode of deformation considered in the analysis. These additional constraint equations can be specified in two additional bottom rows in the system of equations (36).

d) Additional Constraints

The required additional constraints enforce the singularity cancellation in the regularized problem and can be implemented by the cancellation of the regular regular stress components, as

$$\sigma_{ij}^R = 0 \Rightarrow \sigma_{ij} = \sigma_{ij}^S \quad (37)$$

which ensure that, at the crack tip, the initial problem is singular.

In order to be effective, the additional constraints must be defined in terms of the unknown regularized nodal parameters of $\hat{\mathbf{u}}^R$. Conditions (37) can be redefined, in terms of the respective traction components at the crack tip, as

$$t_j^R = \sigma_{ij}^R n_i = 0 \Rightarrow t_j = t_j^S, \quad (38)$$

where n_i denotes the unit normal components of the crack faces. After the MLS approximation, conditions (38), defined at the crack tip \mathbf{x}_{tip} , are written as

$$\mathbf{t}_{\mathbf{x}_{tip}}^R = \mathbf{n}_{\mathbf{x}_{tip}} \mathbf{D} \mathbf{B}_{\mathbf{x}_{tip}} \hat{\mathbf{u}}^R = \mathbf{0}, \quad (39)$$

or

$$\mathbf{C} \hat{\mathbf{u}}^R = \mathbf{0}, \quad (40)$$

in which matrix $\mathbf{C} = \mathbf{n}_{\mathbf{x}_{tip}} \mathbf{D} \mathbf{B}_{\mathbf{x}_{tip}}$ and can now be included in the global system of equations (36), leading to the final system of equations of the order $(2N + 2) \times (2N + 2)$

$$\begin{bmatrix} \mathbf{K} & \mathbf{G} \\ \mathbf{C} & \mathbf{0} \end{bmatrix} \begin{bmatrix} \hat{\mathbf{u}}^R \\ \mathbf{k} \end{bmatrix} = \begin{bmatrix} \mathbf{F} \\ \mathbf{0} \end{bmatrix}, \quad (41)$$

which represents a generalized saddle point problem that can be solved, since the stiffness matrix \mathbf{K} , of the ILMF local mesh free model is always non singular, with very low condition numbers, as reported by Oliveira and Portela [26].

IV. MULTI-OBJECTIVE OPTIMIZATION OF THE MESH-FREE MODEL

The optimization literature contains the basic concepts and terminology required to carry out the optimization process presented in this work, here formally represented by Sawaragi et al. [32], Hwang and Masud [18], Ringuest [30] and Steuer [33].

Multi-objective optimization of the mesh-free model is carried out through an automated procedure that modifies the design or decision variables which are the mesh-free discretization parameters and the nodal distribution. Hence, the optimization process incrementally updates the design variables, carries out a mesh-free numerical analysis of the updated model and scans the results of each increment to check if an optimized solution has been reached. In this process, the objective functions define the goal of the optimization, while constraints keep within bounds the value of a design response. The goal of the optimization aims to minimize the objective functions by finding feasible solutions, which are arrangements of mesh-free discretization satisfying the constraints of the problem. It is important to note that the optimizer never deals with solution errors of the generated arrangements of the mesh-free model.

a) Genetic Algorithm Search Space and Decision Making

Genetic Algorithm (GA) belongs to a class of evolutionary algorithms, defined as a non-derivative global search heuristic, motivated by the principles of natural genetics and natural selection, presented by Holland [16]. GA is an optimization technique that can be applied to a wide range of problems, as seen in Kelner and Leonard [19] and McCall [23], and can also be applied to mesh-free methods, as seen in Bagheri et al. [3] and Ebrahimnejad et al. [12].

The GA keep a population of $\mathbf{P}(t)$ individuals, for generation t . Each of these individuals contain a potential solution to the posed problem that need to be evaluated and its fitness measured. Some of these individuals are randomly selected to undergo a stochastic transformation and become new individuals (genetic operation). Likewise natural genetics, this transformation can be a mutation, which creates new individuals by making changes in a single individual, or crossover, which creates new individuals by combining parts from two others. The offspring from this process, the new individuals $\mathbf{C}(t)$, are evaluated and its fitness measured. A new population is created after selecting the more fit individuals from the parent and the offspring population. In the end, after several generations, the algorithm converges to the best individual, which is a possible optimal or sub-optimal solution to the problem, as stated by Gen and Cheng [13].

The genetic algorithm components need to be carefully addressed in order to provide a good search space and exploit the best solution. A good balance between exploration and exploitation is a must for complex and real-world problems.

b) Design Variables

In a mesh-free discretization, the size of the compact support, where nodal shape functions are defined, and the size of the domain of integration, where the nodal stiffness matrix of the numerical model is computed, must be conveniently defined in any application, since their values strongly affect the performance of the numerical solution. Therefore, the values of the size of the compact support and the values of the size of the local integration domain, are optimized in this paper. They are

defined, respectively in Equations (10) and (11) which show that the accuracy of a mesh-free numerical application can be controlled through a proper specification of the discretization parameters α_s and α_q . Therefore, parameters α_s and α_q are both set as design variables of the multi-objective optimization process, in order to be automatically defined with optimal values.

Additionally, in order to facilitate and automate the pre-processing phase of the mesh-free modeling, the nodal distribution need to be addressed. Therefore, for a bi-dimensional problem, the number of divisions in x and y direction are chosen as design variables. When the number of divisions in both directions are provided, the mesh-free numerical model, can define the nodal coordinates and distribute the nodes along the problem domain and boundary, including crack nodes. For this case, only regular nodal distributions are considered.

c) Objective Functions

The use of efficient objective functions condition the overall performance of the multi-objective optimization process. The objective functions force, through mesh-free numerical simulation, the minimum total mechanical energy of the structure and the conditioning of the final system of algebraic equations which, consequently enforce the solution accuracy of the mesh-free model. Note that solution errors of the mesh-free model are not included in any of the objective functions which, therefore are quite general and do not depend on any analytical solution.

The standing challenge in the application of numerical simulations in the optimization process is the accurate evaluation of objective functions which obviously is dependent upon the automatically generated mesh-free discretization. Since multiple iterations are required during the optimization process, it is necessary to maintain a balance between efficiency and accuracy through constraints of the design variables.

i. Structural Compliance

The definition of this objective function results from the features of the parameter α_s in combination with α_q . Considering a body with the actual elastic field in any state, the strain energy U , and the potential energy P , of external forces, respectively given by

$$U = \int_{\Omega} \frac{1}{2} \boldsymbol{\sigma}^T \boldsymbol{\varepsilon} \, d\Omega \quad (42)$$

and

$$P = - \int_{\Gamma_t} \bar{\mathbf{t}}^T \mathbf{u} \, d\Gamma, \quad (43)$$

can be used to obtain the total potential energy T . The work theorem, when applied to the global domain of the body, for the actual elastic field settled in the body, leads to $P = -2U$ and therefore $T = -U$, as well as $T = P/2$. These results show that the minimum value of the total potential energy of the body corresponds to a minimum value of the potential energy P or a maximum value of the strain energy U .

The energy can be measure both by strain energy U or potential energy P , although evaluation of U is computationally more expensive, since requires the computation of the stress field for all nodal values and derivatives of shape functions. Therefore, the potential energy P is used instead, since it requires the evaluation of displacement fields only at static boundary nodes, the ones with no-null ap-

plied loads, and does not require the computation of derivatives of shape functions, which is computationally efficient in comparison.

Hence, the objective function can be defined with the structural compliance C , as

$$C = \frac{1}{2} \int_{\Gamma_t} \bar{\mathbf{t}}^T \mathbf{u} \, d\Gamma = -\frac{1}{2} P. \quad (44)$$

Consequently, the minimum value of the potential energy P corresponds to a maximum value of $-C$ that is equivalent to a minimum value of C .

d) Algorithm Formulation

The numerical problem optimization aims to minimize the objective function using the mesh-free numerical model, by finding optimum values for the design variables, in this case the geometrical parameters α_s , α_q and the nodal distribution, also satisfying the problem constraints.

The mathematical formulation of the multi-objective optimization scheme for linear elastic fracture mechanics problems is as follows

$$\begin{aligned} & \text{minimize} && C(\alpha_s, \alpha_q, \mathbf{n}_x, \mathbf{n}_y) \\ & && \text{CPU time}(\alpha_s, \alpha_q, \mathbf{n}_x, \mathbf{n}_y) \\ & \text{subject to} && \mathbf{e}(\alpha_s) = \alpha_s^{\min} \leq \alpha_s \leq \alpha_s^{\max} \\ & && \mathbf{e}(\alpha_q) = \alpha_q^{\min} \leq \alpha_q \leq \alpha_q^{\max} \\ & && \mathbf{e}(\mathbf{n}_x) = n_x^{\min} \leq n_x \leq n_x^{\max} \\ & && \mathbf{e}(\mathbf{n}_y) = n_y^{\min} \leq n_y \leq n_y^{\max} \\ & \text{where} && \alpha_s = (\alpha_{s1}, \alpha_{s2}, \dots, \alpha_{sn}) \in \alpha_s \\ & && \alpha_q = (\alpha_{q1}, \alpha_{q2}, \dots, \alpha_{qn}) \in \alpha_q \\ & && \mathbf{n}_x = (n_{x1}, n_{x2}, \dots, n_{xn}) \in (\mathbf{x}) \\ & && \mathbf{n}_y = (n_{y1}, n_{y2}, \dots, n_{yn}) \in (\mathbf{y}), \end{aligned} \quad (45)$$

in which C is the structural compliance, CPU time is the time required to generate and solve the global system of algebraic equations; $\alpha_s^{\min}/\alpha_q^{\min}$ and $\alpha_s^{\max}/\alpha_q^{\max}$ denote the minimum and the maximum allowable limits for the mesh free discretization parameters α_s and α_q , respectively. n^{\min}/n^{\max} denote the minimum and the maximum geometrical values for the number of divisions on both directions (x and y), limited by the geometrical constraint of the problem, for a regular nodal discretization of the posed problem. Therefore, the variable \mathbf{n} also determine the total number of nodes for the problem and node coordinates, automatically defined for a regular nodal distribution.

On this multi-objective optimization, the fitness function, that is the routine containing the mesh-free algorithm, define scalar values for α_s , α_q , n_x and n_y , yielding different objective function outputs. Since there are two objective functions, the Pareto front will be the final result of the optimization, which will provide non-dominant solutions.

The ILMF is the only mesh free method implemented in this paper, but this process can be easily applied to any desired local mesh free method. The whole optimization process is summarized in the flowchart presented in Figure 3.

V. NUMERICAL RESULTS

This section presents numerical results to demonstrate the accuracy and efficiency of the mesh-free numerical method with optimization, through different linear fracture mechanics problems previously presented by Oliveira and Portela [26].

For a regular mesh-free discretization of $n_x \times n_y$ nodes, the size of the local support Ω_s and the size of the local integration domain Ω_q , are respectively parameters α_s and α_q . Good results can be obtained with a mesh-free model if r_{Ω_s} , r_{Ω_q} and the arrangement of nodes are properly refined.

Usually, these parameters and the nodal distribution are heuristically defined. One key advantage of the ILMF modeling process is that it can provide appropriate

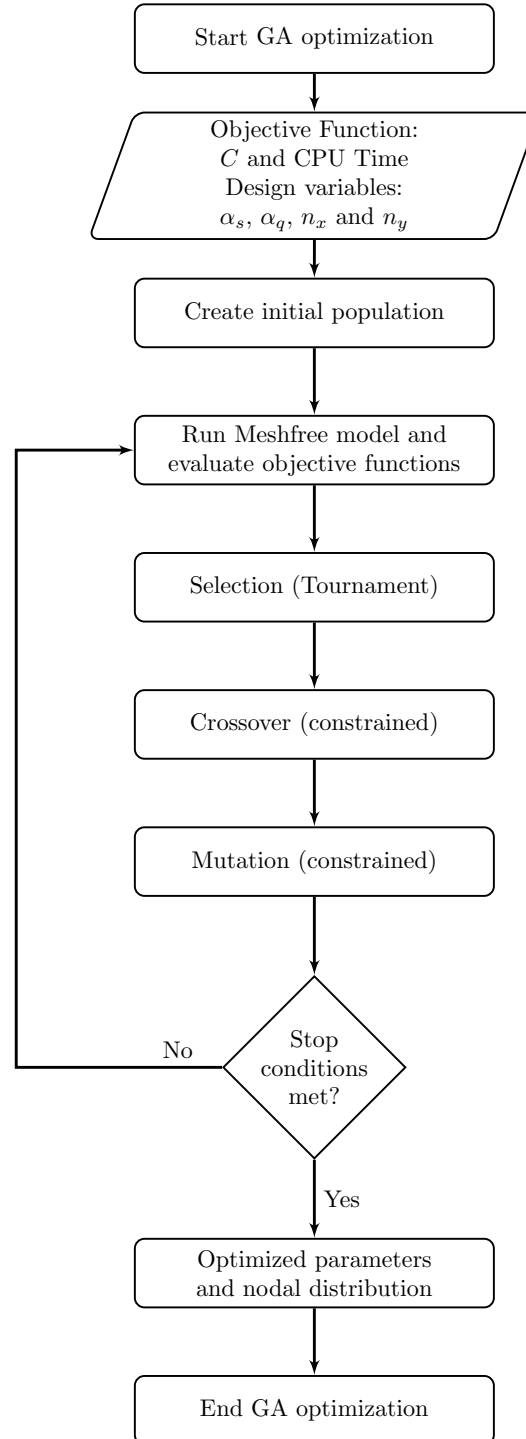


Figure 3: Flowchart of the multi-objective optimization scheme for mesh-free numerical methods.

values for α_s and α_q using genetic algorithms, as initially presented by Santana et al. [31], which greatly improves the model accuracy. Additionally, this work also optimize the nodal distribution, resulting in a fully automated optimization routine for the entire pre-processing phase of traditional numerical methods, which is the definition of the mesh.

a) *Edge-Cracked Plate*

Three cases of edge-cracked square plates, respectively under mode-I, mode-II and mixed-mode deformation are considered.

The discontinuity generated by the presence of the crack requires a special treatment in order to be carried out in this non-convex domain. Therefore, the crack faces are modeled with two lines of overlapping nodes, where the MLS approximation is acting only in their respective influence size, while the crack tip is modeled with one node that can influence both sides of the crack. The visibility criterion is implemented around the crack during the definition of the compact support of each node. Hence, the compact support and the local integration domain of each node of the crack faces are defined as in the case of a traction-free boundary node.

The size of the local integration domain of the crack tip node is defined as $\alpha_k = \alpha_q/2$, to ensure the local aspect of the discretization of the crack. The computation of matrices g and f , of the Williams' singular solution at each crack tip is carried out with Gaussian quadrature, with a single integration point.

The results obtained with the ILMF using the multi-objective optimization are compared with the results originally obtained by Oliveira and Portela [26], without optimization, and by Portela and Aliabadi [28], using the DBEM with the J-integral (J-DBEM) technique, which proved to be a very accurate method. The DBEM modeling strategy considers piecewise-straight cracks which are discretized with straight discontinuous quadratic boundary elements. Continuous quadratic boundary elements are used along the remaining boundaries of the problem, except at the intersection between a crack and an edge, where semi-discontinuous boundary elements are used on the edge. Self-point discontinuous boundary elements are integrated analytically, while Gaussian quadrature, with sub-element integration, is carried out for the remaining integrations.

The GA is set to minimize the Compliance C and CPU time or computational effort, chosen as objective functions for this optimization process. The design variables of the optimization, the number of nodes and the node coordinate are defined within the problem geometry, and the parameters $\alpha_s = 1.5 \sim 10$ and $\alpha_q = 0.1 \sim 0.9$, are defined as continuous in the intervals. Only the major computational cost that is the cost of generating and solving the global system of algebraic equations, was measured.

On this optimization scheme, the initial population is randomly generated according to the predefined population size of 25 individuals. Then, the fitness function is calculated for each member of the population and scaled using a rank process, which is used later in the selection process. The reproduction operator is implemented based on a tournament selection. Both mutation and crossover are constraint dependent. The genetic algorithm described above generates a stochastic values sequence of design variables which are evaluated through the objective functions. Finally, the optimization process is terminated if the number of generations exceeds the predefined maximum number, which is selected as 150 in this scheme, or if the average change in fitness function is less than 1×10^{-6} .

The improved accuracy of the optimization process can be clearly seen on this benchmark problem, regardless of the loading.

i. *Mode-I Loading*

A square edge-cracked plate, represented in Figure 4, is considered for the first analysis. The plate, with crack length a , width w and height $h = w/2$, is loaded

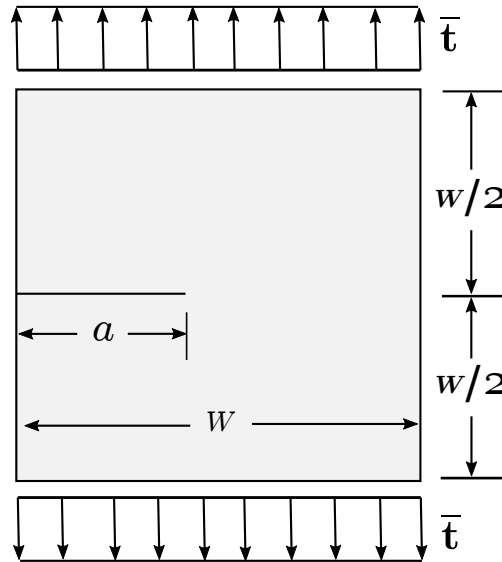


Figure 4: Square plate with a single edge crack under mode-I loading ($h/w = 0.5$).

by a uniform traction $\bar{t} = \sigma$, applied symmetrically at the ends. All the results presented are for $h/w = 0.5$, to be compared with the highly accurate values introduced by Civelek and Erdogan [7]. Therefore, five cases were considered, with $a/w = 0.2, 0.3, 0.4, 0.5$ and 0.6 .

The ILMF model was applied with rectangular local domains of integration, with discretization parameters and nodal configuration automatically defined through GA optimization. The MLS approximation considered a first-order polynomial basis with quartic spline weighting function. It is important to highlight that all nodal distributions were performed without considering any refinement of the discretization around the crack tip, always with regular distributions.

Figure 5 show the Pareto front obtained from the optimization process, containing all feasible solutions for the posed problem. From the frontier solutions,

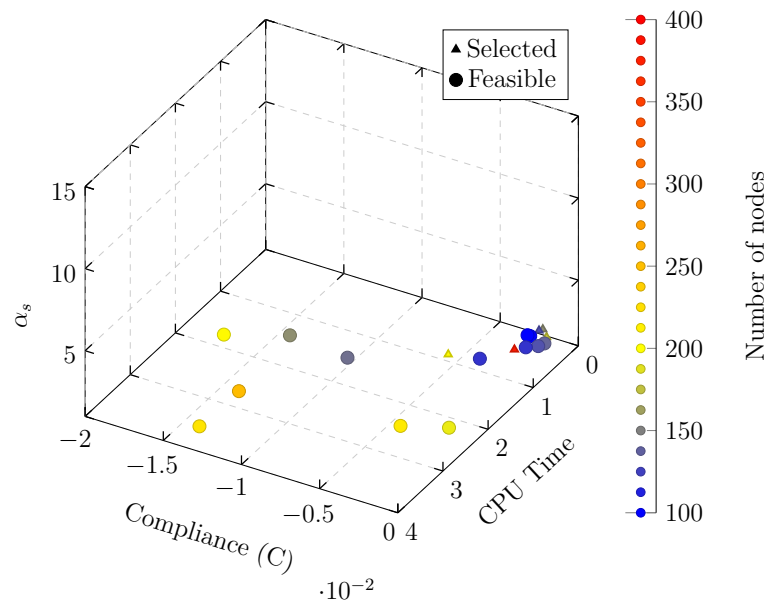


Figure 5: The multi-objective Pareto front of the square plate with a single edge crack under mode-I loading, for $a/w = 0.5$; ILMF with the automatic parameters optimization routine.

a set of solutions were selected and the results presented in Figure 6 and Table 1; where it can be seen that the optimization lead to accurate results for all points

Table 1: The multi-objective Pareto front results of selected feasible solutions for the square plate with a single edge crack under mode-I loading, for $a/w = 0.5$.

Index	CPU Time (s)	Compliance	$K_I/(\bar{t}\sqrt{\pi a})$	α_s	α_q	Nodes
1	0.15	-0.0016	3.534	1.440	0.670	179
2	2.19	-0.0020	3.045	5.459	0.195	203
3	1.07	-0.0010	3.010	3.2	0.505	379
4	0.13	-0.0019	3.010	1.778	0.125	155
5	0.11	-0.0022	3.367	1.563	0.604	131

in the Pareto front, with minimum values for compliance and SIF close to reference values. For this case, α_s greatly varies depending on the nodal distribution, but the best values for α_q are usually closer to 0.5. Table 2 show the results obtained for different a/w , where ILMF represents the values obtained in Oliveira and Portela [26], ILMF⁺ represents the values presented in this work using the optimization routine, Portela and Aliabadi [28] represents the values obtained with

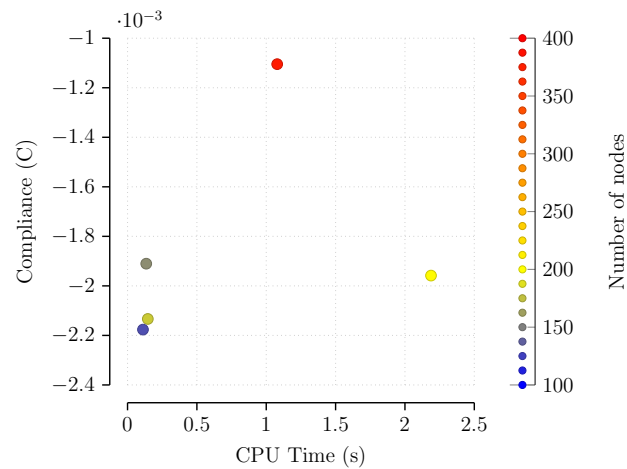


Figure 6: The multi-objective Pareto front of selected feasible solutions for a square plate with a single edge crack under mode-I loading ($a/w = 0.5$).

Table 2: Square plate with a single edge crack under mode-I loading.

a/w	$K_I/(\bar{t}\sqrt{\pi a})$				% Error	
	ILMF	ILMF ⁺	J-DBEM [28]	Reference [7]	ILMF ⁺	J-DBEM
0.2	1.520	1.488	1.495	1.488	9.672E-7	0.005
0.3	1.967	1.848	1.858	1.848	3.53E-6	0.005
0.4	2.413	2.324	2.338	2.324	3.93E-4	0.006
0.5	2.973	3.010	3.028	3.010	1.85E-4	0.006
0.6	3.991	4.152	4.184	4.152	3.12E-5	0.008

the J-integral implemented in the DBEM. Percentage errors are measured from the values of reference provided by Civelek and Erdogan [7]. In this analysis, the SIF values of the mode-II are always below 10^{-7} , since this is a mode-I loading crack problem.

The results highlight the accuracy of ILMF, which was further improved after the optimization process, always very close to reference values and J-DBEM. Even for similar nodal distributions as originally conceived, like index 1 of the Pareto front of selected solutions, the optimization of α_s was enough to improve the overall accuracy. The nodal distribution obtained by the GA optimization scheme and the respective deformed configuration of the plate is schematically represented in Figures 7 and 8.

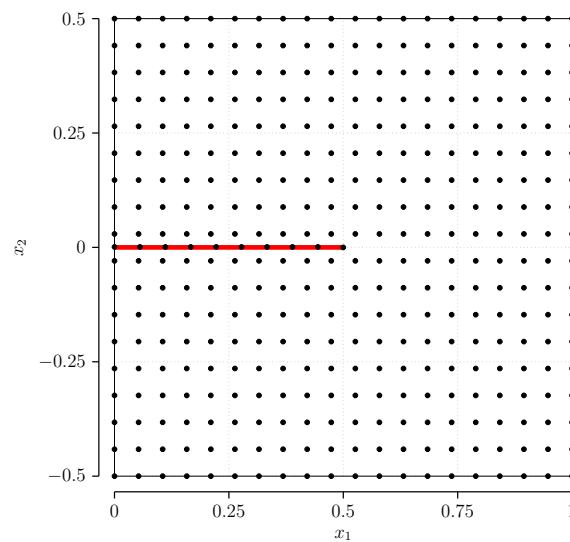


Figure 7: Regular nodal distribution resulting from the optimization scheme, with a regular nodal distribution of $20 \times 18 = 360$ nodes and additional overlapping nodes on the crack faces, for $a/w = 0.5$, under mode-II loading. The red line represents the crack faces.

ii. Mode-II Loading

A square edge-cracked plate, with ratio between the height and the width of the plate as $h/w = 0.5$, schematically represented in Figure 9, is considered for this analysis.

The plate is loaded with a uniform traction \bar{t} , parallel to the crack of length a and is applied anti-symmetrically on the sides which corresponds to a mode-II loading. There are no published benchmark results due to the complexity of the problem and, therefore, they are compared with the results obtained with the J-DBEM, using the software [28].

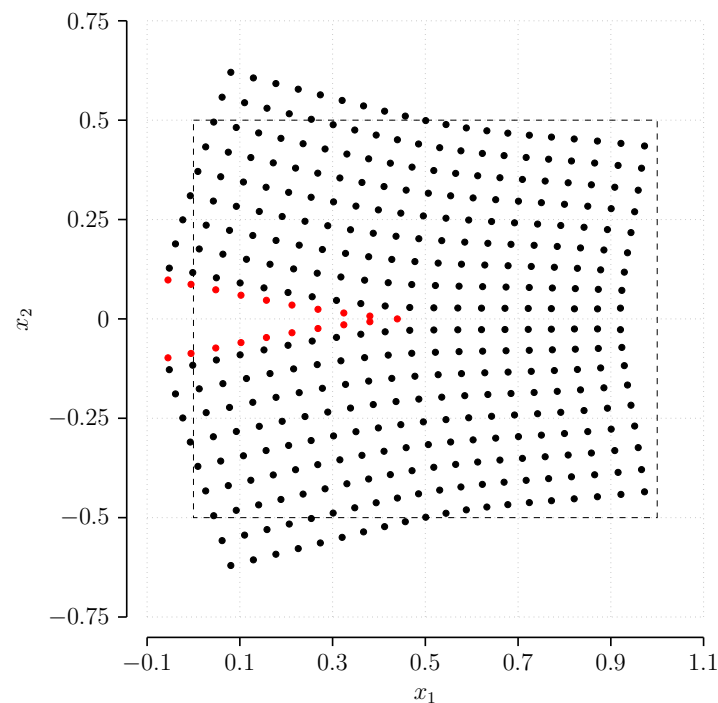


Figure 8: Deformed configuration of the plate resulting from the optimization scheme, for $a/w = 0.5$, under mode-I loading.

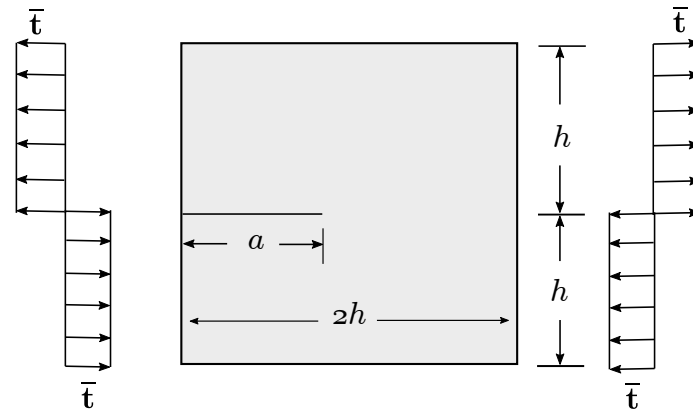


Figure 9: Square plate with a single edge crack under mode-II loading ($w = 2h$).

For this problem, five cases were considered, with corresponding ratios of $a/w = 0.2, 0.3, 0.4, 0.5$ and 0.6 . Rectangular local domains of integration, first-order polynomial basis and quartic spline weighting function are considered on the ILMF model. Like the previous problem, the regular nodal configuration and discretization parameters are automatically defined though GA optimization, without any special refinement around the crack tip.

The results obtained for this multi-objective optimization process are presented in Figure 10, Figure 11 and Table 3; with all point in the Pareto front leading to

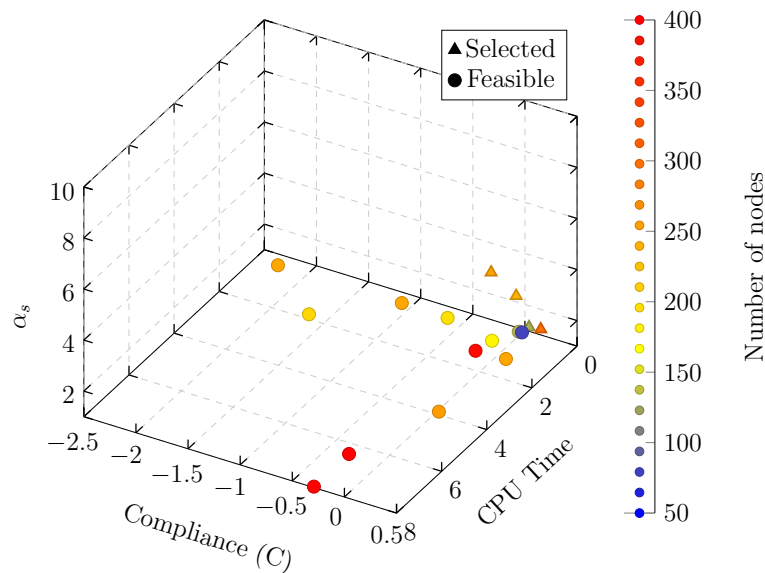


Figure 10: The multi-objective Pareto front of the square plate with a single edge crack under mode-II loading, for $a/w = 0.5$; ILMF with the automatic parameters optimization routine.

Table 3: The multi-objective Pareto front results of selected feasible solutions for the square plate with a single edge crack under mode-II loading ($a/w = 0.5$).

Index	CPU Time (s)	Compliance	$K_I/(\bar{t}\sqrt{\pi a})$	α_s	α_q	Nodes
1	0.394	9.87E-04	0.264	2.662	0.511	237
2	0.241	0.204	0.315	1.485	0.501	299
3	0.967	-0.115	0.281	3.903	0.503	251
4	0.886	0.791	0.231	3.885	0.828	359

accurate results and fast computations. It can be seen that SIF values are close to each other, depending on the minimum value of the compliance indicator. For this optimization, both α_s and α_q values are close to each other due to the similarity between nodal distributions obtained. Once more, $\alpha_q \approx 0.5$ and, for this case, $\alpha_s = 1.4 \sim 4$.

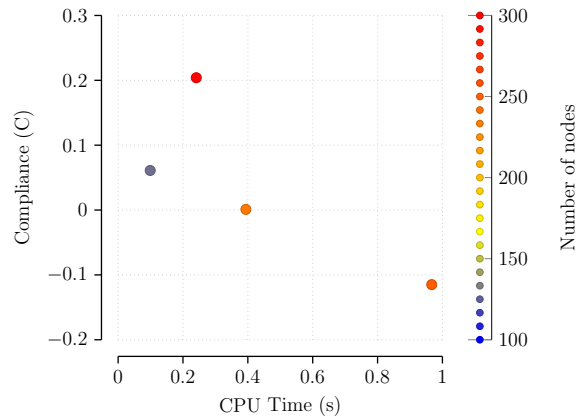


Figure 11: The multi-objective Pareto front of selected feasible solutions for a square plate with a single edge crack under mode-II loading ($a/w = 0.5$).

For different values of a/w , Table 4 show the results obtained from the anal-

Table 4: Square plate with a single edge crack under mode-II loading.

a/w	$K_I/(\bar{t}\sqrt{\pi a})$			% Error
	ILMF	ILMF ⁺	J-DBEM [28]	ILMF ⁺
0.2	0.416	0.436	0.435	0.00309
0.3	0.338	0.359	0.358	0.00360
0.4	0.296	0.309	0.304	0.01686
0.5	0.248	0.264	0.262	0.00932
0.6	0.218	0.224	0.223	0.00397

ysis. Percentage errors are measured from the values obtained with the J-integral implemented in the DBEM provided by Portela and Aliabadi [28]. In this problem, the SIF values obtained for the mode-I are always below 10^{-3} , since this is a mode-II crack problem.

Even though this problem is highly complex, accurate values were obtained after the optimization process, improving the previous results. The nodal distribution obtained by the GA optimization scheme and the respective deformed configuration of the plate is schematically represented in Figures 12 and 13.

iii. Mixed-Mode Loading

Consider now a plate with an edge slant crack, as represented in Figure 14 schematically, in mixed-mode deformation. The length of the crack is denoted by a , the width and height of the plate is denoted by w . The plate is loaded by a uniform traction $\bar{t} = \sigma$, applied symmetrically at the ends.

For this problem analysis, three cases were considered with corresponding ra-

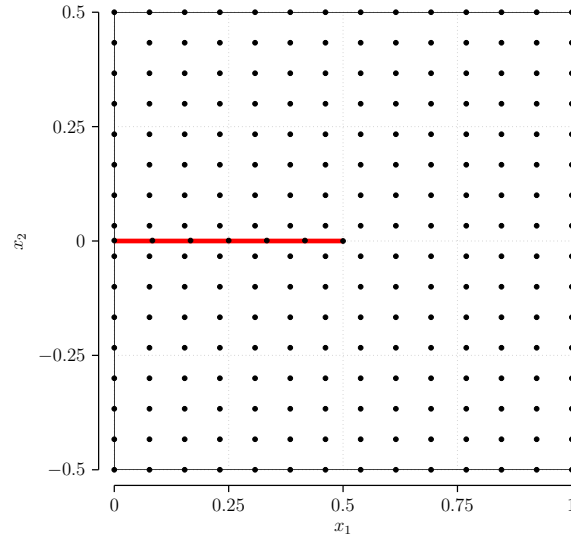


Figure 12: Regular nodal distribution resulting from the optimization scheme, with a regular nodal distribution of $14 \times 16 = 224$ nodes and additional overlapping nodes on the crack faces, for $a/w = 0.5$, under mode-II loading. The red line represents the crack faces.

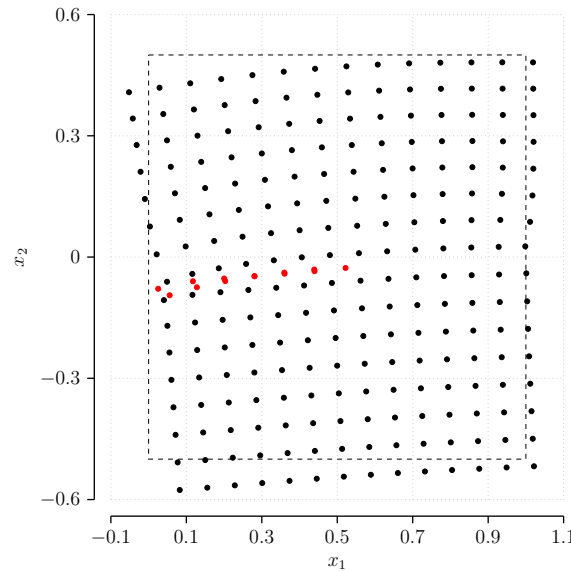


Figure 13: Deformed configuration of the plate resulting from the optimization scheme, for $a/w = 0.5$, under mode-II loading.

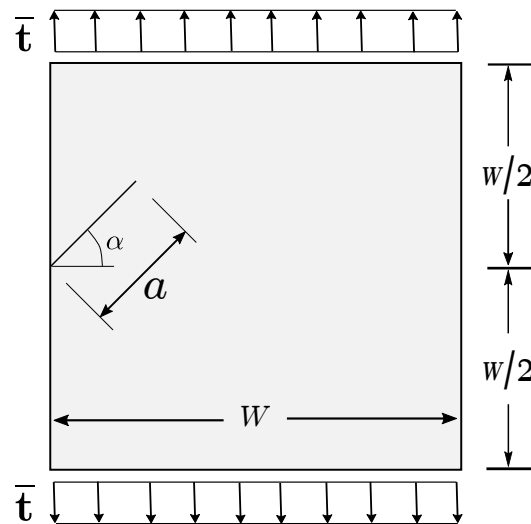


Figure 14: Square plate with an edge slant crack, under remote stress σ loading.

tios of $a/w = 0.2, 0.4$ and 0.6 , for $\alpha = 30^\circ$ and two cases, with corresponding ratios of $a/w = 0.2$ and 0.4 , for $\alpha = 60^\circ$, as originally presented by Murakami [24]. For MLS approximation of the elastic field, a first-order polynomial basis and a quartic spline weighting function were considered, along with rectangular local domains to perform the numerical integration of the ILMF model. The regular nodal configuration and discretization parameters are automatically defined though GA optimization, without any special refinement around the crack tip.

All the results presented are compared with the accurate values provided by Murakami [24] and Portela and Aliabadi [28]. The multi-objective optimization process resulted in the Pareto front of Figure 15, where all feasible solutions are presented. The selected multi-objective optimization are presented in Figure 16 and Tables 5 and 6; where a good accuracy can be seen related to minimum values

Table 5: The multi-objective Pareto front results of selected feasible solutions for the square plate with a single edge crack under mixed-mode loading, for $a/w = 0.4$ and $\alpha = 30^\circ$.

Ind.	CPU T.(s)	C	$K_I/(\bar{t}\sqrt{\pi a})$	$K_{II}/(\bar{t}\sqrt{\pi a})$	α_s	α_q	N.
1	3.08	2.48E-04	1.667	0.505	5.821	0.617	301
2	6.614	-4.68E-02	1.518	0.455	9.769	0.612	455
3	0.329	4.46E-04	1.645	0.494	2.753	0.916	203
4	5.744	-1.34E-04	1.937	0.587	6.56	0.499	331
5	1.437	2.54E-04	1.579	0.479	4.25	0.501	267

for compliance. For $\alpha = 30^\circ$, more point in the Pareto front were found when

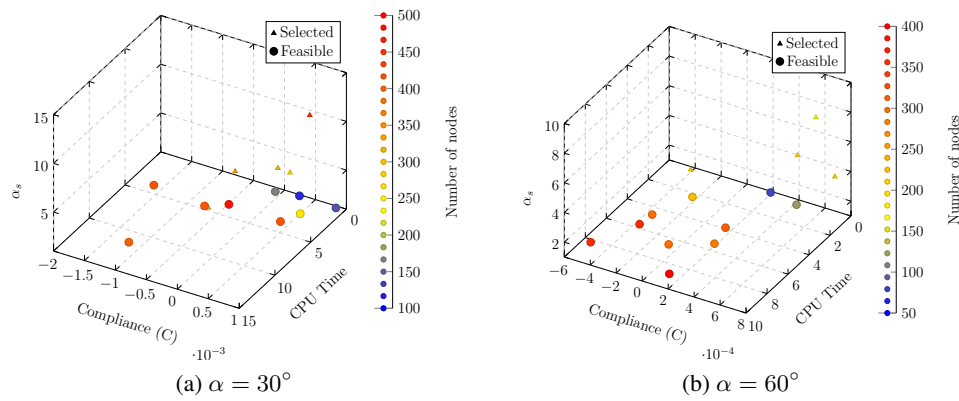


Figure 15: The multi-objective Pareto front of the square plate with an edge slant crack under mixed-mode loading, for $a/w = 0.4$; ILMF with the automatic parameters optimization routine.

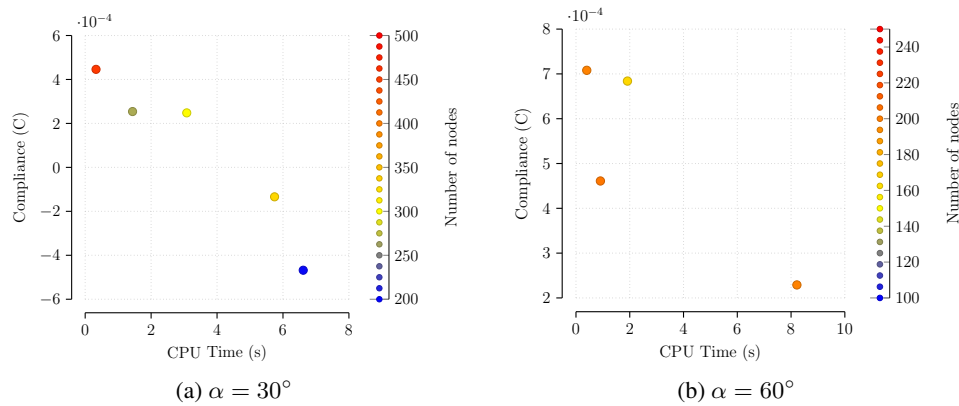


Figure 16: The multi-objective Pareto front of selected feasible solutions for the square plate with an edge slant crack under mixed-mode loading ($a/w = 0.4$).

Table 6: The multi-objective Pareto front results of selected feasible solutions for the square plate with a single edge crack under mixed-mode loading, for $a/w = 0.4$ and $\alpha = 60^\circ$.

Ind.	CPU T. (s)	C	$K_I/(\bar{t}\sqrt{\pi a})$	$K_{II}/(\bar{t}\sqrt{\pi a})$	α_s	α_q	N.
1	0.909	4.61E-04	0.649	0.454	4.761	0.503	203
2	1.915	6.84E-04	0.701	0.491	8.58	0.501	165
3	8.217	2.29E-04	0.713	0.499	7.955	0.498	199
4	0.401	7.08E-04	0.511	0.482	3.659	0.495	199

compared to other examples or $\alpha = 60^\circ$ due to the high difference between K_I and K_{II} , which generates more feasible solutions if no trade-off is established.

For different values of a/w , the results are presented in Tables 7 and 8 for $\alpha = 30^\circ$, and Tables 9 and 10, for $\alpha = 60^\circ$. Percentage errors presented are measured

Table 7: Square plate with a single edge crack under mixed-mode loading, for $\alpha = 30^\circ$ and $K_I/(\bar{t}\sqrt{\pi a})$.

a/w	$K_I/(\bar{t}\sqrt{\pi a})$				% Error	
	ILMF	ILMF ⁺	J-DBEM [28]	Reference [24]	ILMF ⁺	J-DBEM
0.2	1.164	1.1	1.082	1.100	0.009	0.016
0.4	1.513	1.579	1.545	1.550	0.018	0.003
0.6	2.732	2.743	2.572	2.550	0.08	0.009

Table 8: Square plate with a single edge crack under mixed-mode loading, for $\alpha = 30^\circ$ and $K_{II}/(\bar{t}\sqrt{\pi a})$.

a/w	$K_{II}/(\bar{t}\sqrt{\pi a})$				% Error	
	ILMF	ILMF ⁺	J-DBEM [28]	Reference [24]	ILMF ⁺	J-DBEM
0.2	0.325	0.353	0.351	0.350	0.008	0.003
0.4	0.471	0.478	0.474	0.470	0.017	0.009
0.6	0.580	0.748	0.700	0.700	0.07	0.000

from the values obtained with the J-integral implemented in the DBEM, provided by Portela and Aliabadi [28], and Murakami [24]. The nodal distribution obtained by the GA optimization scheme and the respective deformed configuration of the plate is schematically represented in Figures 17 and 18.

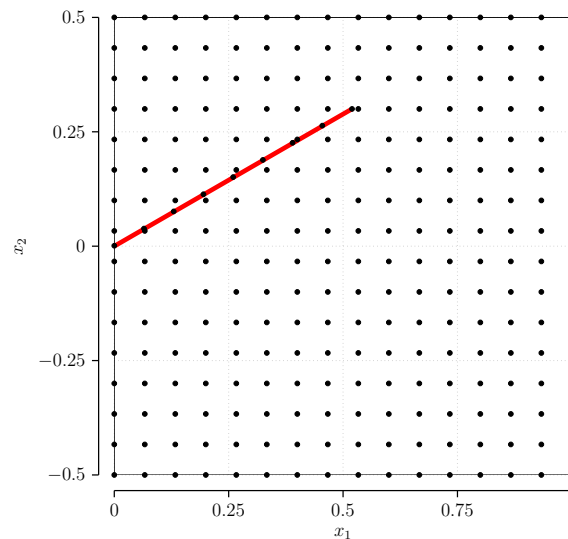
The compliance proved to be an efficient objective function for linear elastic fracture mechanics problems and complement the already efficient SST implementation, without any refinement around the crack tip due to the regularized stress field.

Table 9: Square plate with a single edge crack under mixed-mode loading, for $\alpha = 60^\circ$ and $K_I/(\bar{t}\sqrt{\pi a})$.

a/w	$K_I/(\bar{t}\sqrt{\pi a})$				% Error	
	ILMF	ILMF ⁺	J-DBEM [28]	Reference [24]	ILMF ⁺	J-DBEM
0.2	0.543	0.520	0.495	0.500	0.039	0.010
0.4	0.603	0.604	0.592	0.600	0.005	0.013

Table 10: Square plate with a single edge crack under mixed-mode loading, for $\alpha = 60^\circ$ and $K_{II}/(\bar{t}\sqrt{\pi a})$.

a/w	$K_{II}/(\bar{t}\sqrt{\pi a})$				% Error	
	ILMF	ILMF ⁺	J-DBEM [28]	Reference [24]	ILMF ⁺	J-DBEM
0.2	0.327	0.373	0.356	0.360	0.035	0.011
0.4	0.439	0.422	0.413	0.420	0.005	0.017

**Figure 17:** Regular nodal distribution resulting from the optimization scheme, with a regular nodal distribution of $16 \times 16 = 256$ nodes and additional overlapping nodes on the crack faces, for $a/w = 0.6$, under mixed-mode loading. The red line represents the crack faces.

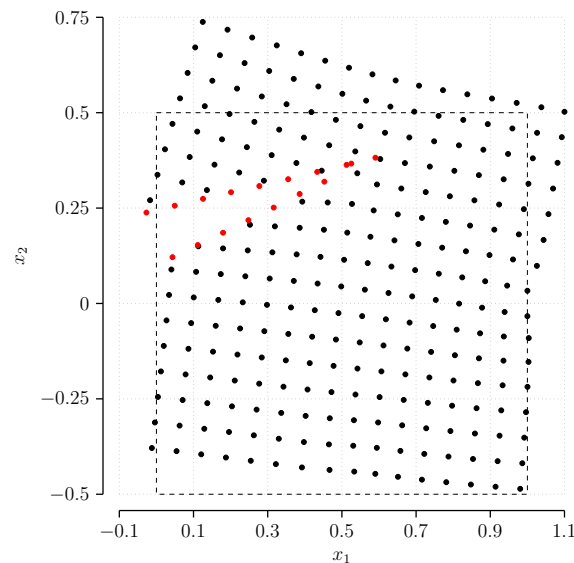


Figure 18: Deformed configuration of the plate resulting from the optimization scheme, for $a/w = 0.6$, under mixed-mode loading.

VI. CONCLUSIONS

The ILMF local mesh free numerical method, implemented with SST, was improved through an optimization scheme that automatically define the nodal distribution and the discretization parameters, for solving two-dimensional problems of the linear elastic fracture mechanics.

The MLS and reduced numerical integrations are considered in the discretization of the elastic field, using a node-by-node process to generate the global system of equilibrium equations, which is very efficient and prone to parallel processing. Also, the reduced integration reduce the stiffness associated with local nodes, leading to an increase in the overall accuracy, without the well-known instabilities associated with the process.

The SST implemented for linear elastic fracture mechanics applications performs a regularization of the stress field, introducing the SIF as additional primary unknowns of the problem. As a consequence, the analysis does not require refined nodal distributions around crack tips, in contrast to other numerical methods. The numerical results are evidence of the efficiency of the modeling strategy, since accurate results were obtained for edge-cracked square plates under mode-I, mode-II and mixed-mode, always without any refinement around the crack tip and relatively small nodal distributions, automatically obtained by the optimization algorithm.

Historically, the nodal distribution, the size of the compact support and the size of the local integration domain are heuristically defined and need to be addressed for every mesh-free application. The ILMF model has the capability of the automatic definition of the discretization parameters and the nodal distribution, through a multi-objective optimization process, based on GA.

The definition of the objective function as a profound impact on the behavior of the optimization process and need to be carefully defined. In this paper, an appropriate objective function is derived from the classical structural theorem of the minimum total potential energy, carried out only at static boundary nodes that does not require the computation of derivatives of shape functions. Therefore, the

optimization scheme is computationally very efficient and as the additional benefit of not requiring the analytical solution to be performed.

The results obtained with the optimization algorithm are in agreement with those of the reference values, where low compliance values are associated with accurate SIF values, as expected. This result show that the local Pareto-optimal is always quite close to the global Pareto-optimal solutions, which is always desirable from a computational point of view. The structural compliance objective function effectively optimized the discretization parameters and the nodal distribution, properly defining these geometrical properties with fast computations and without any user input.

This paper show that mesh-free methods, along with optimization processes, could provide stable and accurate solutions for fracture mechanics problems with minimal user input, contributing to a mainstream use of mesh-free numerical methods in the near future.

REFERENCES RÉFÉRENCES REFERENCIAS

- [1] S.N. Atluri and S. Shen. The meshless local petrov-galerkin (mlpg) method: A simple and less-costly alternative to the finite element and boundary element methods. *CMES: Computer Modeling in Engineering and Sciences*, 3 (1):11–51, 2002.
- [2] S.N. Atluri and T. Zhu. A new meshless local petrov-galerkin (mlpg) approach in computational mechanics. *Computational Mechanics*, 22(2):117–127, 1998.
- [3] A. Bagheri, R. Ehsany, M.J. Mahmoodabadi, and G.H. Baradaran. Optimization of meshless local petrov-galerkin using genetic algorithm for 3d elasto-static problems. *International Journal of Engineering*, 24(2):143–153, 2011.
- [4] G.H. Baradaran and M.J. Mahmoodabadi. Optimal pareto parametric analysis of two dimensional steady-state heat conduction problems by mlpg method. *International Journal of Engineering*, 22(4):387–406, 2009.
- [5] J. Caicedo and A. Portela. Cracked plate analysis with the dual boundary element method and williams' eigenexpansion. *J. of Engineering Analysis with Boundary Elements*, 52:16—23, 2015.
- [6] J. Chen, M. Hillman, and S. Chi. Meshfree methods: Progress made after 20 years. *Journal of Engineering Mechanics*, 143(4):04017001, 2017.
- [7] M.B. Civelek and F. Erdogan. Crack problems for a rectangular plate and an infinite strip. *International Journal of Fracture*, 19:139–159, 1982.
- [8] E. Dede. Multiphysics topology optimization of heat transfer and fluid flow systems. In *Proceedings of the COMSOL Conference*, Boston, 2009. COMSOL.
- [9] L. Dede, M.J. Borden, and T.J.R. Hughes. Isogeometric analysis for topology optimization with a phase field model. *Archives of Computational Methods in Engineering*, 19:427–465, 2012.
- [10] Denk, M., Rother, K., Zinßer, M., Petroll, C., & Paetzold, K. (2021). Nodal cosine sine material interpolation in multi objective topology optimization with the global criteria method for linear elasto static, heat transfer, potential flow and binary cross entropy sharpening. In *Proceedings of the 23th International Conference on Engineering Design* (pp. 2247–2256). Design Society.
- [11] Denk, M., Rother, K., Zinßer, M., Petroll, C., & Paetzold, K. (2021). Nodal cosine sine material interpolation in multi objective topology optimization with the global criteria method for linear elasto static, heat transfer, potential flow and binary



- cross entropy sharpening. In *Proceedings of the 23th International Conference on Engineering Design* (pp. 2247–2256). Design Society.
- [12] M. Ebrahimnejad, N. Fallah, and A.R. Khoei. Adaptive refinement in the meshless finite volume method for elasticity problems. *Computers & Mathematics with Applications*, 69(12):1420–1443, 2015.
- [13] M. Gen and R. Cheng. *Genetic Algorithms and Engineering Optimization*. Wiley, 2000.
- [14] A. Gersborg-Hansen, M.P. Bendsoe, and O. Sigmund. Topology optimization of heat conduction problems using the finite volume method. *Structural and Multidisciplinary Optimization*, 31:251–259, 2006.
- [15] D.K. Gupta, M. Langelaar, M. Barink, and F. van Keulen. Topology optimization of front metallization patterns for solar cells. *Structural and Multidisciplinary Optimization*, 51:941–955, 2015.
- [16] J.H. Holland. *Adaptation in Natural and Artificial Systems*. MIT press, 1975.
- [17] A. Huerta, T. Belytschko, S. Fernández-Méndez, T. Rabczuk, X. Zhuang, and M. Arroyo. Meshfree methods. *Encyclopedia of Computational Mechanics, Second Edition, Edited by Erwin Stein, René de Borst and Thomas J.R. Hughes*, Wiley, 2017.
- [18] C.L. Hwang and A.S.M. Masud. *Multiple Objectives Decision Making—Methods and Applications*. Springer, 1979.
- [19] V. Kelner and O. Leonard. Application of genetic algorithms to lubrication pump stacking design. *Journal of Computational and Applied Mathematics*, 168(1):255–265, 2004.
- [20] W.Y. Kim, R.V. Grandhi, and M. Haney. Multiobjective evolutionary structural optimization using combined static/dynamic control parameters. *AIAA J.*, 44:794–802, 2006.
- [21] G.R. Liu and Y.T. Gu. A local point interpolation method for stress analysis of two-dimensional solids. *Structural Engineering and Mechanics*, 11(2): 221–236, 2001.
- [22] G.R. Liu, L. Yan, J.G. Wang, and Y.T. Gu. Point interpolation method based on local residual formulation using radial basis functions. *Structural Engineering and Mechanics*, 14:713–732, 2002.
- [23] J. McCall. Genetic algorithms for modelling and optimisation. *Journal of Computational and Applied Mathematics*, 184(1):205–222, 2005.
- [24] Y. Murakami. *Stress intensity factors handbook, 1st edition, vol 2*. Pergamon Press, 1987.
- [25] T. Oliveira and A. Portela. Weak form collocation – a local meshless method in linear elasticity. *Engineering Analysis with Boundary Elements*, 73(1): 144–160, 2016.
- [26] T. Oliveira and A. Portela. A local mesh free method with the singularity subtraction technique. *Engineering Analysis with Boundary Elements*, 104: 148–159, 2019.
- [27] T. Oliveira, W. Vélez, E. Santana, T. Araújo, F. Mendonça, and A. Portela. A local mesh free method for linear elasticity and fracture mechanics. *Engineering Analysis with Boundary Elements*, 101:221–242, 2019.
- [28] A. Portela and M.H. Aliabadi. *Crack Growth Analysis Using Boundary Elements – Software*. Computational Mechanics Publications, Southampton, UK and Boston, USA, 1993.



- [29] K. Proos, G. Steven, O. Querin, and Y. Xie. Multicriterion evolutionary structural optimization using the weighting and the global criterion methods. *AIAA J.*, 39:2006–2012, 2001.
- [30] J.L. Ringuest. *Multiobjective Optimization: Behavioral and Computational Considerations*. Kluwer, 1992.
- [31] E. Santana, T. Oliveira, W. Vélez, T. Araújo, F. Martins, and A. Portela. A local mesh free numerical method with automatic parameter optimization. *Engineering Analysis with Boundary Elements*, 113:55–71, 2020.
- [32] Y. Sawaragi, H. Nakayama, and T. Tanino. *Theory of Multiobjective Optimization*. Academic Press, 1985.
- [33] R.E. Steuer. *Multiple Criteria Optimization: Theory, Computation, and Application*. Wiley, 1986.
- [34] M.L. Williams. Stress singularities resulting from various boundary conditions in angular corners of plates in extension. *Journal of Applied Mechanics*, pages 526–528, 1952.
- [35] D.H. Wolpert and W.G. Macready. No free lunch theorems for optimization. *Transactions on Evolutionary Computation*, 1(1):67–82, 1997.
- [36] David W. Zingg, Marian Nemec, and Thomas H. Pulliam. A comparative evaluation of genetic and gradient-based algorithms applied to aerodynamic optimization. *European Journal of Computational Mechanics*, 17(1–2):103–126, 2008.
- [37] A. Zolfagharian, M. Denk, M. Bodaghi, A.Z. Kouzani, and A. Kaynak. Topology-optimized 4d printing of a soft actuator. *Acta Mechanica Sinica*, 33:418–430, 2020.



GLOBAL JOURNALS GUIDELINES HANDBOOK 2021

WWW.GLOBALJOURNALS.ORG

MEMBERSHIPS

FELLOWS/ASSOCIATES OF ENGINEERING RESEARCH COUNCIL

FERC/AERC MEMBERSHIPS

INTRODUCTION



FERC/AERC is the most prestigious membership of Global Journals accredited by Open Association of Research Society, U.S.A (OARS). The credentials of Fellow and Associate designations signify that the researcher has gained the knowledge of the fundamental and high-level concepts, and is a subject matter expert, proficient in an expertise course covering the professional code of conduct, and follows recognized standards of practice. The credentials are designated only to the researchers, scientists, and professionals that have been selected by a rigorous process by our Editorial Board and Management Board.

Associates of FERC/AERC are scientists and researchers from around the world are working on projects/researches that have huge potentials. Members support Global Journals' mission to advance technology for humanity and the profession.

FERC

FELLOW OF ENGINEERING RESEARCH COUNCIL

FELLOW OF ENGINEERING RESEARCH COUNCIL is the most prestigious membership of Global Journals. It is an award and membership granted to individuals that the Open Association of Research Society judges to have made a 'substantial contribution to the improvement of computer science, technology, and electronics engineering.

The primary objective is to recognize the leaders in research and scientific fields of the current era with a global perspective and to create a channel between them and other researchers for better exposure and knowledge sharing. Members are most eminent scientists, engineers, and technologists from all across the world. Fellows are elected for life through a peer review process on the basis of excellence in the respective domain. There is no limit on the number of new nominations made in any year. Each year, the Open Association of Research Society elect up to 12 new Fellow Members.



BENEFIT

TO THE INSTITUTION

GET LETTER OF APPRECIATION

Global Journals sends a letter of appreciation of author to the Dean or CEO of the University or Company of which author is a part, signed by editor in chief or chief author.



EXCLUSIVE NETWORK

GET ACCESS TO A CLOSED NETWORK

A FERC member gets access to a closed network of Tier 1 researchers and scientists with direct communication channel through our website. Fellows can reach out to other members or researchers directly. They should also be open to reaching out by other.

[Career](#)[Credibility](#)[Exclusive](#)[Reputation](#)

CERTIFICATE

CERTIFICATE, LOR AND LASER-MOMENTO

Fellows receive a printed copy of a certificate signed by our Chief Author that may be used for academic purposes and a personal recommendation letter to the dean of member's university.

[Career](#)[Credibility](#)[Exclusive](#)[Reputation](#)

DESIGNATION

GET HONORED TITLE OF MEMBERSHIP

Fellows can use the honored title of membership. The "FERC" is an honored title which is accorded to a person's name viz. Dr. John E. Hall, Ph.D., FERC or William Walldroff, M.S., FERC.

[Career](#)[Credibility](#)[Exclusive](#)[Reputation](#)

RECOGNITION ON THE PLATFORM

BETTER VISIBILITY AND CITATION

All the Fellow members of FERC get a badge of "Leading Member of Global Journals" on the Research Community that distinguishes them from others. Additionally, the profile is also partially maintained by our team for better visibility and citation. All fellows get a dedicated page on the website with their biography.

[Career](#)[Credibility](#)[Reputation](#)

FUTURE WORK

GET DISCOUNTS ON THE FUTURE PUBLICATIONS

Fellows receive discounts on the future publications with Global Journals up to 60%. Through our recommendation programs, members also receive discounts on publications made with OARS affiliated organizations.

Career

Financial



GJ ACCOUNT

UNLIMITED FORWARD OF EMAILS

Fellows get secure and fast GJ work emails with unlimited storage of emails that they may use them as their primary email. For example, john [AT] globaljournals [DOT] org.

Career

Credibility

Reputation



PREMIUM TOOLS

ACCESS TO ALL THE PREMIUM TOOLS

To take future researches to the zenith, fellows receive access to all the premium tools that Global Journals have to offer along with the partnership with some of the best marketing leading tools out there.

Financial

CONFERENCES & EVENTS

ORGANIZE SEMINAR/CONFERENCE

Fellows are authorized to organize symposium/seminar/conference on behalf of Global Journal Incorporation (USA). They can also participate in the same organized by another institution as representative of Global Journal. In both the cases, it is mandatory for him to discuss with us and obtain our consent. Additionally, they get free research conferences (and others) alerts.

Career

Credibility

Financial

EARLY INVITATIONS

EARLY INVITATIONS TO ALL THE SYMPOSIUMS, SEMINARS, CONFERENCES

All fellows receive the early invitations to all the symposiums, seminars, conferences and webinars hosted by Global Journals in their subject.

Exclusive



PUBLISHING ARTICLES & BOOKS

EARN 60% OF SALES PROCEEDS

Fellows can publish articles (limited) without any fees. Also, they can earn up to 70% of sales proceeds from the sale of reference/review books/literature/publishing of research paper. The FERC member can decide its price and we can help in making the right decision.

Exclusive

Financial

REVIEWERS

GET A REMUNERATION OF 15% OF AUTHOR FEES

Fellow members are eligible to join as a paid peer reviewer at Global Journals Incorporation (USA) and can get a remuneration of 15% of author fees, taken from the author of a respective paper.

Financial

ACCESS TO EDITORIAL BOARD

BECOME A MEMBER OF THE EDITORIAL BOARD

Fellows may join as a member of the Editorial Board of Global Journals Incorporation (USA) after successful completion of three years as Fellow and as Peer Reviewer. Additionally, Fellows get a chance to nominate other members for Editorial Board.

Career

Credibility

Exclusive

Reputation

AND MUCH MORE

GET ACCESS TO SCIENTIFIC MUSEUMS AND OBSERVATORIES ACROSS THE GLOBE

All members get access to 5 selected scientific museums and observatories across the globe. All researches published with Global Journals will be kept under deep archival facilities across regions for future protections and disaster recovery. They get 10 GB free secure cloud access for storing research files.

ASSOCIATE OF ENGINEERING RESEARCH COUNCIL

ASSOCIATE OF ENGINEERING RESEARCH COUNCIL is the membership of Global Journals awarded to individuals that the Open Association of Research Society judges to have made a 'substantial contribution to the improvement of computer science, technology, and electronics engineering.

The primary objective is to recognize the leaders in research and scientific fields of the current era with a global perspective and to create a channel between them and other researchers for better exposure and knowledge sharing. Members are most eminent scientists, engineers, and technologists from all across the world. Associate membership can later be promoted to Fellow Membership. Associates are elected for life through a peer review process on the basis of excellence in the respective domain. There is no limit on the number of new nominations made in any year. Each year, the Open Association of Research Society elect up to 12 new Associate Members.



BENEFIT

TO THE INSTITUTION

GET LETTER OF APPRECIATION

Global Journals sends a letter of appreciation of author to the Dean or CEO of the University or Company of which author is a part, signed by editor in chief or chief author.



EXCLUSIVE NETWORK

GET ACCESS TO A CLOSED NETWORK

A AERC member gets access to a closed network of Tier 1 researchers and scientists with direct communication channel through our website. Associates can reach out to other members or researchers directly. They should also be open to reaching out by other.

Career

Credibility

Exclusive

Reputation



CERTIFICATE

CERTIFICATE, LOR AND LASER-MOMENTO

Associates receive a printed copy of a certificate signed by our Chief Author that may be used for academic purposes and a personal recommendation letter to the dean of member's university.

Career

Credibility

Exclusive

Reputation



DESIGNATION

GET HONORED TITLE OF MEMBERSHIP

Associates can use the honored title of membership. The "AERC" is an honored title which is accorded to a person's name viz. Dr. John E. Hall, Ph.D., AERC or William Walldroff, M.S., AERC.

Career

Credibility

Exclusive

Reputation

RECOGNITION ON THE PLATFORM

BETTER VISIBILITY AND CITATION

All the Associate members of AERC get a badge of "Leading Member of Global Journals" on the Research Community that distinguishes them from others. Additionally, the profile is also partially maintained by our team for better visibility and citation. All associates get a dedicated page on the website with their biography.

Career

Credibility

Reputation

FUTURE WORK

GET DISCOUNTS ON THE FUTURE PUBLICATIONS

Associates receive discounts on the future publications with Global Journals up to 60%. Through our recommendation programs, members also receive discounts on publications made with OARS affiliated organizations.

Career

Financial



GJ ACCOUNT

UNLIMITED FORWARD OF EMAILS

Associates get secure and fast GJ work emails with unlimited storage of emails that they may use them as their primary email. For example, john [AT] globaljournals [DOT] org..

Career

Credibility

Reputation



PREMIUM TOOLS

ACCESS TO ALL THE PREMIUM TOOLS

To take future researches to the zenith, associates receive access to all the premium tools that Global Journals have to offer along with the partnership with some of the best marketing leading tools out there.

Financial

CONFERENCES & EVENTS

ORGANIZE SEMINAR/CONFERENCE

Associates are authorized to organize symposium/seminar/conference on behalf of Global Journal Incorporation (USA). They can also participate in the same organized by another institution as representative of Global Journal. In both the cases, it is mandatory for him to discuss with us and obtain our consent. Additionally, they get free research conferences (and others) alerts.

Career

Credibility

Financial

EARLY INVITATIONS

EARLY INVITATIONS TO ALL THE SYMPOSIUMS, SEMINARS, CONFERENCES

All associates receive the early invitations to all the symposiums, seminars, conferences and webinars hosted by Global Journals in their subject.

Exclusive



PUBLISHING ARTICLES & BOOKS

EARN 30-40% OF SALES PROCEEDS

Associates can publish articles (limited) without any fees. Also, they can earn up to 30-40% of sales proceeds from the sale of reference/review books/literature/publishing of research paper.

Exclusive

Financial

REVIEWERS

GET A REMUNERATION OF 15% OF AUTHOR FEES

Associate members are eligible to join as a paid peer reviewer at Global Journals Incorporation (USA) and can get a remuneration of 15% of author fees, taken from the author of a respective paper.

Financial

AND MUCH MORE

GET ACCESS TO SCIENTIFIC MUSEUMS AND OBSERVATORIES ACROSS THE GLOBE

All members get access to 2 selected scientific museums and observatories across the globe. All researches published with Global Journals will be kept under deep archival facilities across regions for future protections and disaster recovery. They get 5 GB free secure cloud access for storing research files.



ASSOCIATE	FELLOW	RESEARCH GROUP	BASIC
\$4800 lifetime designation	\$6800 lifetime designation	\$12500.00 organizational	APC per article
Certificate , LoR and Momento 2 discounted publishing/year Gradation of Research 10 research contacts/day 1 GB Cloud Storage GJ Community Access	Certificate , LoR and Momento Unlimited discounted publishing/year Gradation of Research Unlimited research contacts/day 5 GB Cloud Storage Online Presense Assistance GJ Community Access	Certificates , LoRs and Momentos Unlimited free publishing/year Gradation of Research Unlimited research contacts/day Unlimited Cloud Storage Online Presense Assistance GJ Community Access	GJ Community Access



PREFERRED AUTHOR GUIDELINES

We accept the manuscript submissions in any standard (generic) format.

We typeset manuscripts using advanced typesetting tools like Adobe In Design, CorelDraw, TeXnicCenter, and TeXStudio. We usually recommend authors submit their research using any standard format they are comfortable with, and let Global Journals do the rest.

Alternatively, you can download our basic template from <https://globaljournals.org/Template.zip>

Authors should submit their complete paper/article, including text illustrations, graphics, conclusions, artwork, and tables. Authors who are not able to submit manuscript using the form above can email the manuscript department at submit@globaljournals.org or get in touch with chiefeditor@globaljournals.org if they wish to send the abstract before submission.

BEFORE AND DURING SUBMISSION

Authors must ensure the information provided during the submission of a paper is authentic. Please go through the following checklist before submitting:

1. Authors must go through the complete author guideline and understand and *agree to Global Journals' ethics and code of conduct*, along with author responsibilities.
2. Authors must accept the privacy policy, terms, and conditions of Global Journals.
3. Ensure corresponding author's email address and postal address are accurate and reachable.
4. Manuscript to be submitted must include keywords, an abstract, a paper title, co-author(s) names and details (email address, name, phone number, and institution), figures and illustrations in vector format including appropriate captions, tables, including titles and footnotes, a conclusion, results, acknowledgments and references.
5. Authors should submit paper in a ZIP archive if any supplementary files are required along with the paper.
6. Proper permissions must be acquired for the use of any copyrighted material.
7. Manuscript submitted *must not have been submitted or published elsewhere* and all authors must be aware of the submission.

Declaration of Conflicts of Interest

It is required for authors to declare all financial, institutional, and personal relationships with other individuals and organizations that could influence (bias) their research.

POLICY ON PLAGIARISM

Plagiarism is not acceptable in Global Journals submissions at all.

Plagiarized content will not be considered for publication. We reserve the right to inform authors' institutions about plagiarism detected either before or after publication. If plagiarism is identified, we will follow COPE guidelines:

Authors are solely responsible for all the plagiarism that is found. The author must not fabricate, falsify or plagiarize existing research data. The following, if copied, will be considered plagiarism:

- Words (language)
- Ideas
- Findings
- Writings
- Diagrams
- Graphs
- Illustrations
- Lectures



- Printed material
- Graphic representations
- Computer programs
- Electronic material
- Any other original work

AUTHORSHIP POLICIES

Global Journals follows the definition of authorship set up by the Open Association of Research Society, USA. According to its guidelines, authorship criteria must be based on:

1. Substantial contributions to the conception and acquisition of data, analysis, and interpretation of findings.
2. Drafting the paper and revising it critically regarding important academic content.
3. Final approval of the version of the paper to be published.

Changes in Authorship

The corresponding author should mention the name and complete details of all co-authors during submission and in manuscript. We support addition, rearrangement, manipulation, and deletions in authors list till the early view publication of the journal. We expect that corresponding author will notify all co-authors of submission. We follow COPE guidelines for changes in authorship.

Copyright

During submission of the manuscript, the author is confirming an exclusive license agreement with Global Journals which gives Global Journals the authority to reproduce, reuse, and republish authors' research. We also believe in flexible copyright terms where copyright may remain with authors/employers/institutions as well. Contact your editor after acceptance to choose your copyright policy. You may follow this form for copyright transfers.

Appealing Decisions

Unless specified in the notification, the Editorial Board's decision on publication of the paper is final and cannot be appealed before making the major change in the manuscript.

Acknowledgments

Contributors to the research other than authors credited should be mentioned in Acknowledgments. The source of funding for the research can be included. Suppliers of resources may be mentioned along with their addresses.

Declaration of funding sources

Global Journals is in partnership with various universities, laboratories, and other institutions worldwide in the research domain. Authors are requested to disclose their source of funding during every stage of their research, such as making analysis, performing laboratory operations, computing data, and using institutional resources, from writing an article to its submission. This will also help authors to get reimbursements by requesting an open access publication letter from Global Journals and submitting to the respective funding source.

PREPARING YOUR MANUSCRIPT

Authors can submit papers and articles in an acceptable file format: MS Word (doc, docx), LaTeX (.tex, .zip or .rar including all of your files), Adobe PDF (.pdf), rich text format (.rtf), simple text document (.txt), Open Document Text (.odt), and Apple Pages (.pages). Our professional layout editors will format the entire paper according to our official guidelines. This is one of the highlights of publishing with Global Journals—authors should not be concerned about the formatting of their paper. Global Journals accepts articles and manuscripts in every major language, be it Spanish, Chinese, Japanese, Portuguese, Russian, French, German, Dutch, Italian, Greek, or any other national language, but the title, subtitle, and abstract should be in English. This will facilitate indexing and the pre-peer review process.

The following is the official style and template developed for publication of a research paper. Authors are not required to follow this style during the submission of the paper. It is just for reference purposes.



Manuscript Style Instruction (Optional)

- Microsoft Word Document Setting Instructions.
- Font type of all text should be Swis721 Lt BT.
- Page size: 8.27" x 11", left margin: 0.65, right margin: 0.65, bottom margin: 0.75.
- Paper title should be in one column of font size 24.
- Author name in font size of 11 in one column.
- Abstract: font size 9 with the word "Abstract" in bold italics.
- Main text: font size 10 with two justified columns.
- Two columns with equal column width of 3.38 and spacing of 0.2.
- First character must be three lines drop-capped.
- The paragraph before spacing of 1 pt and after of 0 pt.
- Line spacing of 1 pt.
- Large images must be in one column.
- The names of first main headings (Heading 1) must be in Roman font, capital letters, and font size of 10.
- The names of second main headings (Heading 2) must not include numbers and must be in italics with a font size of 10.

Structure and Format of Manuscript

The recommended size of an original research paper is under 15,000 words and review papers under 7,000 words. Research articles should be less than 10,000 words. Research papers are usually longer than review papers. Review papers are reports of significant research (typically less than 7,000 words, including tables, figures, and references)

A research paper must include:

- a) A title which should be relevant to the theme of the paper.
- b) A summary, known as an abstract (less than 150 words), containing the major results and conclusions.
- c) Up to 10 keywords that precisely identify the paper's subject, purpose, and focus.
- d) An introduction, giving fundamental background objectives.
- e) Resources and techniques with sufficient complete experimental details (wherever possible by reference) to permit repetition, sources of information must be given, and numerical methods must be specified by reference.
- f) Results which should be presented concisely by well-designed tables and figures.
- g) Suitable statistical data should also be given.
- h) All data must have been gathered with attention to numerical detail in the planning stage.

Design has been recognized to be essential to experiments for a considerable time, and the editor has decided that any paper that appears not to have adequate numerical treatments of the data will be returned unrefereed.

- i) Discussion should cover implications and consequences and not just recapitulate the results; conclusions should also be summarized.
- j) There should be brief acknowledgments.
- k) There ought to be references in the conventional format. Global Journals recommends APA format.

Authors should carefully consider the preparation of papers to ensure that they communicate effectively. Papers are much more likely to be accepted if they are carefully designed and laid out, contain few or no errors, are summarizing, and follow instructions. They will also be published with much fewer delays than those that require much technical and editorial correction.

The Editorial Board reserves the right to make literary corrections and suggestions to improve brevity.



FORMAT STRUCTURE

It is necessary that authors take care in submitting a manuscript that is written in simple language and adheres to published guidelines.

All manuscripts submitted to Global Journals should include:

Title

The title page must carry an informative title that reflects the content, a running title (less than 45 characters together with spaces), names of the authors and co-authors, and the place(s) where the work was carried out.

Author details

The full postal address of any related author(s) must be specified.

Abstract

The abstract is the foundation of the research paper. It should be clear and concise and must contain the objective of the paper and inferences drawn. It is advised to not include big mathematical equations or complicated jargon.

Many researchers searching for information online will use search engines such as Google, Yahoo or others. By optimizing your paper for search engines, you will amplify the chance of someone finding it. In turn, this will make it more likely to be viewed and cited in further works. Global Journals has compiled these guidelines to facilitate you to maximize the web-friendliness of the most public part of your paper.

Keywords

A major lynchpin of research work for the writing of research papers is the keyword search, which one will employ to find both library and internet resources. Up to eleven keywords or very brief phrases have to be given to help data retrieval, mining, and indexing.

One must be persistent and creative in using keywords. An effective keyword search requires a strategy: planning of a list of possible keywords and phrases to try.

Choice of the main keywords is the first tool of writing a research paper. Research paper writing is an art. Keyword search should be as strategic as possible.

One should start brainstorming lists of potential keywords before even beginning searching. Think about the most important concepts related to research work. Ask, "What words would a source have to include to be truly valuable in a research paper?" Then consider synonyms for the important words.

It may take the discovery of only one important paper to steer in the right keyword direction because, in most databases, the keywords under which a research paper is abstracted are listed with the paper.

Numerical Methods

Numerical methods used should be transparent and, where appropriate, supported by references.

Abbreviations

Authors must list all the abbreviations used in the paper at the end of the paper or in a separate table before using them.

Formulas and equations

Authors are advised to submit any mathematical equation using either MathJax, KaTeX, or LaTeX, or in a very high-quality image.

Tables, Figures, and Figure Legends

Tables: Tables should be cautiously designed, uncrowned, and include only essential data. Each must have an Arabic number, e.g., Table 4, a self-explanatory caption, and be on a separate sheet. Authors must submit tables in an editable format and not as images. References to these tables (if any) must be mentioned accurately.



Figures

Figures are supposed to be submitted as separate files. Always include a citation in the text for each figure using Arabic numbers, e.g., Fig. 4. Artwork must be submitted online in vector electronic form or by emailing it.

PREPARATION OF ELETRONIC FIGURES FOR PUBLICATION

Although low-quality images are sufficient for review purposes, print publication requires high-quality images to prevent the final product being blurred or fuzzy. Submit (possibly by e-mail) EPS (line art) or TIFF (halftone/ photographs) files only. MS PowerPoint and Word Graphics are unsuitable for printed pictures. Avoid using pixel-oriented software. Scans (TIFF only) should have a resolution of at least 350 dpi (halftone) or 700 to 1100 dpi (line drawings). Please give the data for figures in black and white or submit a Color Work Agreement form. EPS files must be saved with fonts embedded (and with a TIFF preview, if possible).

For scanned images, the scanning resolution at final image size ought to be as follows to ensure good reproduction: line art: >650 dpi; halftones (including gel photographs): >350 dpi; figures containing both halftone and line images: >650 dpi.

Color charges: Authors are advised to pay the full cost for the reproduction of their color artwork. Hence, please note that if there is color artwork in your manuscript when it is accepted for publication, we would require you to complete and return a Color Work Agreement form before your paper can be published. Also, you can email your editor to remove the color fee after acceptance of the paper.

TIPS FOR WRITING A GOOD QUALITY ENGINEERING RESEARCH PAPER

Techniques for writing a good quality engineering research paper:

1. Choosing the topic: In most cases, the topic is selected by the interests of the author, but it can also be suggested by the guides. You can have several topics, and then judge which you are most comfortable with. This may be done by asking several questions of yourself, like "Will I be able to carry out a search in this area? Will I find all necessary resources to accomplish the search? Will I be able to find all information in this field area?" If the answer to this type of question is "yes," then you ought to choose that topic. In most cases, you may have to conduct surveys and visit several places. Also, you might have to do a lot of work to find all the rises and falls of the various data on that subject. Sometimes, detailed information plays a vital role, instead of short information. Evaluators are human: The first thing to remember is that evaluators are also human beings. They are not only meant for rejecting a paper. They are here to evaluate your paper. So present your best aspect.

2. Think like evaluators: If you are in confusion or getting demotivated because your paper may not be accepted by the evaluators, then think, and try to evaluate your paper like an evaluator. Try to understand what an evaluator wants in your research paper, and you will automatically have your answer. Make blueprints of paper: The outline is the plan or framework that will help you to arrange your thoughts. It will make your paper logical. But remember that all points of your outline must be related to the topic you have chosen.

3. Ask your guides: If you are having any difficulty with your research, then do not hesitate to share your difficulty with your guide (if you have one). They will surely help you out and resolve your doubts. If you can't clarify what exactly you require for your work, then ask your supervisor to help you with an alternative. He or she might also provide you with a list of essential readings.

4. Use of computer is recommended: As you are doing research in the field of research engineering then this point is quite obvious. Use right software: Always use good quality software packages. If you are not capable of judging good software, then you can lose the quality of your paper unknowingly. There are various programs available to help you which you can get through the internet.

5. Use the internet for help: An excellent start for your paper is using Google. It is a wondrous search engine, where you can have your doubts resolved. You may also read some answers for the frequent question of how to write your research paper or find a model research paper. You can download books from the internet. If you have all the required books, place importance on reading, selecting, and analyzing the specified information. Then sketch out your research paper. Use big pictures: You may use encyclopedias like Wikipedia to get pictures with the best resolution. At Global Journals, you should strictly follow [here](#).



6. Bookmarks are useful: When you read any book or magazine, you generally use bookmarks, right? It is a good habit which helps to not lose your continuity. You should always use bookmarks while searching on the internet also, which will make your search easier.

7. Revise what you wrote: When you write anything, always read it, summarize it, and then finalize it.

8. Make every effort: Make every effort to mention what you are going to write in your paper. That means always have a good start. Try to mention everything in the introduction—what is the need for a particular research paper. Polish your work with good writing skills and always give an evaluator what he wants. Make backups: When you are going to do any important thing like making a research paper, you should always have backup copies of it either on your computer or on paper. This protects you from losing any portion of your important data.

9. Produce good diagrams of your own: Always try to include good charts or diagrams in your paper to improve quality. Using several unnecessary diagrams will degrade the quality of your paper by creating a hodgepodge. So always try to include diagrams which were made by you to improve the readability of your paper. Use of direct quotes: When you do research relevant to literature, history, or current affairs, then use of quotes becomes essential, but if the study is relevant to science, use of quotes is not preferable.

10. Use proper verb tense: Use proper verb tenses in your paper. Use past tense to present those events that have happened. Use present tense to indicate events that are going on. Use future tense to indicate events that will happen in the future. Use of wrong tenses will confuse the evaluator. Avoid sentences that are incomplete.

11. Pick a good study spot: Always try to pick a spot for your research which is quiet. Not every spot is good for studying.

12. Know what you know: Always try to know what you know by making objectives, otherwise you will be confused and unable to achieve your target.

13. Use good grammar: Always use good grammar and words that will have a positive impact on the evaluator; use of good vocabulary does not mean using tough words which the evaluator has to find in a dictionary. Do not fragment sentences. Eliminate one-word sentences. Do not ever use a big word when a smaller one would suffice.

Verbs have to be in agreement with their subjects. In a research paper, do not start sentences with conjunctions or finish them with prepositions. When writing formally, it is advisable to never split an infinitive because someone will (wrongly) complain. Avoid clichés like a disease. Always shun irritating alliteration. Use language which is simple and straightforward. Put together a neat summary.

14. Arrangement of information: Each section of the main body should start with an opening sentence, and there should be a changeover at the end of the section. Give only valid and powerful arguments for your topic. You may also maintain your arguments with records.

15. Never start at the last minute: Always allow enough time for research work. Leaving everything to the last minute will degrade your paper and spoil your work.

16. Multitasking in research is not good: Doing several things at the same time is a bad habit in the case of research activity. Research is an area where everything has a particular time slot. Divide your research work into parts, and do a particular part in a particular time slot.

17. Never copy others' work: Never copy others' work and give it your name because if the evaluator has seen it anywhere, you will be in trouble. Take proper rest and food: No matter how many hours you spend on your research activity, if you are not taking care of your health, then all your efforts will have been in vain. For quality research, take proper rest and food.

18. Go to seminars: Attend seminars if the topic is relevant to your research area. Utilize all your resources.

19. Refresh your mind after intervals: Try to give your mind a rest by listening to soft music or sleeping in intervals. This will also improve your memory. Acquire colleagues: Always try to acquire colleagues. No matter how sharp you are, if you acquire colleagues, they can give you ideas which will be helpful to your research.

20. Think technically: Always think technically. If anything happens, search for its reasons, benefits, and demerits. Think and then print: When you go to print your paper, check that tables are not split, headings are not detached from their descriptions, and page sequence is maintained.



21. Adding unnecessary information: Do not add unnecessary information like "I have used MS Excel to draw graphs." Irrelevant and inappropriate material is superfluous. Foreign terminology and phrases are not apropos. One should never take a broad view. Analogy is like feathers on a snake. Use words properly, regardless of how others use them. Remove quotations. Puns are for kids, not grunt readers. Never oversimplify: When adding material to your research paper, never go for oversimplification; this will definitely irritate the evaluator. Be specific. Never use rhythmic redundancies. Contractions shouldn't be used in a research paper. Comparisons are as terrible as clichés. Give up ampersands, abbreviations, and so on. Remove commas that are not necessary. Parenthetical words should be between brackets or commas. Understatement is always the best way to put forward earth-shaking thoughts. Give a detailed literary review.

22. Report concluded results: Use concluded results. From raw data, filter the results, and then conclude your studies based on measurements and observations taken. An appropriate number of decimal places should be used. Parenthetical remarks are prohibited here. Proofread carefully at the final stage. At the end, give an outline to your arguments. Spot perspectives of further study of the subject. Justify your conclusion at the bottom sufficiently, which will probably include examples.

23. Upon conclusion: Once you have concluded your research, the next most important step is to present your findings. Presentation is extremely important as it is the definite medium through which your research is going to be in print for the rest of the crowd. Care should be taken to categorize your thoughts well and present them in a logical and neat manner. A good quality research paper format is essential because it serves to highlight your research paper and bring to light all necessary aspects of your research.

INFORMAL GUIDELINES OF RESEARCH PAPER WRITING

Key points to remember:

- Submit all work in its final form.
- Write your paper in the form which is presented in the guidelines using the template.
- Please note the criteria peer reviewers will use for grading the final paper.

Final points:

One purpose of organizing a research paper is to let people interpret your efforts selectively. The journal requires the following sections, submitted in the order listed, with each section starting on a new page:

The introduction: This will be compiled from reference matter and reflect the design processes or outline of basis that directed you to make a study. As you carry out the process of study, the method and process section will be constructed like that. The results segment will show related statistics in nearly sequential order and direct reviewers to similar intellectual paths throughout the data that you gathered to carry out your study.

The discussion section:

This will provide understanding of the data and projections as to the implications of the results. The use of good quality references throughout the paper will give the effort trustworthiness by representing an alertness to prior workings.

Writing a research paper is not an easy job, no matter how trouble-free the actual research or concept. Practice, excellent preparation, and controlled record-keeping are the only means to make straightforward progression.

General style:

Specific editorial column necessities for compliance of a manuscript will always take over from directions in these general guidelines.

To make a paper clear: Adhere to recommended page limits.

Mistakes to avoid:

- Insertion of a title at the foot of a page with subsequent text on the next page.
- Separating a table, chart, or figure—confine each to a single page.
- Submitting a manuscript with pages out of sequence.
- In every section of your document, use standard writing style, including articles ("a" and "the").
- Keep paying attention to the topic of the paper.



- Use paragraphs to split each significant point (excluding the abstract).
- Align the primary line of each section.
- Present your points in sound order.
- Use present tense to report well-accepted matters.
- Use past tense to describe specific results.
- Do not use familiar wording; don't address the reviewer directly. Don't use slang or superlatives.
- Avoid use of extra pictures—include only those figures essential to presenting results.

Title page:

Choose a revealing title. It should be short and include the name(s) and address(es) of all authors. It should not have acronyms or abbreviations or exceed two printed lines.

Abstract: This summary should be two hundred words or less. It should clearly and briefly explain the key findings reported in the manuscript and must have precise statistics. It should not have acronyms or abbreviations. It should be logical in itself. Do not cite references at this point.

An abstract is a brief, distinct paragraph summary of finished work or work in development. In a minute or less, a reviewer can be taught the foundation behind the study, common approaches to the problem, relevant results, and significant conclusions or new questions.

Write your summary when your paper is completed because how can you write the summary of anything which is not yet written? Wealth of terminology is very essential in abstract. Use comprehensive sentences, and do not sacrifice readability for brevity; you can maintain it succinctly by phrasing sentences so that they provide more than a lone rationale. The author can at this moment go straight to shortening the outcome. Sum up the study with the subsequent elements in any summary. Try to limit the initial two items to no more than one line each.

Reason for writing the article—theory, overall issue, purpose.

- Fundamental goal.
- To-the-point depiction of the research.
- Consequences, including definite statistics—if the consequences are quantitative in nature, account for this; results of any numerical analysis should be reported. Significant conclusions or questions that emerge from the research.

Approach:

- Single section and succinct.
- An outline of the job done is always written in past tense.
- Concentrate on shortening results—limit background information to a verdict or two.
- Exact spelling, clarity of sentences and phrases, and appropriate reporting of quantities (proper units, important statistics) are just as significant in an abstract as they are anywhere else.

Introduction:

The introduction should "introduce" the manuscript. The reviewer should be presented with sufficient background information to be capable of comprehending and calculating the purpose of your study without having to refer to other works. The basis for the study should be offered. Give the most important references, but avoid making a comprehensive appraisal of the topic. Describe the problem visibly. If the problem is not acknowledged in a logical, reasonable way, the reviewer will give no attention to your results. Speak in common terms about techniques used to explain the problem, if needed, but do not present any particulars about the protocols here.

The following approach can create a valuable beginning:

- Explain the value (significance) of the study.
- Defend the model—why did you employ this particular system or method? What is its compensation? Remark upon its appropriateness from an abstract point of view as well as pointing out sensible reasons for using it.
- Present a justification. State your particular theory(-ies) or aim(s), and describe the logic that led you to choose them.
- Briefly explain the study's tentative purpose and how it meets the declared objectives.



Approach:

Use past tense except for when referring to recognized facts. After all, the manuscript will be submitted after the entire job is done. Sort out your thoughts; manufacture one key point for every section. If you make the four points listed above, you will need at least four paragraphs. Present surrounding information only when it is necessary to support a situation. The reviewer does not desire to read everything you know about a topic. Shape the theory specifically—do not take a broad view.

As always, give awareness to spelling, simplicity, and correctness of sentences and phrases.

Procedures (methods and materials):

This part is supposed to be the easiest to carve if you have good skills. A soundly written procedures segment allows a capable scientist to replicate your results. Present precise information about your supplies. The suppliers and clarity of reagents can be helpful bits of information. Present methods in sequential order, but linked methodologies can be grouped as a segment. Be concise when relating the protocols. Attempt to give the least amount of information that would permit another capable scientist to replicate your outcome, but be cautious that vital information is integrated. The use of subheadings is suggested and ought to be synchronized with the results section.

When a technique is used that has been well-described in another section, mention the specific item describing the way, but draw the basic principle while stating the situation. The purpose is to show all particular resources and broad procedures so that another person may use some or all of the methods in one more study or referee the scientific value of your work. It is not to be a step-by-step report of the whole thing you did, nor is a methods section a set of orders.

Materials:

Materials may be reported in part of a section or else they may be recognized along with your measures.

Methods:

- Report the method and not the particulars of each process that engaged the same methodology.
- Describe the method entirely.
- To be succinct, present methods under headings dedicated to specific dealings or groups of measures.
- Simplify—detail how procedures were completed, not how they were performed on a particular day.
- If well-known procedures were used, account for the procedure by name, possibly with a reference, and that's all.

Approach:

It is embarrassing to use vigorous voice when documenting methods without using first person, which would focus the reviewer's interest on the researcher rather than the job. As a result, when writing up the methods, most authors use third person passive voice.

Use standard style in this and every other part of the paper—avoid familiar lists, and use full sentences.

What to keep away from:

- Resources and methods are not a set of information.
- Skip all descriptive information and surroundings—save it for the argument.
- Leave out information that is immaterial to a third party.

Results:

The principle of a results segment is to present and demonstrate your conclusion. Create this part as entirely objective details of the outcome, and save all understanding for the discussion.

The page length of this segment is set by the sum and types of data to be reported. Use statistics and tables, if suitable, to present consequences most efficiently.

You must clearly differentiate material which would usually be incorporated in a study editorial from any unprocessed data or additional appendix matter that would not be available. In fact, such matters should not be submitted at all except if requested by the instructor.



Content:

- Sum up your conclusions in text and demonstrate them, if suitable, with figures and tables.
- In the manuscript, explain each of your consequences, and point the reader to remarks that are most appropriate.
- Present a background, such as by describing the question that was addressed by creation of an exacting study.
- Explain results of control experiments and give remarks that are not accessible in a prescribed figure or table, if appropriate.
- Examine your data, then prepare the analyzed (transformed) data in the form of a figure (graph), table, or manuscript.

What to stay away from:

- Do not discuss or infer your outcome, report surrounding information, or try to explain anything.
- Do not include raw data or intermediate calculations in a research manuscript.
- Do not present similar data more than once.
- A manuscript should complement any figures or tables, not duplicate information.
- Never confuse figures with tables—there is a difference.

Approach:

As always, use past tense when you submit your results, and put the whole thing in a reasonable order.

Put figures and tables, appropriately numbered, in order at the end of the report.

If you desire, you may place your figures and tables properly within the text of your results section.

Figures and tables:

If you put figures and tables at the end of some details, make certain that they are visibly distinguished from any attached appendix materials, such as raw facts. Whatever the position, each table must be titled, numbered one after the other, and include a heading. All figures and tables must be divided from the text.

Discussion:

The discussion is expected to be the trickiest segment to write. A lot of papers submitted to the journal are discarded based on problems with the discussion. There is no rule for how long an argument should be.

Position your understanding of the outcome visibly to lead the reviewer through your conclusions, and then finish the paper with a summing up of the implications of the study. The purpose here is to offer an understanding of your results and support all of your conclusions, using facts from your research and generally accepted information, if suitable. The implication of results should be fully described.

Infer your data in the conversation in suitable depth. This means that when you clarify an observable fact, you must explain mechanisms that may account for the observation. If your results vary from your prospect, make clear why that may have happened. If your results agree, then explain the theory that the proof supported. It is never suitable to just state that the data approved the prospect, and let it drop at that. Make a decision as to whether each premise is supported or discarded or if you cannot make a conclusion with assurance. Do not just dismiss a study or part of a study as "uncertain."

Research papers are not acknowledged if the work is imperfect. Draw what conclusions you can based upon the results that you have, and take care of the study as a finished work.

- You may propose future guidelines, such as how an experiment might be personalized to accomplish a new idea.
- Give details of all of your remarks as much as possible, focusing on mechanisms.
- Make a decision as to whether the tentative design sufficiently addressed the theory and whether or not it was correctly restricted. Try to present substitute explanations if they are sensible alternatives.
- One piece of research will not counter an overall question, so maintain the large picture in mind. Where do you go next? The best studies unlock new avenues of study. What questions remain?
- Recommendations for detailed papers will offer supplementary suggestions.



Approach:

When you refer to information, differentiate data generated by your own studies from other available information. Present work done by specific persons (including you) in past tense.

Describe generally acknowledged facts and main beliefs in present tense.

THE ADMINISTRATION RULES

Administration Rules to Be Strictly Followed before Submitting Your Research Paper to Global Journals Inc.

Please read the following rules and regulations carefully before submitting your research paper to Global Journals Inc. to avoid rejection.

Segment draft and final research paper: You have to strictly follow the template of a research paper, failing which your paper may get rejected. You are expected to write each part of the paper wholly on your own. The peer reviewers need to identify your own perspective of the concepts in your own terms. Please do not extract straight from any other source, and do not rephrase someone else's analysis. Do not allow anyone else to proofread your manuscript.

Written material: You may discuss this with your guides and key sources. Do not copy anyone else's paper, even if this is only imitation, otherwise it will be rejected on the grounds of plagiarism, which is illegal. Various methods to avoid plagiarism are strictly applied by us to every paper, and, if found guilty, you may be blacklisted, which could affect your career adversely. To guard yourself and others from possible illegal use, please do not permit anyone to use or even read your paper and file.



CRITERION FOR GRADING A RESEARCH PAPER (COMPILATION)
BY GLOBAL JOURNALS

Please note that following table is only a Grading of "Paper Compilation" and not on "Performed/Stated Research" whose grading solely depends on Individual Assigned Peer Reviewer and Editorial Board Member. These can be available only on request and after decision of Paper. This report will be the property of Global Journals.

Topics	Grades		
	A-B	C-D	E-F
<i>Abstract</i>	Clear and concise with appropriate content, Correct format. 200 words or below	Unclear summary and no specific data, Incorrect form Above 200 words	No specific data with ambiguous information Above 250 words
<i>Introduction</i>	Containing all background details with clear goal and appropriate details, flow specification, no grammar and spelling mistake, well organized sentence and paragraph, reference cited	Unclear and confusing data, appropriate format, grammar and spelling errors with unorganized matter	Out of place depth and content, hazy format
<i>Methods and Procedures</i>	Clear and to the point with well arranged paragraph, precision and accuracy of facts and figures, well organized subheads	Difficult to comprehend with embarrassed text, too much explanation but completed	Incorrect and unorganized structure with hazy meaning
<i>Result</i>	Well organized, Clear and specific, Correct units with precision, correct data, well structuring of paragraph, no grammar and spelling mistake	Complete and embarrassed text, difficult to comprehend	Irregular format with wrong facts and figures
<i>Discussion</i>	Well organized, meaningful specification, sound conclusion, logical and concise explanation, highly structured paragraph reference cited	Wordy, unclear conclusion, spurious	Conclusion is not cited, unorganized, difficult to comprehend
<i>References</i>	Complete and correct format, well organized	Beside the point, Incomplete	Wrong format and structuring



INDEX

A	T
Amenable · 15	Torsion · 22, 23
Arbitrarily · 11	
Asymptotic · 13, 14	
C	
Cantilever · 23	
E	
Erosion · 16	
G	
Girder · 21	
Gravel · 16	
I	
Integrals · 11, 13, 14, 15	
P	
Perturbation · 9	
Q	
Quadratic · 1, 2, 3, 6	
R	
Reciprocity · 9, 13	



save our planet



Global Journal of Researches in Engineering

Visit us on the Web at www.GlobalJournals.org | www.EngineeringResearch.org
or email us at helpdesk@globaljournals.org



ISSN 9755861

© Global Journals